RSC Advances

REVIEW

View Article Online
View Journal | View Issue

Cite this: *RSC Adv.*, 2021, **11**, 31884

On the diatomite-based nanostructure-preserving material synthesis for energy applications

Patrick Aggrey, *[a] Martinson Nartey, [b] Yuliya Kan,[a] Julijana Cvjetinovic, [c] Anthony Andrews,[b] Alexey I. Salimon, [a] Kalin I. Dragnevski[d] and Alexander M. Korsunsky *[d]

The present article overviews the current state-of-the-art and future prospects for the use of diatomaceous earth (DE) in the continuously expanding sector of energy science and technology. An eco-friendly direct source of silica and the production of silicon, diatomaceous earth possesses a desirable nano- to micro-structure that offers inherent advantages for optimum performance in existing and new applications in electrochemistry, catalysis, optoelectronics, and biomedical engineering. Silica, silicon and silicon-based materials have proven useful for energy harvesting and storage applications. However, they often encounter setbacks to their commercialization due to the limited capability for the production of materials possessing fascinating microstructures to deliver optimum performance. Despite many current research trends focusing on the means to create the required nano- to micro-structures, the high cost and complex, potentially environmentally harmful chemical synthesis techniques remain a considerable challenge. The present review examines the advances made using diatomaceous earth as a source of silica, silicon-based materials and templates for energy related applications. The main synthesis routes aimed at preserving the highly desirable naturally formed neat nanostructure of diatomaceous earth are assessed in this review that culminates with the discussion of recently developed pathways to achieving the best properties. The trend analysis establishes a clear roadmap for diatomaceous earth as a source material of choice for current and future energy applications.

Received 30th July 2021
Accepted 6th September 2021

DOI: 10.1039/d1ra05810j

rsc.li/rsc-advances

[a]*Hierarchically Structured Materials, Center for Energy Science and Technology, Skolkovo Institute of Science and Technology, Bolshoy Boulevard 30, bld. 1, Moscow, Russia 121205*

[b]*Department of Materials Engineering, Kwame Nkrumah University of Science and Technology, Private Mail Box, Kumasi, Ghana*

[c]*Center for Photonics and Quantum Materials, Skolkovo Institute of Science and Technology, Bolshoy Boulevard 30, bld. 1, Moscow, Russia 121205*

[d]*Department of Engineering Science, University of Oxford, Parks Road, Oxford OX1 3PJ, UK. E-mail: alexander.korsunsky@eng.ox.ac.uk*

Patrick Aggrey is a PhD student in Materials Science and Engineering at Skoltech. Patrick's research work aims at understanding the effects of transformations within the silicon oxygen system on the structure and properties of nanostructured silicon and silica-based energy materials and designing cost effective and environmentally friendly synthesis routes to produce them. Some of his results have been recently published. At present his main focus of research is centered on hierarchically structured silica and silicon-based anode materials obtained from naturally occurring diatomaceous earth for applications in energy harvesting and storage.

Dr. Martinson Nartey recently received his PhD from the Zhejiang University, Hangzhou, China and joined the Materials Engineering Department of KNUST, Ghana as a lecturer. His research spans advanced composites, functional alloy development and finding alternative materials for sustainable development. Currently, Dr Nartey is working on diatomaceous earth as potential materials for energy sector applications, building industry as partial replacement of cement and wastewater treatment.

1. Diatomaceous earth

Advances in scientific imaging have enabled researchers to unveil the intricate structural details of nature's own hierarchically structured materials. The use of imaging techniques based on light and electron beams have progressively revealed the micro- to nano-structures of both natural and engineered materials down to the atomic scale that could not be seen previously. Indeed, the majority of naturally occurring materials possess multi-scale, hierarchical organization that to date remains an area of keen interest for researchers. One such naturally occurring material is diatomaceous earth (DE), which is formed following the build-up of amorphous silica cell walls of dead diatoms in marine sediments.[1] Originally discovered by a German peasant Peter Kasten in 1836,[2] diatomaceous earth, also known as diatomite, has for some time now been mined in close to thirty countries globally.[3] Presently, the leading producer of diatomite is the United States, accounting for close to 35% of the total world production.[3] DE is characterized by unique properties such as high porosity, light weight, small particle size and high surface area, chemical inertness and low thermal conductivity[3] thus paving the way for numerous applications. It normally has the appearance of a pale-colored powder. The typical particle size range reported for DE is

Yuliya Kan graduated Master's degree in Material Science from Tomsk Polytechnic University in 2018. Her thesis was focused on the glass–ceramic interlayer of the coating and alumina ceramic composite for biomedical applications. In the 2nd year of her Master's degree, she participated in the academic exchange program at Technical University in Dresden. At Skoltech she keeps working with the hierarchical nanostructures for biomaterial application.

Julijana Cvjetinovic received her M. S. in Condensed Matter Physics from National University of Science and Technology "MISiS", Moscow, Russia and currently a PhD student at the Center for Photonics and Quantum Materials at Skolkovo Institute of Science and Technology. During her Master's degree studies she worked on development of hybrid materials based on natural and synthetic polymers for reconstructive surgery. Her current research is focused on using different photonic and bioimaging techniques to study composite multifunctional nanostructured particles for application in medicine and dentistry. Julijana's research interests include bioimaging, photoacoustic and fluorescence visualization, spectroscopy and analysis of compounds, unicellular microalgae, nanoparticles, drug delivery systems.

Anthony Andrews is an Associate Professor in the Department of Materials Engineering, in the College of Engineering, Kwame Nkrumah University of Science and Technology, Kumasi – Ghana. His research interest is in materials synthesis and development of ceramic-based composites using both traditional and advanced processing routes. His current research activities include surface modification, corrosion, tribology, and ceramic processing. He has over 30 publications in reputable journals.

Alexey Salimon is senior research engineer in the field of hierarchically structured materials having energy, biomedical and structural applications. He received a Candidate of Science (PhD) degree from the Department of Physical Materials Science of NUST MISiS (1997). His doctoral thesis was devoted to the investigation of the structure changes in metal powders under high-energy mechanical activation and alloying. Dr Alexey Salimon for more than 20 years works in the field of new materials and technologies: nanostructured metals and alloys, quasicrystalline intermetallics (University of Newcastle, UK, 1997–1998), bulk metallic glasses, composites, elastomers resistant to explosion decompression. In 2002–2004 Dr Salimon developed the expert system for the finding of application for new materials under Professor M.F. Ashby leadership in INPG (Grenoble, France).

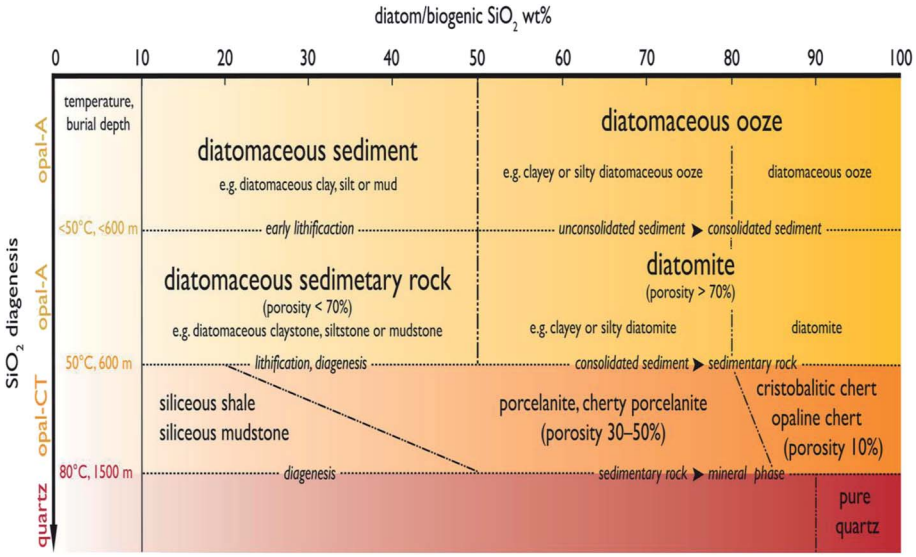

Fig. 1 Classification system of diatom based sediments proposed by Zahajská *et al.*[4] The *x*-axis showing the weight percentage (wt%) of diatom/biogenic SiO_2 contained in sediments and their corresponding transformations as a function of burial depth on the *y*-axis.

about 10–200 μm.[3] Diatomite, regardless of the source, contains SiO_2 as the main phase. Other phases present in DE are CaO, MgO, Fe_2O_3, and Al_2O_3. Lately, the number of literature reports dedicated to DE has increased, but the fundamental requirement for the powder to be classed as DE remains unresolved, creating significant inconsistency with the term Diatomaceous Earth. However, in a study by Zahajská *et al.*,[4] an approach to resolving these issues has been presented. In the report, a classification of sediment containing diatoms into diatomite and diatomaceous ooze is reported. This work was carried out to address the inconsistency in the use of terms 'diatomite' and 'diatomaceous ooze' in previous studies.[5–14] Fig. 1 illustrates the classification system proposed by Zahajská *et al.*[4] to group the powders into diatomite and diatomaceous ooze. From their system, a powder is considered as diatomite when consolidated siliceous/opaline sediment contains more than 80% diatom SiO_2 by weight and porosity higher than 70%. It is worth noting that while other forms of diatomite are available per the classification of Zahajská *et al.*[4] it remains a difficult task to distinguish between the diatomite precursors used in the current literature. This is due to the lack of detail provided by the authors regarding the precursors used. For this reason, the

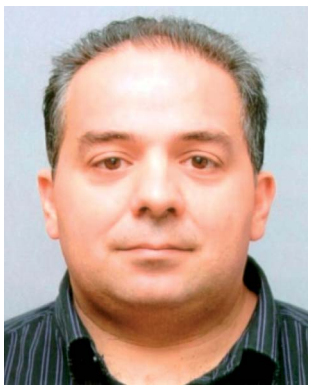

Kalin Dragnevski obtained his MSc from the University of Chemical Technology & Metallurgy, Sofia, Bulgaria & his PhD from the Institute of Materials at Leeds University. Following a short spell in industry, he took a research position in the Cavendish Laboratory at the University of Cambridge. Kalin joined the Engineering Science Department at the University of Oxford in 2008, where he established & leads the Laboratory for In situ *Microscopy & Analysis (LIMA). His research is aimed at developing methodologies for better understanding the structure–property–composition relationship in advanced materials systems on a micro- & nano-scale using novel* in situ *micromechanical testing techniques. His work recently received the prestigious DR Harting Award for best paper of the year given by the Society of Experimental Mechanics.*

Alexander M. Korsunsky is a leading expert in engineering microscopy of materials for optimisation of design, durability and performance. He is Fellow of the Institute of Physics, London, UK, and Editor-in-Chief of Materials & Design. *Prof. Korsunsky's research interests concern improved understanding of engineered and natural structures and systems, from high-performance metallic alloys to polycrystalline ceramics to natural hard tissue such as seashell nacre and human enamel, the subject of a major research project he leads on the understanding and combatting human dental Caries. He co-authored books on fracture mechanics (Springer), elasticity (CUP) and residual stress (Elsevier), and published ~500 articles in scholarly periodicals on subjects ranging from multi-modal 'live' microscopy, neutron and synchrotron X-ray analysis, contact mechanics and structural integrity to micro-cantilever biosensors, and size effects.*

definition of diatomite given by Zahajská *et al.*[4] cannot be applied strictly in the discussion of the existing reports, so that all reports related to diatom silica, diatomite, diatomaceous earth, diatom frustules, diatom algae, diatom earth and bio-silica diatomite will be included in the scope of this review paper. It is however important that full details of precursors be used in future to establish a clearer roadmap to advanced technology use.

The use of diatomite dates as far back as 2000 years ago. It is reported that the Greeks used diatomite in pottery and bricks.[2] Conventionally, DE finds applications as filter aids, functional additives, absorbents, natural insecticide, and materials for soil improvement.[15–19] Recently, diatomite has attracted significant attention in the scientific community. DE provides a unique way to mimic nature by using it as both template and precursor for materials with desirable nanostructures. Most of today's materials are expected to possess nano to micro-structures to meet several functionalities of specific applications. Often, materials exhibiting desirable properties at the macro-scale suffer setbacks arising from chemical, thermal, electronic or mechanical processes at the nano and micro-scale. One notable example is the potential use of silicon as an anode material in lithium-ion batteries. This area has been well studied, continues to be studied and remains a potential game changer in battery technology.[20–26] Silicon is known to have a theoretical capacity an order of magnitude higher than graphite. Coupled with the aforementioned advantages of silicon as a suitable anode material, it is highly abundant and non-toxic. Nevertheless, silicon has not found commercial use as an anode material due to the low cycling stability. Volume changes (up to about 300%) during lithiation have been reported to lead to internal stresses, electrode pulverization, loss of electrical contact between the active material and the current collector, all of which eventually led to poor reversibility and rapid decline in capacity.[22,27] These setbacks are peculiar to bulk silicon, particularly ball-milled Si obtained from bulk silicon. This is because the structure of bulk silicon is unable to meet a combination of functionalities required at the nanoscale. For this reason, several attempts have focused on nanostructuring silicon-based anodes to harness the full potential of silicon in battery technology.[28–34] This new approach to nanostructuring Si based anodes has been reported to offer a better response to volume changes from the surface to center as shown in Fig. 2.[35] As shown in Fig. 2, the ball-milled Si particle disintegrates during the lithiation process while the porous Si powder accommodates the volume changes during lithiation. Another observation of the same kind has been reported in the potential use of bulk silicon as a thermoelectric material.[36] Here also, bulk silicon has not found huge applications due to the difficulty in generating a temperature gap across it. As a semiconductor made up of covalent bonds, heat at one end is almost entirely transferred to the other end by lattice vibrations. Without a temperature gradient, it is difficult to generate a significant voltage in thermoelectrics. Again, nanostructuration of silicon has been studied as a way to resolve issues related to its potential use in thermoelectric energy generation.[36] Another case is the use of bulk silicon, which is widely used in photovoltaic applications. In spite of gaining commercial attention, a number of drawbacks are still persistent. Notable among these drawbacks is the high surface reflectivity of bulk silicon based solar cells.[37–39] A lot of progress has been made in this area, prompting a number of review papers[40–42] on the improved surface reflectance of silicon based solar cells with a nanostructured surface. All these reports point to the importance and role of silicon nano-structuration in energy related science. Most importantly, it reveals the potential of siliceous materials with desirable nanostructures and for that matter diatomaceous earth.

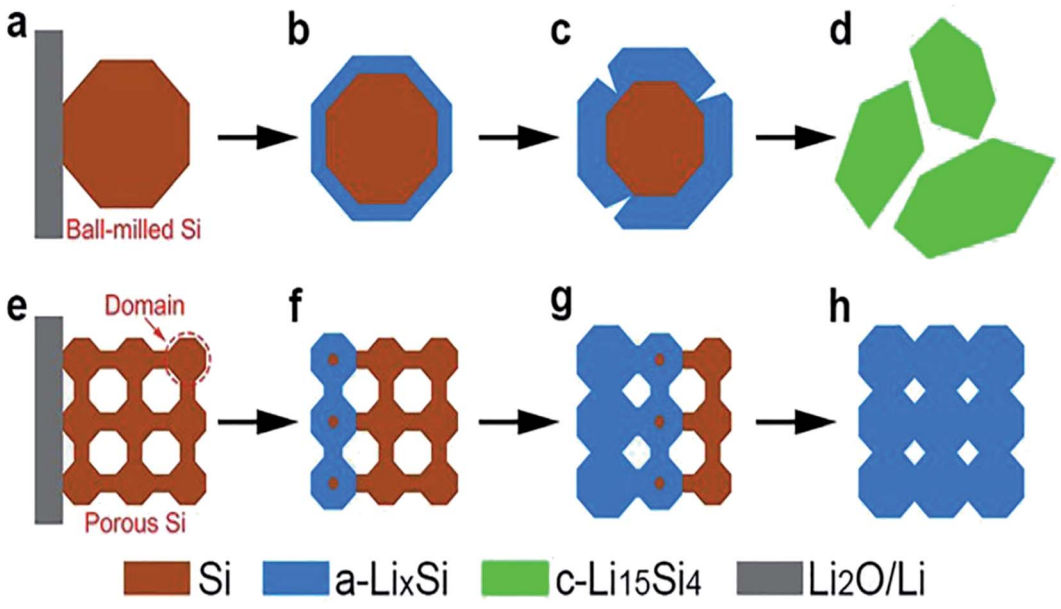

Fig. 2 Lithiation manners presented in ball-milled Si and porous Si nanoparticles. (a–d) Response pattern of ball-milled Si from the surface-to-center during lithiation. (e–h) Response pattern of porous Si particle from the surface-to-center during lithiation.[35]

The attention towards DE has produced a lot of interesting results[43–53] based on which a number of excellent reviews on the application of diatomite in energy harvesting and storage have been reported.[54–57] Nevertheless, these excellent reviews do not fully elaborate on the processing routes and their translation into desired properties. Thanks to a recent review by Ragni *et al.*[58] a detailed description of some of the processes used in synthesizing nanostructured materials from diatom microalgae was presented. As DE continues to gain more attention in energy applications, it is essential to provide a comprehensive report of the major synthesis used in DE related studies for energy application which is not fully addressed in the previous reviews. This review seeks to expand and cover all the major processing routes as far as diatomite in energy applications are concerned. Also, quite a lot of progress has been made in this area since the publication of these reviews[36,59–63] and for that matter we present a report of the current progress made with biosilica diatomite for potential energy application while focusing deeply on the main synthesis routes common to most of the reports. Considering the fast progress in this area, we also report on unexplored areas related to energy research.

2. Nano-scale morphology of diatomaceous earth

The structure of DE has been studied over the years using state-of-the-art scientific equipment including Scanning/Transmission Electron Microscopy (SEM and TEM),[64] Atomic

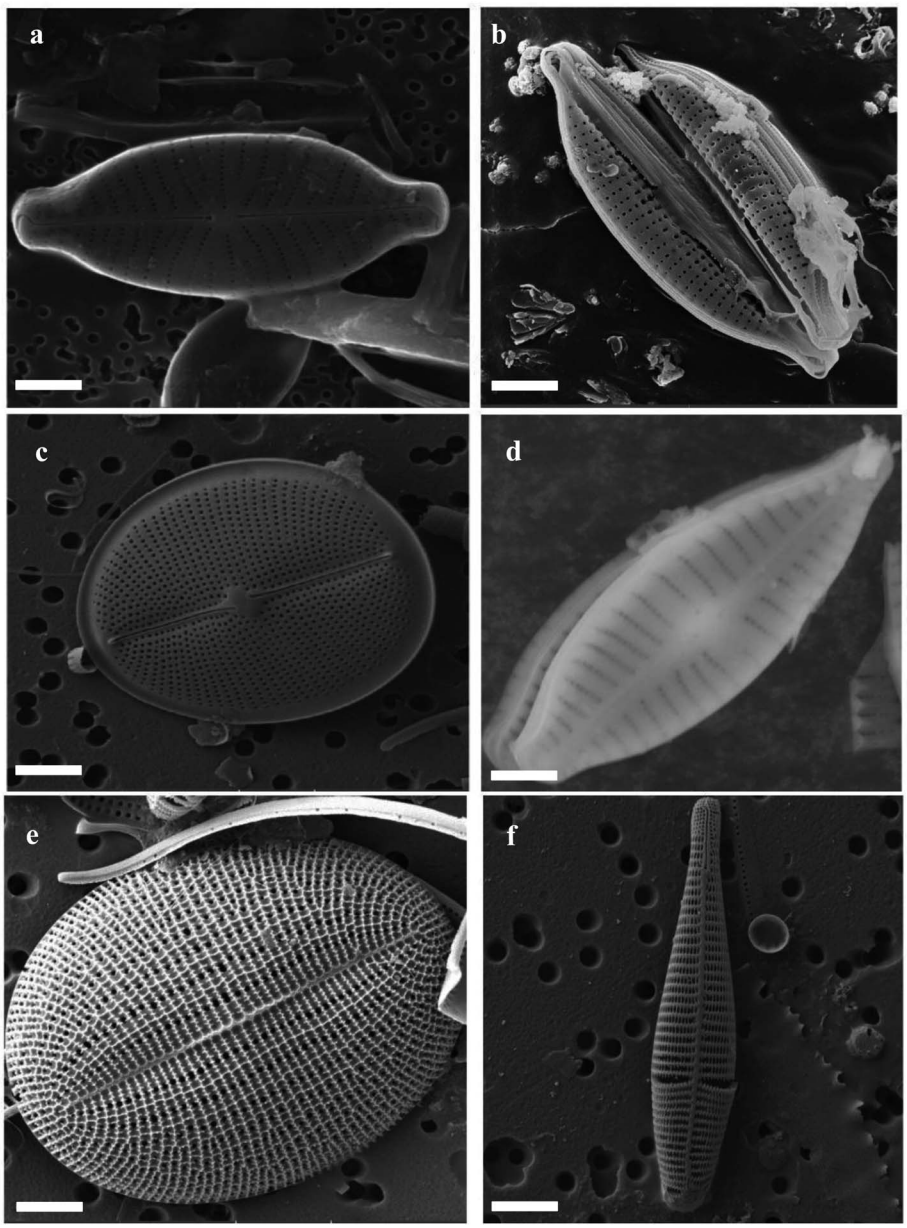

Fig. 3 Different shapes and structure of diatoms (a–f) SEM images of different marine diatoms (source: Lake Baikal, Arabian Sea, and Skolkovo Pool) scale bar: 5 μm.[70]

Force Microscopy (AFM),[65] X-ray Photoelectron Microscopy,[66] Fourier Transform Infrared Spectroscopy (FTIR)[67] and Small Angle X-ray Scattering (SAXS).[68] Individual diatom frustules within a diatomite powder are characterized by a silica cell wall consisting of two overlapping thecae (epitheca as the larger part and hypotheca, the smaller), each consisting of a valve. These valves are separated by an accompanying series of girdle bands.[55] Frustules are characterized by a row of pores known as interstriae. Between the interstriae are ribs, called striae. The interstriae are mainly responsible for the uptake of nutrients.[69] The frustules vary greatly, so there is no simple summary of the morphology. In Fig. 3, the SEM images of different diatoms collected from Lake Baikal, Arabian Sea and Skolkovo Pool clearly show diatoms with different shapes and structures.[70] However, frustules have been traditionally classified into two groups namely; centric diatoms (Centrales) and pennate diatoms (Pennales). The centric diatom frustules have surface features arranged around a point while the pennate frustules have major features at right angles to the striae. In a classification by round and Crawford diatoms have been classified into three groups.[69] They are the centric diatoms (Coscinodiscophyceae), pennate diatoms without a raphe (Fragilariophyceae), and pennate diatoms with a raphe (Bacillariophyceae).

3. Classification of the role of DE

Diatomite plays different roles in experimental research. These roles are classified under three main groups with regards to energy related studies. These groups have been created based on the state of diatomite in particular experimental works. The three groups, namely, synthesis involving the use of raw DE, the use of DE frustules as a sacrificial material (template), and DE as a precursor for silicon-based materials are shown in Fig. 4. The main motivation behind the use of DE is to preserve and translate the nanoscale morphology of diatomite into new functional materials, either as a precursor or template. This is quite different for some studies that require the use of raw diatomite as a supporting material to host the active material especially in thermal energy storage applications. All the groups have some reports using pre-treatments, mostly thermal and mechanical. The prospect of the entire diatom macrocosm in the energy industry is further showcased in an isolated report by Chen *et al.*[71] A rather unconventional approach with respect to most reported DE based materials for energy applications saw Chen *et al.*[71] exploring the optical properties of a chlorophyll extract from diatom algae for solar energy harvesting. Diatom algae are known to be one of the most photosynthetic organisms. It is reported to contribute about 40% of the aquatic primary production using chlorophyll a [chl-a] component.

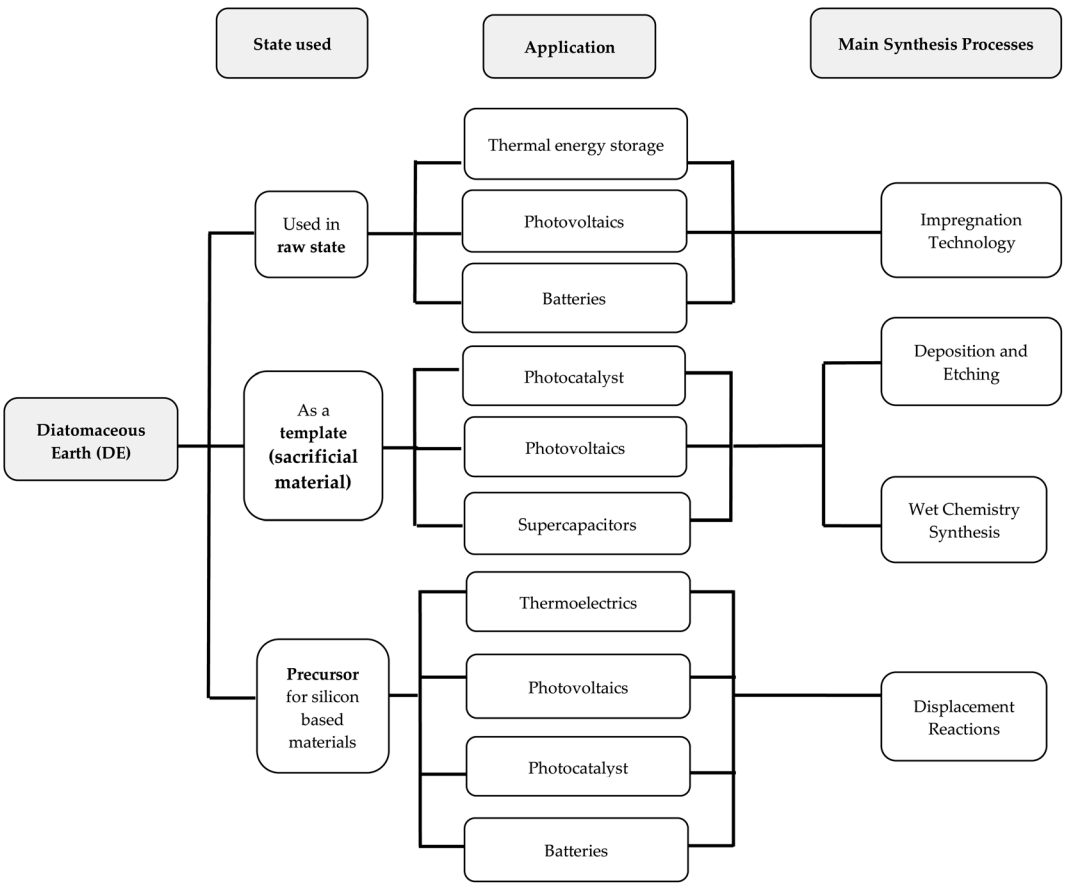

Fig. 4 Schematic representation of the relationship between the state of DE, intended applications and main synthesis.

Other important light absorption components found in diatoms are chlorophyll c [chl-c] and fucoxanthin. In their work, Chen *et al.*[71] studied the anti-reflective property of diatom extract obtained *via* a facile process where the diatom extract contained chlorophyll a as the primary active component for photon energy conversion suitable for blue to red photon conversion. As expected, the diatom extract reduced the surface reflectance of Si over the entire light spectrum (350–1100 nm) up to 13%. Apart from its anti-reflective (AR) properties, the extract showed strong photon down-conversion effect where the blue light portion of light is converted to red. Both properties were credited for the enhanced short circuit current and power conversion efficiency (PCE) of the Si solar cell. Most importantly Chen *et al.*[71] confirmed the thermal stability of the diatom extract up to 90 °C without changes in neither the optical properties nor the color.

3.1 Raw DE for energy applications

Energy applications involving the use of raw diatomaceous earth without further chemical synthesis, capable of dissolving it or transforming it to silicon-based materials, have been majorly associated with thermal energy storage (TES)[72–82] although recent isolated applications in Li-ion[63] and Li–sulphur[83] batteries and polymer solar cells[84] have been reported as presented in Fig. 4. Diatomaceous earth normally serves as a supporting material and no form of templating or chemical reduction is required. Rather, facile processes such as mixing and impregnation are normally used to form a composite with the active material. Even though DE is applied in its raw state, pre-heat treatments such as vacuum drying, microwave heating, and calcination are sometimes performed.[85–90] Thermal energy storage has long been seen as an eco-friendly approach to sustainable energy for future energy demands.[91] Using phase change materials (PCMs), latent heat can be effectively used to store thermal energy. Over the years of studies, modifications with PCMs have been reported to result in substantial increase in desired properties. Notable among these modifications is the use of diatomaceous earth. DE assumes the role of a supporting material in the modification of PCMs. It is known that the higher the mass ratio of the PCM in DE, the greater the latent heat of the composite PCM.[91,92] Thermal energy storage is realized through three routes namely, sensible heat, latent heat, thermochemical or a combination of these.[91] Among the possible thermal energy storage routes, latent heat storage is known to be the most attractive due to its ability to provide a higher energy storage density and to store heat at a constant temperature corresponding to the phase transition temperature of PCM. In latent heat storage, a storage material undergoes a phase change from solid to liquid or liquid to gas or *vice versa* upon the absorption or release of heat.[91] PCMs are available in three forms. They are organic, inorganic and eutectic PCMs.[91] Recently, raw diatomite was studied as a potential negative electrode for Li-ion batteries and a polysulfur absorbent for Li–S batteries. In another isolated study,[84] raw DE was used in a polymer solar cell to improve light trapping. In all these reports,[72–82] diatomite is used in its raw state without complex chemical reactions to dissolve, precipitate or reduce silica to silicon-based compounds and does not involve templating.

3.2 DE as sacrificial material for energy applications

Inspired by the neat nanostructured patterns in diatom frustules, newly engineered structured materials/composites have been produced with similar patterns using diatom frustules as templates.[93–105] Ever since Losic *et al.*[93] reported on the fabrication of nanostructured gold using diatom frustule as a template, a number of advances pertaining to the application of this fabrication route for new engineered materials have been reported[94–105] mostly for energy applications. Specifically, these materials have been found useful for photovoltaics,[95,97] supercapacitors[99–101] and photocatalysts[98] which is shown in Fig. 4. Apart from the dissolution process often executed at the end of the synthesis protocol to dissolve DE, there is mostly no chemical reaction involving DE prior to the dissolution process. The main synthesis processes used are deposition techniques and wet chemistry routes, however, some pre-treatments such as vacuum drying and calcination are sometimes applied as a means to free the pores of all impurities.

3.3 Precursor for silicon based materials for energy applications

Pure elemental silicon, silicon oxide and other silicon-based materials have found diverse applications in energy related applications to date.[106–109] Bulk silicon is widely known for its application in photovoltaics, existing as monocrystalline and polycrystalline silicon based solar cells.[106] With the advent of nanotechnology, nanostructured silicon-based materials have paved the way for novel applications in batteries and thermoelectrics.[22,36,109] The desire for facile and cost-effective ways of producing nanostructured silicon-based materials has led the attention of the scientific community towards diatomite, as a precursor for silicon-based materials. Diatomite happens to be the only siliceous material exhibiting a neatly formed nanoporous structure, at least to the best knowledge of the authors. It must be noted that, while the primary focus is as a silica precursor, DE eventually serves as a template for the silicon-based materials formed. There appears to be a narrow margin of difference between this category and the previous section (4.2). Here, the chemistry of DE is altered through chemical reduction reactions best known as displacement reactions, discussed in subsequent sections, but no such chemical reactions are reported for diatoms used as a template (4.2). Interestingly, some studies have combined both approaches and notable among them is a report by Le *et al.*[110] In their work, DE initially served as a precursor for nanostructured Si. The nanostructured Si possessing the framework of the precursor DE, subsequently played the role of a template for MnO_2, therefore obtaining a nanocomposite for supercapacitor applications. Potential energy applications involving the use of diatomite as a precursor for silicon-based materials are mostly batteries[44,49,59,60,111], photovoltaics,[112] supercapacitors[110] and thermoelectrics[36] as shown in Fig. 4. Widely reported materials

obtained from diatomite are mostly elemental Si, Si/SiO_2, Si/MgO, SiC, SiGe, and Mg_2Si.

4. Synthesis routes for energy applications

The most crucial aspect of synthesis involving diatomite is the ability to preserve the nanoscale structure and translate it into the new material. For that matter, all efforts to preserve the structure are vital in research. The processing routes used in diatomite related studies are numerous,[58] however, a number of these processing routes are peculiar to energy related reports. Herein, the major synthesis routes and their respective field of application are addressed. While these synthesis routes are reported as the primary process, the majority of these studies involved pre-treatments of DE, thermal or mechanically driven.

4.1 Pre-treatments of diatomaceous earth

DE pre-processing techniques have become popular when synthesizing DE-based energy materials. In most cases, these treatments were thermally or mechanically motivated. Thermal pre-treatment such as calcination,[36,44,45,51,52,59,73,74,113] drying[43,45,49,52,59,61,72] and microwave heating[87,88] have been widely used. Mechanical milling has also been reported.[49,63,113] Among the two, thermal pre-treatments have received more attention in energy related studies. Prior heat treatments are reported to cause changes in the powder characteristics of DE including the color, particle size, specific surface area, pore size and volume, crystalline state and crystallite size.[63,114] Diatomite is usually dried in vacuum between 80–100 °C prior to further synthesis. This is usually done to reduce the moisture content of the powder.[115] In some isolated cases, microwave heating was applied prior to further synthesis, and this affected the porous structure to some extent,[87,88] notably particle size increment and an unclogged pore structure. To the best of our knowledge, no further changes are reported for vacuum drying and microwave heating of diatomite unlike other prior heat treatments. As far as diatomite is concerned, calcination involves a controlled high temperature (500–1200 °C) treatment under controlled environment. Calcination of diatomite is mostly preceded by vacuum drying. Unlike low vacuum drying and microwave heating, calcination causes a wide range of changes in the powder characteristics including color changes,[114] phase composition,[36,114,116] crystallite size[114] and particle size.[114] Clearly, calcination has serious consequences on the powder characteristics of diatomite, yet the selection of the right precursor remains a concern for some intended applications. In most reports, either a raw (dried powder) DE is used or a calcined powder (dried and calcined), particularly reports in battery, supercapacitor, and thermoelectric applications.[36,44,49,50,99,117] Choosing the right DE precursor for such applications is quite a challenge as far as these reports are concerned since either raw or calcined DE powders have different consequences on the final properties. Thanks to some reports where both raw diatomite (only dried) and calcined diatomite (dried and calcined) are compared, we have some guidelines to help select the right DE precursor for specific applications. These reports, especially in filtration,[118] cement production,[119] thermal energy storage[73,89] and photocatalyst[120] carried out a comparative study of the performance of both calcined and uncalcined DE powders in a single work, providing some insight into the right candidate for these applications. This particular issue not given much attention was recently raised by Korsunsky *et al.*,[121] where the importance of choosing the right DE precursor (calcined or raw), specifically for silica to silicon-based materials synthesis was addressed. Raw diatomite is amorphous while the calcined counterpart is crystalline (cristobalite). Understanding their individual reaction kinetics may be crucial for selecting the right precursor as well as controllable synthesis parameters. Even though both calcined and raw DE powders have successfully been reduced to silicon-based materials, it is still unclear the ideal state of the DE precursor for silicon-based material conversion.

Mechanical pre-treatments of DE normally involve high energy ball milling. In some recent studies high energy ball milling was performed on DE prior to the main synthesis process.[63,122,123] Like some thermal pre-treatments, ball-milled DE normally shows significant changes in the particle size, pore size and specific surface area. Powder characteristics such as crystallinity, phase composition and color changes are not affected by ball milling. Although ball milling of DE has not received much attention like thermal processes, recent reports show it is a crucial step for some intended applications. A study by Blanco *et al.*[63] reported the effects of ball milling of DE on the electrochemical properties of the negative electrode produced. In that work, the ball milled DE powder showed an increase in specific surface area from 1.2 $m^2\ g^{-1}$ (pristine DE) to 17.3 $m^2\ g^{-1}$. Additionally, the mean particle size of the ball-milled DE powder was significantly lower (470 nm) than the pristine DE (17 μm). They also reported an increased presence of mesopores in the ball-milled powder compared to the pristine powder. Blanco *et al.*[63] indicated that although the mesopores could have been present in the pristine powder, they became accessible after ball milling. The powder characteristics reported for the ball-milled powder subsequently influenced the electrochemical performance of the DE-based negative electrode. As evidenced in Fig. 5,[63] the DE based negative electrode prepared from the milled powder showed a higher capacity of 750 mA h g^{-1} (milled) than the pristine powder (550 mA h g^{-1}). This was attributed to the shortening of the Li-ion diffusion path and the increased surface area of the powders achieved through particle size reduction. Ball milling offers a cheap and simple way to alter the powder characteristics of DE for intended applications, especially in silicon-based anode materials. The right combination of both mechanically and thermally motivated pre-treatments may lead to a range of functionalities for new materials.

4.2 Impregnation technology

The impregnation technology is a well-known manufacturing process which has been widely used in the synthesis of nano-catalyst, composite materials, foundry technology, energy

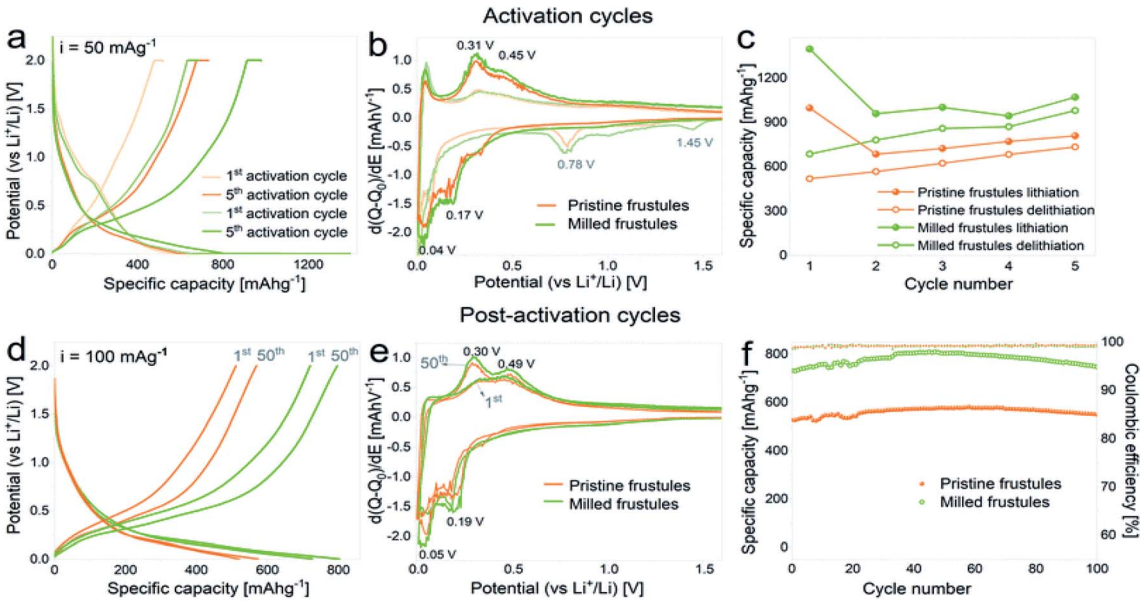

Fig. 5 The electrochemical performance of the milled and pristine DE-based negative electrodes: (a and d) voltage profile curves, (b and e) differential capacity plots, (c and f) specific capacity against cycle number for activation (a–c) and post-activation (d–f) curves (green points: milled DE) and (orange points: pristine DE).[63]

materials and eco-efficient construction.[124–129] In advanced composite manufacture, impregnation is used in making the starting material, prepreg, which comprises the resin and reinforcement. Recently, impregnation technology has become a useful process for the synthesis of nanocatalyst.[124] The impregnation technology has been utilized in the protection of wooden structures from destruction.[129] Herein, the combustibility of constructions made from wooden structures are reduced by the impregnation of fire-retardant solutions. In the impregnation technology, a solution (impregnant) is infused to fill the invisible pores in a material. The impregnation technology comes in two forms: dry/incipient-wetness technology and wet impregnation.[130,131] In dry/incipient-wetness technology, the volume of the impregnate matches exactly the pore volume of the support while in wet impregnation, an excess volume of impregnate is used.[130] The impregnation technology has widely been used in the production of nanocomposite phase change materials (nPCMs) based on diatomaceous earth for TES. The principle behind this synthesis is identical to the ones presented above. Diatomaceous earth, as a supporting material in this area, offers the ability to load sufficient PCM without leakage due to their attractive sorption ability.[43] Based on accounts provided in existing reports on DE-based materials prepared by impregnation technology, the wet impregnation method was mostly used. Impregnation technology is further categorized as direct or vacuum impregnation, both widely reported in recent studies.

4.2.1 Direct impregnation. Quite a number of reports on DE based nPCMs employed the impregnation technology without vacuum, well known as the direct impregnation technology.[73,75,86,89] This type of impregnation process appears to provide a simple and low-cost set-up for synthesis unlike the vacuum-assisted type. In the direct impregnation process, the PCM (impregnate) is mixed with the porous powder (supporting material) at a specific melting temperature of the PCM, without prior air suction. Konuklu *et al.*[75] showed the effectiveness of using the direct impregnation process to synthesize a DE based nPCM, with paraffin as the PCM. They reported a maximum paraffin absorption of 32%, obtained from a mixing ratio of 40 : 60 (paraffin : DE) as compared to other mixing ratios; 16% for 20 : 80 and 24% for 30 : 70. Their nPCM with the highest absorption showed very good thermal stability and successfully passed the leakage test performed at 95 °C. This test is carried out at high temperatures, especially in the vicinity of the PCMs melting point, as a quality check to confirm the active materials does not leak out. DE pre-treatments have received considerable attention in the preparation of nPCMs.[73,87–89] As far as the impregnation method is concerned, an improved sorption ability of DE can accommodate for more PCM.[91,92] Xu *et al.*[74] studied the potential application of calcined DE as a supporting material for a nPCM based on paraffin using a direct impregnation method. In their work, they recorded an optimum paraffin absorption of 47.44% obtained from a mixing ratio of 0.9 : 1.0 (paraffin : DE). As expected, the nPCM with the optimum absorption capacity showed superior TES properties compared to powders with different mixing ratios. In another study showing the effects of pre-treatments on the absorption capacity of DE, microwave heating was utilized.[91] Konuklu *et al.*,[88] prepared nPCMs fabricated *via* the direct impregnation method using microwave modified diatomite, using lauric acid (LA). In that study, the microwave modification of diatomite led to an increased absorption of the PCM on its surface and thus showed an increase in the TES capacity as compared to nPCM without microwave modification. They also reported an

Table 1 Studies on diatomite based nPCMs synthesized *via* the impregnation technology[a]

PCM	State of DE	Optimum quantity of impregnant	Type of impregnation	Reference
Polyethylene glycol	Raw	50 wt%	Vacuum impregnation	43
GHL and GHM	Raw	55 wt%	Vacuum impregnation	81
Binary forms of (*n*-octadecane, paraffin wax and liquid paraffin)	Raw and calcined	36 wt% and 39 wt%	Direct impregnation	73
Paraffin	Raw and calcined	47.37 wt% and 52.63 wt%	Direct impregnation	74
Fatty acids	Raw	40 wt%	Fusion adsorption/ direct impregnation	78
Hexadecane, octadecane, and paraffin	Raw	80 wt%	Vacuum impregnation	72
Lauric–stearic acid	Microwave modified	n/a	Vacuum impregnation	87
Lauric acid	Microwave modified	n/a	Direct impregnation	88
Methyl stearate	Dried at 120 °C for 24 hours	51.3 wt%	Direct impregnation	86
Capric acid	Raw diatomite	50 wt%	Direct impregnation	132
Palmitic acid	Dried at 120 °C for 8 hours	55 wt%	Direct impregnation	134
Stearic–palmitic acid	Dried at 105 °C for 1 hours	65.2 wt%	Vacuum impregnation	139
Capric–lauric acid	Raw	53.6 wt%	Vacuum impregnation	80

[a] GHL = galactitol hexa laurate; GHM = galactitol hexa myristate.

optimum microwave heating time of 1 minute, beyond which TES properties deteriorated. To better predict the right DE precursor for nPCMs, a number of studies focused on both calcined and uncalcined DE powders.[73,89] Sun *et al.*[73] prepared nPCMs made from both raw and calcined opal using a direct impregnation process. Here, nPCMs made from calcined opal showed optimum absorption of the binary paraffin blends than the raw opal sample. The highest absorption obtained were 39% and 36% for the calcined and raw powders respectively. The superior absorption (39%) of the calcined opal was attributed to the increase in pore size and increased specific surface area (61.56 to 84.79 $m^2\ g^{-1}$). The nPCM based on calcined opal showed greater latent heat than the one based on the raw opal. Other previous and recent reports that utilized the direct impregnation method in the preparation of DE based nPCMs are by Liu *et al.*[132,133] and Jia *et al.*,[134] which are presented in Table 1. It must be emphasized that in all these reports, the interaction between the PCMs and the diatomite was confirmed to be physical, without any chemical interaction from FTIR measurements. The direct impregnation method is a facile, cheap and eco-friendly route to commercially produce nPCMs based on DE. Regardless of these attractive attributes, some researchers use vacuum impregnation towards expecting considerable improvements in the TES capacity of prepared nPCMs. A study by Nomura *et al.*,[77] however, alleged that a trivial difference in the latent heat was obtained for both direct and vacuum impregnation making the direct impregnation method a cost-effective route to prepare DE based nPCMs. Diatomaceous earth undergoes no chemical transformation when subjected to an impregnation process, whether directly or using vacuum. Away from thermal energy storage, Li *et al.*[83] reported on the use of raw diatomite as a polysulfur absorbent for lithium–sulfur batteries. In their work, the sulfur–diatomite–acetylene black composite was prepared *via* the direct impregnation technology. The calculated adsorption capacity of diatomite was $6.14 \times 10^{-3}\ g\ g^{-1}$, proving to be a better absorbent compared to acetylene black ($5.31 \times 10^{-2}\ g\ g^{-1}$). Schematically shown in their work and presented in Fig. 6,[83] a diatomite-based sulfur electrode is seen to suppress the polysulfide diffusion significantly.

4.2.2 Vacuum impregnation. Although vacuum impregnation comes with a complex set-up and relatively high cost, this impregnation process has interesting applications.[135,136] The vacuum-assisted impregnation/vacuum impregnation could allow for shorter synthesis time coupled with void-free systems due to the absence of obstruction posed by impurities trapped within the pores. Herein, air is sucked out of the porous powder using a vacuum system prior to the loading process. Potentially, the entire porosity of the supporting DE material could be utilized to obtain optimum mass ratio of the PCMs for optimum TES capacity. In a report by Karaman *et al.*,[43] a PEG/diatomite composite PCM was prepared using vacuum impregnation.

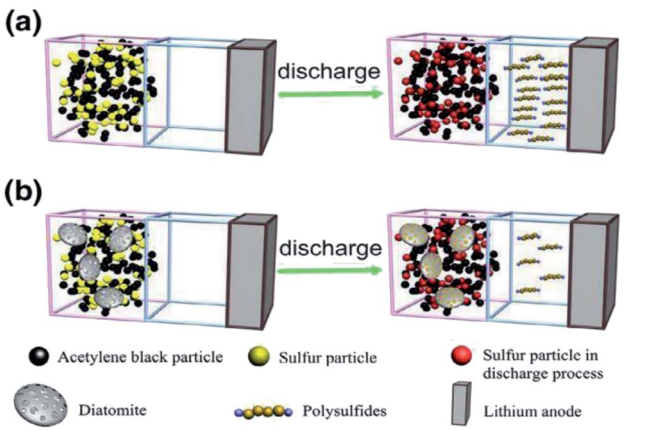

Fig. 6 Polysulfide suppression behaviour schematically illustrated for (a) sulfur electrode without DE (b) sulfur electrode with DE.[83]

Herein, they reported that air was initially evacuated from the pores on the surface of the diatomite sample followed by injection with the liquid PEG. In their work, they reported a complete dispersion of PEG into diatomite pores. This, they claim, provided mechanical stability to the composite, hence preventing seepage of melted PEG until a threshold of about 50% PEG in diatomite. Additionally, there was no chemical interaction between PEG and diatomite composite prepared using vacuum impregnation as confirmed by FTIR analysis. Physical forces including capillary and surface tension forces were observed between the functional groups of PEG and diatomite, preventing leakage and retaining PEG molecules within the diatomite pores. Sarı *et al.*[81] reported on the use of vacuum impregnation for the synthesis of galactitol hexa-myristate (GHM)/diatomite and galactitol hexa laurate (GHL)/diatomite nPCMs. In their work, they also reported that the porous structure of the supporting material provided good mechanical properties to the composite. The maximum mass percentage of GHM and GHL confined in diatomite were 52 and 51 wt% respectively. Sarı *et al.*[81] also attributed the leakage behavior of the PCM to the capillary and surface tension forces addressed earlier, made possible through vacuum impregnation. Like the nPCM reported by Karaman *et al.*,[43] Sarı *et al.*[81] also reported no chemical interaction between the components of their nPCMs. In both reports discussed above, raw (uncalcined) diatomite and the impregnation process involved the use of vacuum. Efforts to improve the sorption ability are crucial for enhanced TES application of DE based nPCMs. Growing attention given to pre-treatments especially microwave heating has received equal consideration prior to the vacuum impregnation process.[87] Microwave heating is known to provide a uniform and rapid heating compared to traditional heating methods.[137,138] Li *et al.*[87] recently reported an improvement in the loading capacity of diatomite after microwave-acid treatment compared to raw diatomite using the vacuum impregnation method. As reported, a certain amount of DE was mixed with 8% HCl solution and irradiated at 700 W for 5 minutes in a microwave oven. Subsequently, air was sucked from the pores using vacuum and loaded with LA–SA composition (lauric acid–stearic acid). Prior treatment of diatomite *via* the microwave-acid route led to the removal of impurities which blocked the pores, hence significantly improving loading capacity. Albeit clear evidence of the role conditions such as vacuum, in enhancing the absorption properties of DE, detailed information about the effects of all the processing parameters like vacuum level, time and temperature on the structure and absorption properties of DE remains lacking. A study by Qian *et al.*[139] investigated the effects of immersion time and temperature variations on the absorption capacity of DE. Their work illustrated in Fig. 7 showed that PEG absorption increased significantly within the first 60 minutes, but remained almost unaffected beyond 60 minutes. It was also demonstrated that an increase in temperature to 90 °C at immersion times (10 and 30 minutes) resulted in significant increase in PEG absorption. But after 60 minutes, they observed almost no further increase in PEG absorption with increasing temperature, thus proposing the optimal conditions as 60 minutes immersion time and maximum temperature of 90 °C. To fully appreciate the effects of vacuum on the immersion process, they repeated the protocol without vacuum and found that the nPCMs prepared *via* the vacuum impregnation process

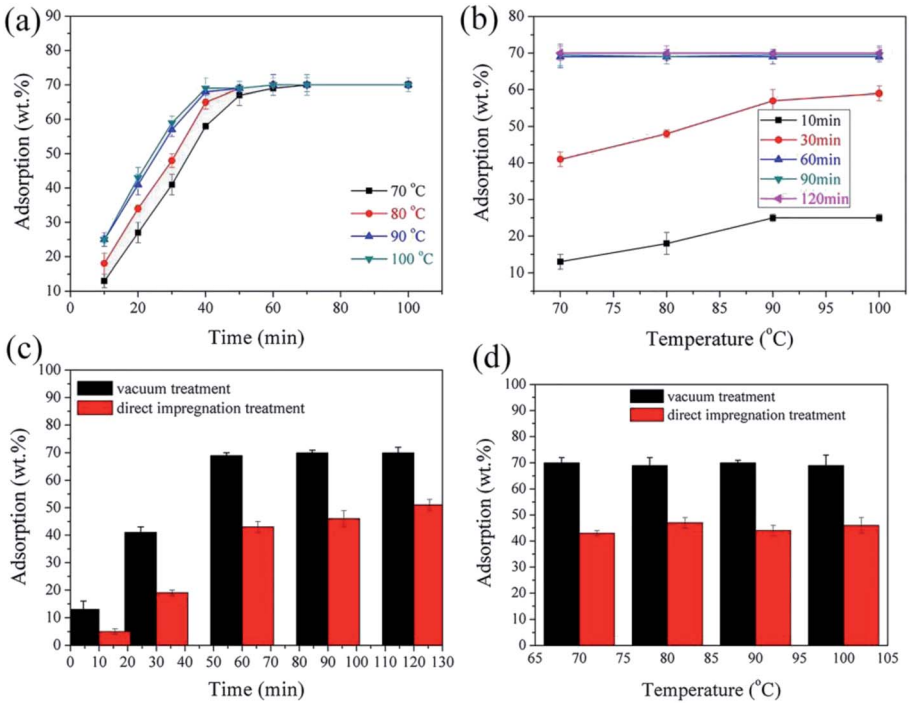

Fig. 7 (a and b) Adsorption capacity of diatomite as a function of temperature and time (c and d) adsorption capacity of diatomite in vacuum and direct impregnation.[139]

had a higher PEG ratio than the direct impregnation process. Another work by Zong *et al.*,[140] explored the effects of vacuum level, soaking time, and temperature on the content of their PCM (stearic acid) in DE. Like Qian *et al.*,[139] Zong *et al.*[140] reported a significant increase in the amount of PCM in DE with increasing temperatures until 80 °C, where it begins to reduce. Increasing temperature improved the viscosity of the PCM and made it easy for it to occupy the internal pores of DE. The downside however is that further increase in temperature promotes the volatilization of the PCM, subsequently leading to a dramatic drop in its content in the supporting material. Another important parameter, immersion time, proved to be very crucial for the impregnation technology. Similar to the report by Qian *et al.*,[139] Zong *et al.*[140] also observed a gradual increase in the absorption capacity with increasing time till a limiting time of 2 hours, beyond which no further changes were observed. The inconsistency between the reported peak times depends on a lot of other synthesis parameters such as, the PCM used, the state of the DE powder and the presence of vacuum or direct immersion. Regardless of these parameters, allowing enough time has the likelihood of yielding optimum PCM amount in the supporting material. Having identified the optimal time and temperature, Zong *et al.* further analyzed the effects of vacuum levels on the absorption capacity of DE in their nPCM using the pre-established conditions. They observed an increase in the absorption capacity when vacuum level increase from 0.01 to 0.03 MPa. Beyond 0.03 MPa, the absorption capacity remained unchanged. It is without doubt that DE, as a supporting material is ideal for TES, as such finding optimal parameters to synergistically improve the impregnation of PCMs is of the highest demand. It must however be noted that, these conditions may differ for different systems, considering the different characteristics of various PCMs. A number of recent studies reported successes in preparing DE based nPCMs using the vacuum impregnation method[72,80,141] as shown in Table 1.

4.3 Deposition and etching

As a highly porous 3D structure with unique properties, diatomite represents a promising carrier and template for synthesizing various composite materials for energy storage applications. However, diatomite's primary limitations are its high resistivity and low conductivity, making it not favorable for energy conversion and other applications. Therefore, in the last decade, significant research has been devoted to functionalizing and modifying diatom silica by different materials to obtain novel composite structures with more efficient optical and electrical properties using several strategies such as chemical vapor deposition, atomic layer deposition and some wet chemistry approaches. Deposition techniques enable the coating of diatomite with metal nanoparticles, semiconductors, carbon, polymers, and other materials while preserving the 3D micro- and nanostructure and porosity. In most cases,[101,102] where the focus is placed on the newly structured products, the active component of interest is deposited on diatomite and subsequent acid washing (etching) is done to get rid of the DE. Elsewhere,[105] acid washing (etching) is not utilized since they mostly focus on preparing DE based nanocomposites.

One material that is widely used for the decoration of diatomite is graphene. Despite the excellent physical, mechanical, optical and electronic properties of graphene and the achievements in advancing its use as a supercapacitor electrode and electrocatalyst, there is still a need to improve capacitive performance and electrocatalytic efficiency.[101] This improvement can be achieved through hybridization with, for example, porous diatomite and transition metal oxides such as manganese dioxides MnO_2, due to their non-toxicity, low fabrication cost, good catalytic activity, abundant availability and high specific capacitance.[142] A small-methane-flow chemical vapor deposition process was used by Chen *et al.*[102] for growth of hierarchical biomorphic graphene (HBG) on diatomite. A pre-cleaned diatomite powder was held under a mixed gas flow of H_2/Ar and methane to support the growth of the graphene layer whose thickness can be changed by varying the concentration of methane gas. Diatomite template was removed by immersing it in a hydrofluoric acid (HF) (molar ratio of HF : H_2O : EtOH (ethanol) is 6.7 : 27.8 : 5.1) at room temperature. Afterwards, the graphene powder was obtained by freeze-drying at – 90 °C and reduced pressure. This new approach utilizes diatomite as the growth template so that the derived HBG sample is highly crystallized, retains the porous structure of diatomite and contains fewer impurities. Flexible graphene films made by adding graphene powder to an ethanol/terpineol solution containing ethyl cellulose (EC) had much higher conductivity and good bending resistance compared to reduced graphene oxide and liquid-phase layered graphene, which opens the way for applications in flexible transparent electrodes, polymer composites, conductive inks, and printed electronics.

In a recent study by Le *et al.*,[101] natural diatomite was used as the bio-template for the chemical vapor deposition (CVD) growth of 3D graphene structure subsequently doped with nitrogen and deposited on MnO_2 nanosheets. The prepared bifunctional material can be used as a high-performance supercapacitor and oxygen reduction reaction catalyst. The CVD method consisted of several stages: placing diatomite into an Al_2O_3 boat and a CVD system, reducing the pressure, heating to 1050 °C, and annealing in an Ar gas flow at a pressure of 26.5 kPa. The growth of graphene started with the introduction of H_2 and CH_4 into the system. The next step was etching the diatomite template by mixing the resulting composite with a KOH solution in an autoclave at 80 °C for 16 h. After etching, 3D graphene was doped with nitrogen (3D N-G) using a hydrothermal reaction to improve the electrochemical properties of the obtained porous graphene structure. Finally, N-doped graphene was mixed with $KMnO_4$ and ultrasonically treated to obtain a MnO_2 decorated (3D N-G) labelled as N-doped 3D graphene@MnO_2. Four different N-doped 3D graphene@MnO_2 hybrid systems were obtained depending on how long the mixture was autoclaved (1, 3, 5, 7 h). SEM and TEM images illustrated that graphene retained the diatomite's porous structure and morphology after removing the template. Moreover, hierarchical channels and pores that penetrate through the graphene walls can facilitate contact between the electrode

and the electrolyte and improve ion/electron transfer so that redox reaction can occur at high current density without the loss of capacitance. Uniformly deposited MnO_2 nanosheets, the size and density of which are directly dependent on the reaction time, improved the electrochemical characteristics. N-doped graphene@MnO_2 has proven to be an effective electrocatalyst in the oxygen reduction (ORR) reaction due to the more active surface area and accelerated O_2 diffusion and electron transfer. The results obtained in this article clearly show that such hybrid structures are very promising for use in ORR catalysts and supercapacitor electrodes.

Another recently published study[105] found that manganese oxide deposited onto carbon nanotubes (CNTs)/graphene/diatomite substrate exhibits high specific capacitance, good rate capability, and excellent cyclic stability and therefore has great potential for energy storage applications. In this work, graphene was deposited on diatomite through the CVD process. At the same time, the carbon nanotube seeds were uniformly grown by bimetal seeds deposition and subsequent CVD on the surface of the prepared graphene/diatomite. In the final stage, MnO_2 nanosheets were attached to the surface of the CNTs/graphene structure *via* a one-pot hydrothermal method. The preparation process of the MnO_2@CNTs/G/diatomite composite is illustrated in Fig. 8.[105] An interconnected network of CNTs with a diameter of around 10–50 nm and 3D porous graphene facilitates the electron transfer rate and increases active surface area whereas uniformly encapsulated porous MnO_2 nanosheets provide the infiltration of electrolyte and decreased ion diffusion path. The authors also investigated the asymmetric supercapacitor (ACS) based on MnO_2@CNTs/G/diatomite and microwave exfoliated graphite oxide (a-MEGO) as positive and negative electrodes. The ACS capacitor revealed high energy density (64.4 W h kg^{-1} at a power density of 451.5 W kg^{-1}) and power density of 19.8 kW kg^{-1} (at an energy density of 6.7 W h kg^{-1}).

The studies mentioned above have shown that diatomite can be used as a template for the fabrication of three-dimensional newly structured/hybrid materials with improved photocatalytic and electrochemical performances through a deposition process often followed by etching of the template. Deposition techniques, although reliable come with a lot of complexities and high cost, raising a lot of concerns about potential commercialization. As mentioned earlier, depositing new materials on diatom silica can equally be achieved *via* facile wet chemistry routes which are discussed in the subsequent section.

Fig. 8 Illustration of the MnO2@CNTs/G/diatomite composite fabrication.[105]

4.4 Wet chemistry synthesis

For energy storage applications, the large surface area and highly porous network structure of diatomite provides the opportunity to maximize electrochemical reactions. Earlier sections have confirmed the prohibitively high synthesis cost and the 'ungreen' nature of some processing techniques as a major limitation to the commercialization of processes that offer alternate materials for energy storage applications. Wet chemistry synthesis shows high potential in enhancing the usability of diatomite for energy applications with the hydrothermal method receiving quite an attention in the past years. Hydrothermal synthesis is a process that produces single crystals that depend on the solubility of minerals in hot aqueous medium under high pressure.[143]

Jiang *et al.*[104] dissolved purified diatomite and other inorganic compounds in an aqueous solution under magnetic stirring and later utilized Teflon-lined stainless steel autoclave at a 180 °C for 24 hours to achieve the hot medium–high pressure step of the hydrothermal synthesis after which subsequent washing was carried out. Through this approach, the inner and outer surfaces of diatomite were successfully decorated with η-Fe_2O_3 to form 3D porous structure that enhanced the specific capacitance of η-Fe_2O_3 nanospheres/diatomite composites. Similarly, Jing *et al.*[144] used the hydrothermal synthesis to form a Ni–Co LDH@diatomite composite which exhibited capacitance retention of 94.2% after the 5000-cycle test at a current density of 2 A g^{-1}. Yang *et al.*,[100] employed diatomite as a template in the preparation of a MoS_2/amorphous carbon composite for supercapacitor applications. After the hydrothermal synthesis, the diatomite was removed by using a 40% HF solution for 12 hours. The retention of the diatomite structure after the HF soaking ensured a unique microstructure of the MoS_2/amorphous carbon composite which is shown in Fig. 9.[100] This led to improved electrochemical properties with 93.2% capacitance retention after 1000 cycles. Li *et al.*[145] used a two-step hydrothermal synthesis followed by an *in situ* polymerization route to form a D@FeOOH@PPy complex which showed enhanced electrochemical performance and potential for electrode material for energy storage.

Li *et al.*[103] studied the MnO_2 nanostructures replicated from diatoms using a simple hydrothermal process for applications in high-performance capacitors. Their study showed that MnO_2 diatom replicas exhibit high specific capacitance, good cyclability and rate capability, which depend on the diatoms' shape. Guo *et al.*[51] demonstrated a new and facile approach for the fabrication of supercapacitors based on hollow diatom silica structures coated with TiO_2 nanospheres and MnO_2 mesoporous nanosheets (diatomite@TiO_2@MnO_2). The fabrication

route of the complex composite included three steps: purification of diatomite to obtain hollow silica microshells, the deposition of the TiO_2 nanospheres layer by hydrolysis, and metathetic reaction using TiF_4 precursor, followed by deposition of the MnO_2 nanosheets using hydrothermal decomposition of $KMnO_4$. It was shown that the diatomite@TiO_2@MnO_2 electrode exhibits larger specific capacitance, better rate capability, lower resistance, as well as long cyclic stability, and a high coulombic efficiency in comparison with literature data on MnO_2 capacitors. This is because the deposition of TiO_2 on porous diatomite represents the appropriate highly aligned substrate with open-pore channels for improved electronic transport of MnO_2, thus increasing the specific surface area and enhancing the electrical conductivity of diatomite. At the same time, MnO_2 ensures a high surface for contact with ions in the electrolyte.

Diatom coated nanocomposite materials have been widely studied for potential applications as photocatalysts.[48,53,98,120,146–149] Among the many materials reported, diatomite coated with nanosized semiconducting TiO_2 particles has been extensively used as a photocatalyst. In the study by Jia *et al.*,[146] TiO_2 was deposited onto the diatomite by employing layer-by-layer (LbL) assembly method, which is based on the electrostatic interactions between oppositely charged surfaces. The pre-calcined diatomite was firstly immersed into a colloidal solution of TiO_2, followed by filtration and rinsing with distilled water and then the immersion of the derived product in phytic acid, which served as a molecular binder which was subsequently removed by thermal treatment at 400 °C. The obtained results demonstrated the uniform distribution of TiO_2 nanocrystals with a size of *ca.* 5–10 nm. The surface area and volume of mesopores increased with an increasing amount of the deposited TiO_2 which strongly depends on the number of deposition cycles. The TiO_2–diatomite hybrid structure prepared by the LbL method represents promising candidature of such a route for photocatalytic applications.

He *et al.*[147] used HCl-treated diatom cells as a template to obtain TiO_2-coated SiO_2 photocatalyst. In this study, titania-coated diatom frustules were prepared by immersing cleaned frustules in a vessel containing 5% titanium tetraisopropoxide (TTIP) in isopropanol for 24 h with subsequent calcination treatment at 773 K in air to remove residual organic parts. X-ray fluorescence (XRF) measurements confirmed the preservation of SiO_2 and carbon contained in diatom cells which was self-doped into this structure upon treatment with the calculated molar ratio of Ti, Si, and C 8 : 1 : 4. According to the FTIR spectra, diatom-templated TiO_2 consists of matrix-isolated TiO_2 layers on silica frustules' surface while TEM images revealed the fine hierarchical structure of such a composite, where the diameter of a titania nanoparticle was approximately 10 nm. Due to biomorphic hierarchical structures, TiO_2 coating, and carbon doping, a higher absorbance in the visible region and an improved photocatalytic efficiency was obtained for the photodegradation of rhodamine B under visible-light irradiation in comparison with the commercial Degussa P25 TiO_2.

Another approach for preparing TiO_2/diatomite composites for photocatalytic applications is demonstrated by Wang *et al.*[148] TiO_2 was immobilized on diatomite by adding dropwise tetrabutyl titanate (TBOT) as a precursor into the diatomite suspension under stirring. The subsequent addition of ethanol–water solution led to the hydrolysis of the TBOT at a moderate rate followed by stirring for 12 h, oven drying at 105 °C and calcination at 450–950 °C for two hours in the air. XRD results showed an increase in crystallite size and content of the rutile phase with the increase in calcination temperature. TiO_2 nanoparticles with an average size in the region of 15–30 nm were uniformly distributed on the diatomite surface. TiO_2/diatomite composites with a 90/10 mixing ratio of anatase/rutile phase, calcined at 750 °C for two hours, showed the best results of the photocatalytic degradation of Rhodamine B under UV-light. The photoactivity of the catalyst is mostly affected by calcination temperature but also depends on the crystalline size and anatase/rutile ratio.

The photocatalytic performance of TiO_2-functionalized diatom samples for indoor air purification was evaluated by Ouwehand and colleagues.[149] Acid-treated and calcined diatom frustules were added to the dissolved titanium(IV) oxysulfate–sulfuric acid hydrate, and the mixture was stirred and heated until all the liquid evaporated followed by calcination in air at 500, 550, 600, and 650 °C for 3 or 6 h using different precursor ratios. XRD analysis showed that the only crystalline phase present in the calcined samples is anatase with no rutile phase observed at calcination temperatures of 550–650 °C. It was also demonstrated that the silica substrate limited the nanoparticle growth and effectively thermally stabilized the TiO_2. The sample with 18.2 wt% titania loading, calcined at 550 °C for three hours showed 2.5 times higher catalytic activity in the decomposition of gaseous acetaldehyde in comparison with the P25 TiO_2 due to a smaller particle size of the active anatase phase and a stabilization of the titania particles on the silica surface. Titania-functionalized samples showed promising results in realistic conditions for the purification of indoor air as well.

The Cu_2O–ZnO/diatomite composite was also reported as a potential photocatalyst in the treatment of red water from TNT manufacturing.[150] The sulfuric acid-treated diatomite was added to the mixture of zinc chloride solution with different concentrations (0.05 M, 0.1 M, 0.2 M, and 0.3 M), 1 M sodium potassium tartrate, and 5% (w/v) polyvinyl pyrrolidone. Zinc oxide was deposited on the diatomite surface upon heating of this mixture to 95 °C. The next step was immobilization of cuprous oxide by adding 0.5 M copper sulfate and 1 M reductant glucose, stirring, and heating with subsequent drying of the precipitates. According to the results, the photocatalytic performance of such composites depends on the concentration of zinc oxide. The optimal optical properties and photocatalytic activity were achieved in the sample with the molar ratios of ZnO *versus* Cu_2O 4 : 2.5 since the degradation rate of red water was 72.8% after illumination by visible light for 4 h.

Fang *et al.*[151] investigated a highly efficient solar vapor generator obtained by the deposition of Ag nanoparticles on diatomite using a chemical plating process. Diatomite treated with a mixture of concentrated H_2SO_4, and H_2O_2 was added into a 2.3 wt% $SnCl_2$. After stirring and rinsing with distilled water, the sample was mixed with silver–ammonia solution and

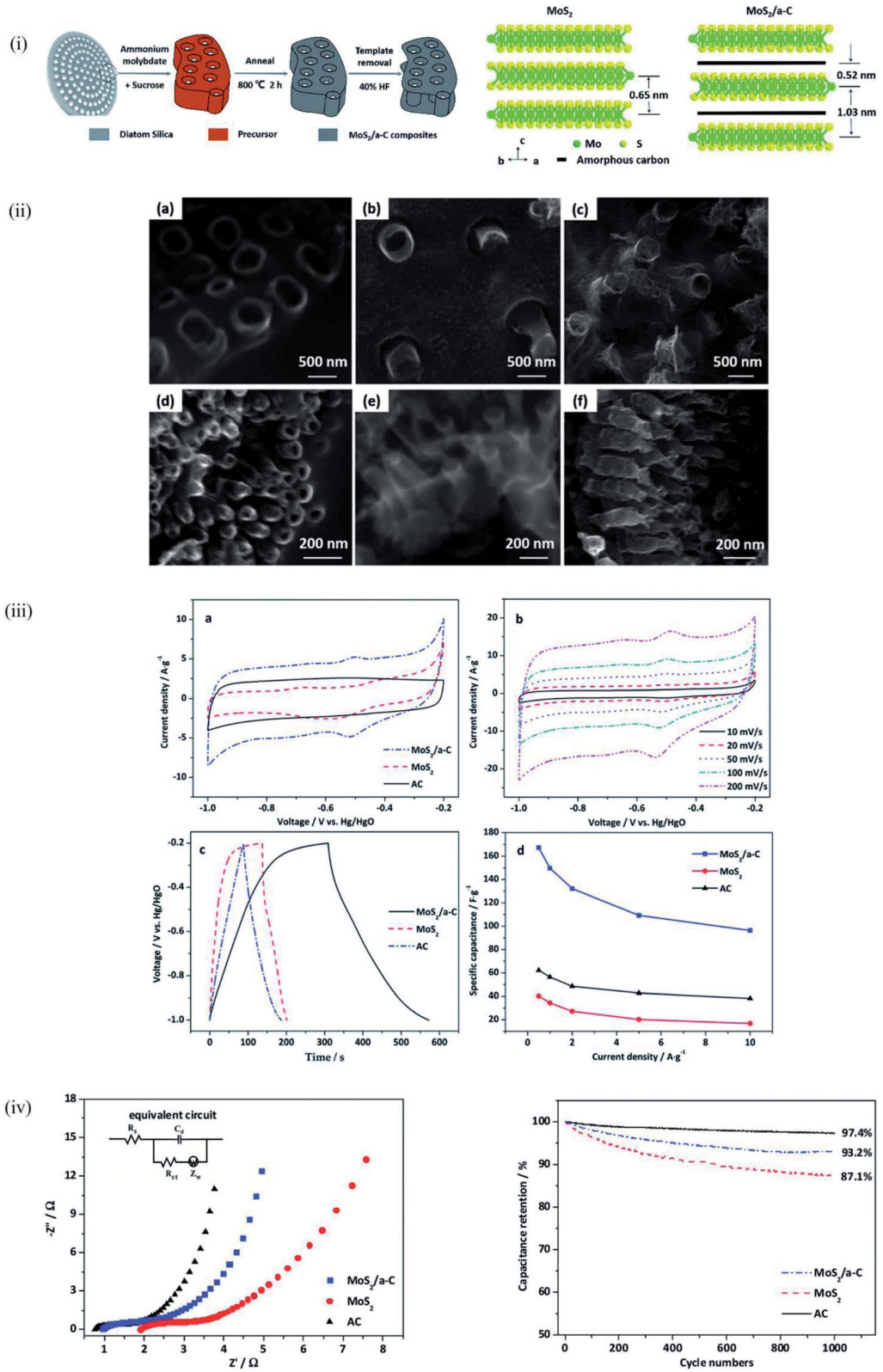

Fig. 9 MoS_2/a-C composite prepared using DE templating (i) schematic representation of the synthesis process (ii) schematic representation of the microstructure of MoS_2 and MoS_2/a-C composite (a and d) AC, (b and e) MoS_2, and (c and f) MoS_2/a-C composite (iii) and (iv) electrochemical performance of MoS_2/a-C, MoS_2, and AC.[100]

$C_4H_4O_6KNa \cdot 4H_2O$ to finish the chemical plating process. Ag/diatomite composite combined with a filter paper, an air-laid paper, and a polystyrene foam showed excellent vapor generation performance under one-sun illumination at room temperature due to the synergy of the localized surface plasmon resonance (LSPR) effect of Ag nanoparticles and the confinement effect in porous micrometer sized diatomite.

Wet chemistry syntheses are efficient ways to structure new materials and prepare hybrid products using diatomite as the base component. These wet chemistry processes end up depositing a material on diatomite just like the deposition method discussed earlier. These techniques have shown that the processes efficiently yield positive outcomes. Also, they are quite straightforward and environmentally friendly. Future works that may consider these techniques could focus on processing parameters such temperature and time on the overall properties. Note here that the DE samples used in these works were in purified form.

4.5 Displacement reactions

The quest to produce nanostructured materials has witnessed a number of new synthesis techniques.[152–156] Among the many interesting techniques, metallothermic reduction reaction (MRR), a type of displacement reaction has gained a lot of attention. A mini review by Xing *et al.* provides a historical view of the process and highlights current trends using this technique.[157] This displacement reaction type employs highly reactive metals to produce a wide range of products from stable compounds such as oxides, sulfides and halides.[158–161] Materials obtained from MRR are metals, alloys and composites.[157] Typical reactive elements used in MRR are lithium, sodium, magnesium, aluminum and intermetallics like Mg_2Si for the reduction of oxides and sulfides.[158–161] Aside MRR, a number of reduction methods are known to the scientific community. Most popular among them are the carbothermal process and the electrolytic process.[162,163] It is through one of these routes (carbothermal process) that the metallurgical grade of silicon is produced. This technique involves the use of a carbon source where reaction temperatures can go as high as 2200 °C.[164] Although useful for commercial production of high purity silicon, the carbothermal process is not highly regarded as the best approach to achieve silicon nanostructuration. This high temperature process poses a huge concern for silicon-based materials with nano-scale morphology. At high temperatures, particles may agglomerate and pores may disappear. For these reasons, MRR is highly touted as an appropriate route to reduce diatomite to nanostructured silicon-based materials for energy applications. In recent times, a number of different modifications to this technique have been reported, giving rise to a conventional and non-conventional MRR.

4.5.1 Conventional MRR. Ever since Sandhage *et al.*[165] reported on the use of Mg vapor to reduce diatom frustules to porous silicon, several groups have also reported on the synthesis of silicon nanostructures such as nanocrystals,[166] nanoporous films,[167] porous silicon[168] and 1D nanostructures[169,170] from the same metallothermic reduction reaction. Most of these publications have focused on magnesiothermic reduction reaction, often referred to as MRR. Apart from magnesiothermic reduction reaction, other potentially interesting processes are aluminothermic reduction reaction and silicothermic reduction reactions.[171–179] Metallothermic reduction reactions, based on the reductant, offer a rather lower synthesis temperature to producing new materials and high purity products. The criteria for selecting a particular processing route when it comes to diatomite are always influenced by the ability to preserve the morphology. This definitely makes MRR a better candidate over carbothermal reduction. Even though MRR is suitable, a number of factors are crucial for effective control of the morphology. In an excellent review by Entwistle *et al.*,[180] the parameters which affect the size and structure of the silicon-based material were addressed, although very little attention was given to pretreatments such as calcination and ball-milling. In their review, the following reaction conditions were reviewed;

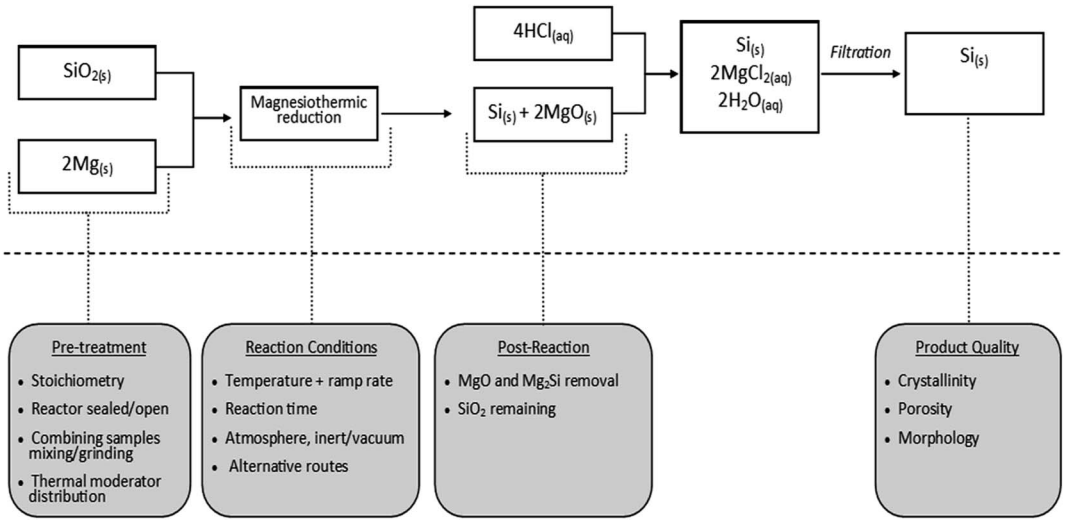

Fig. 10 Flowchart of the magnesiothermic reduction reaction and the key design parameters at specific stages.[180]

reaction temperature, reaction time, crystallite size, ramping rate, reaction ratio, powder mixing and heat scavengers. The summary of their study is presented in Fig. 10 (ref. 180) and shows the critical reaction conditions at various stages of the synthesis process. Lately, a new trend in MRR[181] used purposely for structural control has caught the attention of many.[182–185] Albeit MRR being suitable over the conventional carbothermal reduction process, structural control is not a guarantee. The amount of heat released in this highly exothermic reaction raises the temperature of the system to temperatures significantly higher than the actual experimental temperature. This poses another concern which was recently tackled through the use of inorganic salts. The pioneering work of Batchelor *et al.*[181] revealed the role of salt as a thermal moderator in the highly exothermic reduction reaction using magnesium vapor. Following this great lead, a number of works centered on diatomite made use of inorganic salts to complement the already favored MRR process.[36,112,182–185] In all these reports, the reductant used was magnesium. The ready availability, low cost, low toxicity and low melting temperature make magnesium the most preferred reductant among the lot. On the contrary, a recent study by Lai *et al.*[175] showed huge structural changes and damage to morphology with the use of Mg even though it proved to be an effective reducing agent below its melting point. Aluminum, however, was an effective reducing agent at its melting point or above and offered a better structural and morphological control as compared to Mg. The improved structural control was attributed to the presence of alumina, which enhances the mechanical properties of the product silicon. It was also reported that calcium was an ineffective reducing agent for silica. Due to this, Lai *et al.*[175] suggested a reducing mixture of 70% Mg and 30% Al which could offer the least amount of morphological damage and present a lower temperature than that required when using Mg or Al individually. This recommendation coupled with thermal moderators in the form of inorganic salts could help address the challenges faced with MRR. MRR is well-known in diatomite nanotechnology as a means to obtain pure elemental silicon or other silicon-based materials. Applications where MRR was selected as the synthesis route include both energy harvesting and storage technologies. These are battery anodes, thermoelectric generators, nano-Si coating on Si based solar cells and design of electrodes for supercapacitors. In a study by Shen *et al.*,[186] Si was synthesized from diatomite using the MRR route. A porous Si powder with pore size identical to that of the precursor diatomite powder was obtained after magnesiothermically reducing the precursor powder at 650 °C for 6 hours as shown in eqn (1). The centric diatom frustule described in their work as a sunflower was damaged after the MRR and subsequent HCl washing while the powder particle size decreased from 25 μm to 10 μm for both precursor diatomite and obtained porous silicon respectively. Also, an increase in the surface area of the diatom-based silicon (96 $m^2 g^{-1}$) and original DE with surface area of 6 $m^2 g^{-1}$, a requirement for most energy applications was reported. In addition to the native nanopores inherent to the precursor diatomite, mesopores were found in the porous silicon powder. This, they attributed to the formation of MgO and the subsequent washing with HCl varied significantly. Albeit the sunflower shape of the frustule not being preserved, the porous structure remained almost the same, suggesting MRR as an efficient approach to retain the porous structure of DE. To obtain pure silicon after the MRR, HCl is frequently used to dissolve MgO and further rinsing with deionized water. In quite a number of works,[36,112,182,183] HF was used following HCl washing to dissolve all unreacted silica as a way to obtain pure Si. In the work of Shen *et al.*[186] only HCl was reported, suggesting an eco-friendlier approach but also accounting for the traces of unreacted silica in the porous silicon powder as detected by Raman spectroscopy. However, in a later work,[187] the possibility to fully reduce diatomite to silicon was demonstrated. The protocol used was almost the same with the exception of an adequate powder mixing made possible through ball milling. The powders prior to the MRR process were ball milled at 350 rpm for 5 hours to decrease the particle size of diatomite and obtain a homogenous mixture. This additional step may have provided more reaction sites, promoting full reduction of diatomite to silicon. The high purity silicon obtained possessed a high specific surface area (131 $m^2 g^{-1}$) compared to the as-purchased diatomite (1 $m^2 g^{-1}$) due to the small particles size (less than 2 μm) and porous structure (10–70 nm). In a similar work by Wang *et al.*,[44] a porous silicon powder was obtained after magnesiothermically reducing a purified diatomite powder. This diatomite powder was purified prior to the MRR process. Apart from the purification process, the protocol was almost the same as reported by Shen *et al.*[186] Aside the retained mesopores and macropores retained from the diatomite powder in the product silicon powder, there was an increase in micropores after the MRR process. The use of an inorganic salt for scavenging excess heat produced from the MRR of diatomite was reported by Luo *et al.*[182] In their work, the use of NaCl resulted in a product silicon with cylindrical architectural features retained from the precursor diatomite. This particular trend has been reported in a number of studies,[36,112,183–185] suggesting an effective way to control the overall temperature in the MRR. This high purity silicon had a rough surface occupied with ultrafine Si particles ($\simeq$10 nm). In a more recent work by Zhang *et al.*,[60] a Si/SiO_2 composite was synthesized *via* MRR. Here, the effect of the reaction time during MRR on the phase composition of the reaction product was explored. Reduced reaction time is reported to lead to optimal ratio between the formed silicon and DE based silica. Most importantly, aside from the possibility to create a Si/SiO_2 composite, Zhang *et al.*[60] report that increasing reduction time had significant effects on the specific surface area of the diatomite-silicon sample (D-Si). The specific surface area increased from 78 (D-Si-2 h) to 14 8 $m^2 g^{-1}$ (D-Si-6 h) when the reaction time was increased from 2 to 6 hours which could be attributed to the removal of organic moieties and a subsequent creation of mesopores during the reduction reaction. On the other hand, a decline in the specific surface area was observed after further increase in reaction time to 10 hours. D-Si samples reduced for 10 hours had a specific surface area of 85 $m^2 g^{-1}$. This decline was attributed to an increase in the crystalline silicon domain and a possible collapse/widening of the pores

after a prolonged reduction. D-Si-6 h (diatomite-silicon-reaction time of 6 h) sample showed an optimal ratio of crystalline Si domains embedded within the amorphous SiO_2 matrix. All the D-Si samples synthesized in their work showed small ($\approx$10 nm) and large pores ($\approx$30 nm), signifying a hierarchical structure. The D-Si-6 anode showed almost the same morphology as the precursor diatomite which had the potential to enhance electrolyte diffusion inside the bulk electrode and as well limiting the volume changes in Si during charge/discharge cycles. Interestingly, as the Si domains provide lithium storage capacity, the amorphous SiO_2 matrix provides stability. This synthesis approach by Zhang *et al.*[60] offers greater control of the outcome of MRR, leading to the development of other potentially applicable anode composites. Not only has conventional MRR dominated the scientific headlines, it has also led to the introduction of other facile synthesis routes, also referred to as non-conventional MRR.

4.5.2 Non-conventional MRR. A number of non-conventional MRR have been reported.[188,189] In a study by Wu *et al.*,[188] SiO_x was produced *via* the magnesio-mechanochemical reduction reaction of diatomite. The partial reduction by magnesium was induced by high powder milling which led to a highly porous SiO_x powder after HCl purification. Wu *et al.*[188] demonstrated the possibility to use mechanical milling to promote MRR in the presence of magnesium termed as Magnesio-Mechanochemical Reduction process (MMR). Unlike the aforementioned displacement reactions which require somewhat high reaction temperatures (650–900 °C), this approach did not require an external heat source. As compared to the majority of the previously reported MRR routes, the MMR process reported by Wu *et al.*[188] offers the easiest, cheapest and simplest synthesis route to produce silicon-based anode materials from diatomite. The resulting diatomite-based anode (MMRD_Si indicating magnesio-milling reduced diatomite_Si) exhibited desirable powder characteristics for optimum batteries, markedly an enlarged Brunauer–Emmett–Teller (BET) surface area (from 25 $m^2\ g^{-1}$ for the DE to 134 $m^2\ g^{-1}$ for MMRD_Si) and a simultaneous increase in pore volume in the likewise manner (0.02 $cm^3\ g^{-1}$ to 0.10 $cm^3\ g^{-1}$). The MMRD_Si anode, identical to the SiO_2/Si network reported by Zhang[60] consisted of SiO_2 nanodomains with highly crystalline Si domains in the ratio 51.4%, 48.6% respectively. Such a system, otherwise known as SiO_x, has been identified as a better candidate than pure silicon. The highly desired silicon oxide (SiO_x) is best described as nano-sized clusters of SiO_2 and Si with suboxide-type interface[190] and reportedly show the smallest volume changes (160%) in comparison with SiO_2 and Si[191] upon lithiation. The derived MMRD_Si anode without C-coating, showed excellent cycling stability up to 2000 cycles with a capacity retention of 71.3% after cycling at 4 A g^{-1}. Wu *et al.*[188] attributed the exceptional electrochemical performance of the anode to factors including the presence of both nano-sized Si domains and retained SiO_2 at the nanoscale and the intrinsic porous structure, all of which contribute synergistically to the properties of MMRD_Si anode. Another type of a non-conventional reduction process was demonstrated by Liang *et al.*[189] Described as deep reduction and partial oxidation, this process relies on the use of excess Mg which favors the formation of otherwise unwanted by-product (Mg_2Si) as the main product as depicted in the reaction in eqn (2), with by-product MgO and unreacted Mg. The product Mg_2Si is further oxidized, yielding both Si and MgO is shown in eqn (3). This synthesis route ensures a full reduction of the starting silica powder and thus requires no HF purification to wash unreacted DE. This could potentially increase the silicon yield. Aside from the yield, a silicon product with nanostructure identical to the parent DE was formed. A major concern for this approach is the *in situ* oxidation of silicon produced from Mg_2Si. According to Liang *et al.*[189] *via* a controlled annealing temperature, no significant formation of SiO_2 was observed. Even though the oxidation rate of Si by O_2 at the partial oxidation process is slow, a thin layer of SiO_x was formed around the product silicon.

$$Mg + SiO_2 \rightarrow Si + MgO \quad (1)$$

$$4Mg + SiO_2 \rightarrow Mg_2Si + MgO + \text{unreacted Mg} \quad (2)$$

$$Mg_2Si + O_2 + Mg \rightarrow Si + MgO \quad (3)$$

Even though the conventional and non-conventional MRR appear somewhat less expensive to use and eco-friendly compared to other complex synthesis routes, they still have not reached a full scale commercialization due to issues such as yield and less control over outcome of synthesis. Diatomite has seen extensive research involving displacement reactions because it is the most suitable, cheapest and eco-friendliest precursor for silicon-based materials with nanoscale morphologies. Undoubtedly, displacement reactions lead to a wide range of possibilities and significant modifications in this area could potentially bridge the gap between current state of progress and commercialization. Tuning the parameters of MRR has also shown incredible results. Crucial among the list of tunable parameters are the reaction time and molar ratio as reported by Liang[189] and Zhang *et al.*[60] Further studies of these approaches could lead to a more controllable synthesis process.

Although synthesis processes delivered interesting DE-based materials that led to significant breakthroughs in their respective areas of application, a number of challenges remain that require further attention and improvement. The advantages and disadvantages of these synthesis processes are summarized in Table 2.

5. Energy storage applications

The potential application of diatomite in the energy industry covers a broad spectrum of energy storage systems. Here, a summary of previous and current progress made with the use of diatomite in energy storage systems are briefly discussed.

5.1 Thermal energy storage (TES)

Following the thorough review of processing techniques to preserve the highly porous and desirable structure of DE, this section provides up-to-date review of literature that incorporates DE as a supporting material for PCMs. In earlier sections,

Table 2 Merits and Demerits of the main synthesis processes

Main synthesis process	Merits	Demerits
Impregnation technology	1. Eco-friendly, low cost and facile synthesis 2. Purely physical interaction between precursors maintains a high purity PCM 3. Suitable for a wide range of PCMs	1. Requires unclogged and undamaged frustules 2. Extra vacuum system may be required to achieve maximum encapsulation
Deposition and etching	1. Less time required for large scale production 2. Uniform and homogeneous coatings of new material produced 3. High purity DE-templated materials produced after etching	1. Requires a complex set-up and expertise 2. Could require high synthesis temperatures 3. High cost of synthesis 4. Unbroken frustules needed
Wet chemistry synthesis	1. Fast and facile approach to immobilizing new materials on DE 2. No complex set-up required for synthesis 3. Relatively low synthesis temperatures	1. Unbroken frustules needed 2. Large scale synthesis may require more time 3. Relatively low quality coating compared to vapour deposition routes
Displacement reactions	1. Relatively lower synthesis temperature as compared to carbothermal reduction of SiO_2 2. A wide range of products and composites possible; Si, Si/SiO_2, Mg_2Si, Si/Mg_2Si and MgO when Mg is the reductant 3. Reductant such as Mg and Al are cheap and readily available	1. Highly exothermic reaction could raise the local temperature beyond the set temperature and offer less control over reaction outcome 2. Contamination of product such as Si due to difficulty etching or rinsing by-products (mostly Mg_2Si and MgO) 3. Low structural control

latent heat storage derived through PCMs was determined to be highly efficient amongst the categories of TES where the effectiveness of such TES with PCM has been attributed to the large storage density and narrow temperature variation during the charge–discharge process. Thus, PCMs play a critical role in thermal energy storage capacity where earlier works have classified PCMs as organic or inorganic.[192] Albeit PCMs being effective instruments for thermal energy storage, the works of Sarier *et al.*[192] and Zhang *et al.*[193] have shown leakage during solid–liquid phase changes as a major hindrance that limits the applications of PCMs. To overcome this, several approaches have been used to generate composite PCMs. Not too long ago, Jeong *et al.*[194] proposed the incorporation of porous diatom silica as an alternate approach to realizing light-weight and economical PCMs for thermal energy storage.

Following this proposal, Xu and Li[89,195] prepared paraffin/diatom; paraffin/diatom/MWCNT and Li *et al.*[76] prepared diatom/paraffin composite PCMs which showed enhanced performance. In the case of the paraffin/diatom/MWCNT PCM, a melting temperature of about 27.12 °C and a latent heat of 89.4 J g^{-1} were realized. Through a vacuum impregnation route, Jeong *et al.*[72,194] successfully formed PCM/diatom composites and obtained a latent heat storage of 61.96 J g^{-1} at 54.2 °C. Sun *et al.*[73] obtained a latent heat storage of 89.54 J g^{-1} at a transition temperature of 33.04 °C for a paraffin/diatom composite PCM. Xu and co-workers also successfully produced paraffin/diatomite composite PCM which had a melting temperature of 41.11 °C and latent heat storage of 70.51 J g^{-1}.[74] Li *et al.*[76] formed a form-stable diatomite/paraffin PCM for energy storage using different grades of diatomite particles. So far, the few studies that have considered composite PCMs based on paraffin/diatom have shown great potential. Recently, Zhang *et al.*,[90] used an oleophobic surface modification on diatomite in a paraffin/diatomite composite PCM and reported an enhancement in the latent storage capacity as well as the melting temperature (Table 3). They reported an encapsulation ratio of 84.5% for the paraffin/diatomite composite, suggesting a high efficiency in the impregnation of paraffin into diatomite. However, a noted trend for all the studies undertaken suggests that high phase change temperature/melting temperature results in lower latent heat storage capacity. Furthermore, paraffin has proven to be a major component for PCMs based on paraffin/diatoms but the arduous processes involved in their preparation continues to remain a concern especially when such methods are only applicable at the laboratory scale. In an attempt to overcome the challenge of laboratory scale production, Konuklu *et al.*[75] proposed a direct impregnation method that required no pre-treatment of diatoms and capable of being fabricated on a large scale. Their work showed that for the preparation of PCM nanocomposites based on diatom/paraffin, the direct impregnation method yielded positive results without any chemical reaction between the diatomite and paraffin. It was also shown that the PCM filled the pores of frustules with phase changes occurring within the nanopores. Further studies could concentrate on finding a blend of high storage capacity at high temperatures and also explore the potential of other processing routes.

In other works, the potential of other forms of diatomite based PCM composites have been explored. Nomura *et al.*[77] used erythritol/diatomite and obtained a latent heat of up to 70% of the theoretical value. Li *et al.*[78,79] fabricated shape-stable fatty acid/diatomite composite PCMs for thermal energy storage. The study revealed that the latent heat of capric–lauric acid/diatomite PCM decreased by 57% relative to the latent heat

Table 3 Thermal properties of reported PCMs based on diatomite and other material constituents[a]

PCM	Melting temperature (°C)	Latent heat storage (J g^{-1})	Reference
n-Hexadecane/diatomite	23.68	120.1	192
n-Octadecane/diatomite	31.29	116.8	192
Paraffin wax/diatomite	54.24	61.96	192
Hexadecane/diatomite/*x*GnP	22.09	120.8	72
Octadecane/diatomite/*x*GnP	30.2	126.1	72
Paraffin wax/diatomite/*x*GnP	54.87	63.77	72
Paraffin/diatom/MWCNT	27.12	89.4	89
Paraffin/calcined diatomite	33.04	89.54	73
Paraffin/diatomite	36.55	53.1	75
Paraffin/diatomite	45.70	114.21	90
(Liquid paraffin + *n*-octadecane)/Opal	24.91	59.04	82
Paraffin/diatomite particle	41.11	70.51	74
Polyethylene glycol/diatomite	27.7	87.09	43
LA-SA/Dm/EG	31.17	117.3	87
Methyl stearate/diatomite	36.5	111.8	86
Capric acid/diatomite	34.9	89.2	132
Palmitic acid/diatomite	63	88	134
(SA + PA)/diatomite	52.93	106.7	139
CA-LA/diatomite	23.61	87.33	80
CA/diatomite/CNT	31.38	79.09	133

[a] LA = lauric acid; SA = stearic acid; PA = palmitic acid, CA = capric acid; EG = expanded graphite; CNT = carbon nanotube; GnP = graphene nanoparticle; MWCNT = multi wall carbon nanotube, Dm = microwave-acid treated diatomite.

of capric–lauric acid while a slight increase in phase transition temperature was recorded. The drop in latent heat was attributed to the reduction in percentage of capric–lauric acid. Sarı and Biçer[81] studied the potential of fatty acid ester/building material as potential form-stable PCMs. By infusing galactitol hexa myristate (GHM) and galactitol hexa laurate (GHL) esters into porous networks of diatomite, perlite and vermiculite, they were able to optimize the thermal durability above the working temperature range of the monolithic materials. Karaman *et al.*[43] used polyethylene glycol (PEG)/diatomite to make PCMs. They obtained a latent heat storage of 87.09 J g^{-1} at a melting temperature of 27.7 °C. Qian *et al.*[139] prepared PEG/diatomite composites *via* vacuum impregnation and obtained the highest impregnation of PEG into diatomite. For a diatomite pre-treatment using NaOH leaching, a 70 wt% impregnation was recorded while for nano-silica decorated pre-treatment an impregnation ratio of 66 wt% was obtained. Subsequently, latent heat storage and melting temperatures were 127.0 J g^{-1} at 58.75 °C and 120.2 J g^{-1} at 57.96 °C respectively.

Through microwave-acid treatment of diatomite and the introduction of expanded graphite, Li *et al.*[87] simultaneously enhanced the volume of lauric acid–stearic acid (LA–SA) content impregnated into diatomite matrix and the thermal conductivity of the composite PCM. Comparing the LA-SA/Dm/EG to LA-SA/Dm and LA-SA/D, a 54% and 98.6% increase in the latent heat storage was respectively recorded. Here, Dm denotes microwave-acid treated diatomite while D denotes raw diatomite. Konuklu *et al.*[88] also reported improvement in storage capacity after modifying diatomite by subjecting the diatomite to microwave radiations in a home-style microwave at 700 W. A recent work by Huang *et al.*[196] which used an artificial culture method to generate PEG/diatomite composites exhibited high latent heat values. For the melting and crystallization processes, 121.54 J g^{-1} and 127.20 J g^{-1} were respectively obtained for the latent storage of PEG/sintered-diatom composite with an improved enthalpy efficiency of about 98.1%. The enhancement in latent storage was attributed to the high absorption and improved phase interface.

Table 3 summarizes reported properties of PCMs based on paraffin and other materials. As evident from the work of,[72,194] it is observed that the incorporation of nanoparticles into already existing composite PCMs results in no significant property enhancement while PCMs containing higher constituent volume result in pronounced decline in the melting temperature. Thus, to ensure effective diatomite based PCMs, the composite constituents, method of production and volume fractions are key parameters to be considered. It is seen from these reports that the PCM composites with fatty acids compared to paraffin based PCMs possess high latent storage density but the rather high melting temperature limits their applications in buildings. Thus, for full potential of fatty acid based PCMs, future works must concentrate on lowering the melting temperature hence sustaining the high latent storage ability.

The 3-D network structure offered by DE has proven to be an effective template/building block for the optimization of thermal energy storage capacity. However, with the increasing demand for high performing energy materials, it can be inferred from the presented literature that the full potential of the DE is yet to be realized. Thus, to reap the full benefits, future works need to focus on process optimization, powder/particle size effect as well as further stabilization of properties.

5.2 Supercapacitors

Considered as the next-generation energy saving technology, supercapacitors have been widely studied.[45,50,51,99–101,103] Supercapacitors offer a high energy density, a sustainable cycling life, excellent cycling stability and fast charging/discharging rates. Transition metal oxides (TMO), studied in recent times due to their superior specific capacitance over counterpart carbonaceous materials and conducting polymers have a number of setbacks stalling their commercialization. Typical among these setbacks are low electronic conductivity, low ionic diffusion constant, and structural susceptibility.[197,198] Among the many transition metal oxides studied (CuO, TiO_2, MnO_2, RuO_2, NiO, NiCo, Fe_2O_3, FeOOH, MoO_3, V_2O_5, MoS_2 and Co_3O_4),[100,144,199–202] MnO_2 is reported to be the most promising due to their low fabrication cost, high specific capacitance (theoretical capacity is 1370 F g^{-1}), abundant availability, environmental compatibility, and a high cyclic stability in alkaline/neutral media.[203,204] Highly porous templates have been identified as a solution to these setbacks,[57,205] most especially DE, due to the recent attention it has received. The first attempt to create diatom frustule inspired MnO_2 was made by Zhang *et al.*[45] Apart from MnO_2, diatom frustule templated NiO have also been studied due to their chemical/thermal stability, high specific capacitance, lower cost, eco-friendly nature and ready availability.[206,207] Despite these competitive properties, the full implementation of NiO as a material for supercapacitors is stalled by their low ionic diffusion constant and structural instability.[208,209] In a comprehensive review by Sun *et al.*[57] and a chapter by Zhang *et al.*[205] earlier reports of modifications of MnO_2 and NiO have been discussed in full details. In recent times, a lot of progress has been made with templating new materials especially TMO. Yang *et al.*,[100] for the first time applied diatom frustule templating to synthesize a porous MoS_2/a-C (amorphous carbon) composite. The MoS_2/a-C composite showed high specific capacitance (167.3 F g^{-1} at 0.5 A g^{-1}), high-rate capability (96.4 F g^{-1} at 10 A g^{-1}) and excellent cycling stability (93.2% retention after 1000 cycles) as shown in Fig. 9.[100] These great results were partially due to the well-defined microstructure inspired by the diatomite frustules, with the amorphous carbon playing an equally important role. It is reported that a combination of pores of different sizes for ion-buffering reservoirs causes an increase in the diffusion rate of ions within the porous electrode material. Undoubtedly, the high surface area of diatomite also inspired a specific surface area and nanoscale size of MoS_2. This eventually leads to a substantial decrease in the diffusion lengths for ions and electrons which ultimately improves the capacitive performance. A cost effective and facile one-step hydrothermal process of synthesizing 3D porous structures of NiCo layered double hydroxide (NiCo LDH@DE) was reported by Jing *et al.*[144] Common to most of the reports is the ability of DE to provide a nanoscale morphology suitable for the prevention of agglomerates and reduced volume changes during cycling. Apart from diatomite proving crucial in the overall performance of NiCo LDH@DE, the molar ratio is reported to have a huge impact on the structure of NiCo LDH on diatomite. Jing *et al.*[144] reported that based on the molar ratio used, the morphology of the NiCo LDH could change from nanowires to nanosheets, thus eventually improving the electrochemical performance due to an enlarged surface area. The nanosheet morphology was obtained by increasing the Ni^{2+} concentration, since higher concentrations of Co favors the formation of nanowires. The porous Ni_3Co_1 LDH@DE reportedly showed ultrahigh specific capacitance of 514 F g^{-1} and an excellent capacitance retention (94.2%) after 5000 cycling tests. The combined effect of the porous structure and the nanosheets were credited for the impressive electrochemical properties of NiCo LDH@DE. Another interesting work involving the use of diatomite was reported by Jiang *et al.*[104] Their as-synthesized η-Fe_2O_3/diatomite composite showed good capacitance retention of 73.92% after 1000 cycles. Their composite also showed good cycling stability coupled with a high reversibility during a repetitive charge–discharge cycling. These properties were attributed to the unique morphology of the composite characterized by a high surface area and a high porosity.[104] The as-formed η-Fe_2O_3 decorated both the outer and inner surface of diatomite and this could have potentially led to more active sites to enhance electrochemical reaction. In a more recent work focusing on MnO_2, Le *et al.*[101] demonstrated the use of diatomite as a bio-template for the production of three-dimensional (3D) porous graphene for both supercapacitors and oxygen reduction reaction catalysts. After further doping and deposition of the porous graphene with nitrogen and MnO_2 nanosheets respectively, a hybrid N-doped 3D graphene@MnO_2 (N-G@MnO_2) was obtained. The porous N-G@MnO_2 showed a high specific capacitance (411.5 F g^{-1}) coupled with a good cycling performance (88.3%) after 4000 charge and discharge cycles. The excellent results were partly due to the N-doped graphene, MnO_2 nanosheets and the porous structure triggered by diatomite. Indeed, the porous structure was reported to provide a good contact between the electrode and the electrolyte, resulting in an improved ion transfer and decrease in the contact resistance. Additionally, the porous structure of the N-doped graphene ensured a uniform distribution of the MnO_2 nanosheets on the surface. This prohibits aggregation during charging/discharging reactions. Hu *et al.*[105] recently reported the progress made using diatomite template to create a MnO_2@CNTs/G/diatomite hybrid. Their hybrid exhibited a high specific capacitance (264.0 F g^{-1}) and excellent cyclic stability partly due to the enlarged surface area of the 3D framework provided by DE for the optimum loading of MnO_2 without compromising the electrolyte infiltration and diffusion and thus having no adverse effects on electron and ion transfer. Also, DE primarily provided a platform to form 3D porous graphene. This porous graphene inspired by diatomite allowed for the immobilization of the metallic seeds used for the decomposition and *in situ* growth of the vertically aligned CNT. This eventually resulted in a conductive network which was reported to enhance electron transfer and increase active surface area. Li *et al.*[145] demonstrated the effectiveness of diatomite templating in the supercapacitive properties of diatomite@FeOOH/conductive polypyrrole (D@FeOOH/PPy). In their work, a double shell FeOOH/PPy on DE was synthesized *via* two-step hydrothermal method and *in situ* polymerization routes.

Although the improved electrochemical properties of D@FeOOH/PPy compared with D@FeOOH were hugely attributed to PPy nanoparticles, the use of diatomite played a crucial role for the latter to excel. Already stated from previous reports,[100,101,104,105,144] DE primarily provided a highly porous structure which sufficiently exposed the PPy nanoparticles. This led to shortened ionic transport path and diffusion time, thus accelerating the electrolyte ion transport during charging/discharging cycles. The as-synthesized D@FeOOH/PPy electrode showed a high specific capacitance (417.8 F g^{-1}) and a good capacitance retention (80.6%). The inclusion of DE in the electrode materials for supercapacitors have demonstrated huge potentials to improve the efficiency of already existing electrode material and most importantly allow for a cost effective and eco-friendly way to optimize electrode materials. To fully realize this, facile synthesis processes, with the ability to synthesis in large yields need to be developed.

5.3 Battery technology

Battery materials, especially anodic components have attracted the most attention involving the incorporation of diatomite in their synthesis. Over the past few years, a number of researchers working with silicon-based anode materials have included this silica type in their synthesis protocols.[49,59,60,62,63,111] The choice of this siliceous component is justified by earlier recommendations to produce silicon-based anodes with nanoscale morphologies capable of remedying setbacks with their bulk counterparts.[22,210] As the only naturally occurring siliceous material with attractive nanoscale morphology, DE presents a pathway to obtain nanostructured silicon based anodic materials or templates for other potential ones. Such anode types are highly preferred over carbon-based materials, transition metal oxides and other alloys due to a combination of superior electrochemical properties, cost and environmental factors.[211] These interesting characteristics have not translated into rapid commercialization due to the large volume changes (up to about 300%) during charging/discharging cycles observed for silicon-based anodes from bulk silicon.[22,27] Such volume changes cause strain-induced crumbling and eventually lead to discontinuities rendering the anode ineffective in carrying charges to current collectors. Ever since this setback was identified, several silicon nanostructures have been reported including silicon nanosheets,[212] nanowires,[22] nanospheres[213] and nanotubes[214] which have birthed several comprehensive reviews.[215–217] Recently, a large number of groups have focused on DE, as it provides a ready nanoscale morphology for the synthesis of nanostructured silicon-based materials. The increasing number of reports in this area has in the recent past prompted excellent reviews by Sun *et al.*[57] and Jeffryes *et al.*[55] In both reviews, a detailed report of previous successes obtained for mostly silicon and titanium-based anode materials *via* diatomite addition is given. Since these reviews, some progress has been recorded in DE-based anode materials for battery applications. Recently, a diatomite-derived hierarchical porous crystalline and amorphous Si-based network for battery anodes was magnesiothermically produced by Zhang *et al.*[60]

By adjusting the MRR time (2–10 h, with interval of 2 hours), Si/SiO_2 composites of varying characteristics were produced with 10–30 nm crystalline Si domains distributed within an amorphous SiO_2 matrix. A Si/SiO_2 composite denoted as D-Si-6 (reaction time of 6 h) showed the highest capacity retention ($\approx$80%) after 200 cycles when coupled with a $LiNi_{0.8}Co_{0.1}Mn_{0.1}O_2$ cathode material in a full cell. Also, their D-Si-6 anode showed high discharge capacity ($\approx$1000 mA h g^{-1}), about three times that of commercial graphite anode at 0.2 C without significant capacity decay after 200 charge/discharge cycles. The superior electrochemical properties of their D-Si-6 anode, comparable to reported silicon-based anode materials[218–220] was attributed to the heterogeneous (crystalline Si/amorphous SiO_2) network as well as the porous structure.

The potential of using "fresh" diatom earth as an anode material was recently reported by Blanco *et al.*[63] In their work, they investigated the electrochemical properties of both carbon (C) coated and uncoated milled diatomite powders. Additionally, the electrochemical properties of pristine diatomite were investigated. It was reported that the uncoated milled diatomite powder (470 nm particle size) showed a higher specific capacity (740 mA g^{-1}) than the pristine diatomite with particle size of 17 μm (575 mA h g^{-1} after 100 cycles). After a facile carbon coating process, the C-coated milled diatomite showed the highest specific capacity (840 mA h g^{-1} after 100 cycles). It is almost certain that C-coating will improve the electrochemical properties of milled diatomite due to increased electronic conductivity, however different electrochemical properties observed in the pristine and milled diatomite originate from the increased surface area of the milled diatomite. The milling of diatomite produces powders with ultra-small particle size (470 nm), thus increasing the surface area and eventually reducing the Li-ion diffusion length for optimum electrochemical performance. This places a lot of importance on particle size of materials intended for use as negative electrodes for batteries such as Si, SiGe, SiO_2, SiC, Mg_2Si, Mg_2Si/C *etc.* It must be noted that even though majority of the published reports have focused on liquid or polymer-based Li-ion batteries, not only these battery types are subjects of studies, a growing interest in all solid state batteries drew attention to diatomite-based anodes for such batteries. In a recent report by Zhou *et al.*,[59] a hierarchical hybrid anode material synthesized from diatomite for an all-solid state lithium metal battery is reported. Their hierarchical hybrid (PEO-SPE/Li–Si) was based on a combination of suitable materials for all-solid state batteries namely; polyethylene oxide (PEO) based solid polymer electrolyte (SPE), lithium metal and silicon obtained from diatomite framework. Lithium metal, even though boasting of superior electrochemical properties is not applicable in liquid or polymer electrolyte-based batteries, due to the flammability of liquid electrolytes and the instability of alkali elements. All-solid state batteries provide the perfect opportunity to use Li metal, allowing for the fabrication of stable solid-state batteries exhibiting superior electrochemical properties. Solid polymer electrolytes combined with Li ion salts enable intimate interface

contact and reduce interfacial resistance by providing better flexibility and wettability with Li metal than counterparts inorganic solid electrolytes (ISE).[221–223] Moreover, the use of a diatomite framework is to provide a nature inspired hierarchical structure capable of accommodating volume changes and inhibiting dendrite formation. For these reasons, their hybrid anode showed stable Li stripping/plating performance over 1000 h with average overpotential lower than 100 mV without any short circuit. Coupled with a lithium iron phosphate cathode in a full cell, an excellent cycling stability (0.04% capacity decay rate for 500 cycles at 0.5 C) and high rate capability (65 mA h g^{-1} at 5 C) were obtained. The superior electrochemical performance compared to a lithium foil as demonstrated in Fig. 11,[59] was attributed particularly to the 3D Li^+ ion-conductive framework provided by diatomite inspired-silicon.

Aside from their use in anode material for batteries, diatomite has recently been studied as a key material in the design of other battery parts, specifically as part of the cathode for lithium sulfur batteries by Li *et al.*[83] Lithium sulfur batteries have been identified as promising candidates for energy applications due to attractive electrochemical properties (theoretical specific capacity 1672 mA h g^{-1} of sulfur and energy density 2500 W h kg^{-1}), low cost, natural abundance and eco-friendly nature of sulfur.[224,225] Nevertheless, there are a number of reported shortcomings,[83] and notable among them is the shuttling of soluble polysulfides (Li_2Sn, $4 \leq n \leq 8$) which undermines battery performance over time.[226,227] Even though some progress has been reported in this area,[83] these solutions are known to be expensive and require complex processing routes. Naturally abundant diatomite presents a good approach to reduce the shuttling rate of the polysulfides due to their excellent chemical stability and sorption ability.[228,229] In their work, two composite cathodes were prepared (S-DM-AB) and (S-AB), where sulfur (S), diatomite (DM), and acetylene black (AB) as shown in Fig. 6. The composite cathode with diatomite (S-DM-AB) showed better electrochemical performance (discharge capacity of 531.4 mA h g^{-1} after 300 cycles at 2 C and a capacity retention of 51.6%) than the cathode without diatomite (capacity of 196.9 mA h g^{-1} and capacity retention of 18.6% under the same conditions). Prior to the electrochemical measurements the adsorption capability of diatomite and acetylene black for Li_2S_6 was investigated, with quantitative results showing that diatomite has a higher adsorption capacity (5.31×10^{-2} g g^{-1}) than acetylene black (6.14×10^{-3} g g^{-1}). The addition of diatomite is justified through a significant decline in the diffusion of polysulfides into the electrolyte thus improving the cycling performance. This preliminary result suggests that prior modification of the sorption capability of diatomite *via* pre-treatments such as calcination, roasting and drying may result in improved adsorption ability for optimum electrochemical performance of lithium sulfur batteries. DE has shown tremendous ability to be fully incorporated in the design of new battery cathode and anode materials and this could be fully realized with the combination of suitable pre-treatments.

6. Energy harvesting applications

The study of diatomite for energy harvesting has equally seen tremendous progress rising from very keen interest by

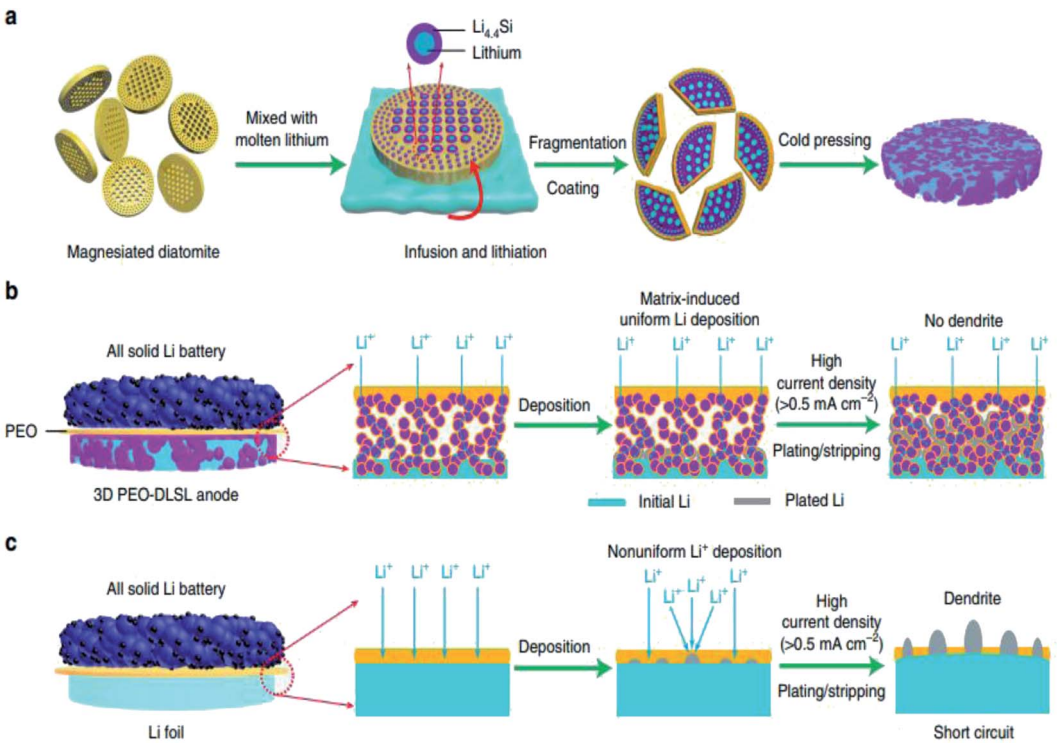

Fig. 11 (a) Flowchart of PEO-DLSL fabrication process and (b and c) mode of lithium stripping/plating in all-solid-state Li metal battery with PEO-DLSL anode and planar Li-foil anode.[59]

researchers. In this section, a brief summary of recent and previous reports are presented.

6.1 Thermoelectric energy harvesting

Complementing their applications in thermal energy storage, diatomite has recently been studied for their potential applications in thermal energy harvesting (thermoelectrics). Based on the same knowledge of their neat nanoporous structure, diatomite could potentially contribute immensely in developing new materials for thermoelectrics. This area of application has not been addressed in previous reviews[54–57] and deserves to be included in the current timeline of diatomite energy related applications. The major classes of materials studied for applications in thermoelectric generators (TEG) are chalcogenide, clathrate, skutterudite, half-Heusler, silicide, and oxide.[230] Bismuth telluride and lead telluride, belonging to the chalcogenide, are the most prominent of thermoelectric materials. Chalcogenides in general have a long history of applications as thermoelectrics.[230] The desire for low cost and abundant material has led to the recent attention on new material for improved and sustainable thermoelectric energy harvesting. Among these, silicides have received a lot of attention due to their availability and low.[230] In order to fully realize the potential of these prospective materials, nanostructuration has been identified as key in their processing.[231–235] The requirement for improved thermoelectric properties through this approach places more importance on the versatility of naturally occurring and readily available diatomaceous earth. One material which emphasizes the importance of nanoscale morphologies for thermoelectrics is Si. Silicon, well known for its applications in semiconductors, offers competitive advantages ranging from low cost, easy integration with systems, abundance and low toxicity.[236] Even though it is tempting to use bulk silicon as a thermoelectric material, the very high thermal conductivity of silicon remains a concern. Efforts have been made to account for this problem with the likes of silicon nanowires[237,238] and nanocrystalline bulk silicon obtained *via* ball milling.[239] Although these efforts present positive results, they are limited by their inability to be integrated on the industrial scale and a high energy consumption. In recent times, porous structures have also been identified as a means to enhance phonon scattering, leading to reduced heat loss through lattice vibrations.[240,241] Even though porous silicon produced *via* anodic etching appears to be a suitable option, porous Si is limited to the micrometer scale and does not affect the bulk silicon material. Based on the requirements for nanocrystalline and nanoporous materials, Zong *et al.*[36] magnesiothermically reduced diatomite to doped silicon for thermoelectric applications. The Sb and B doped nanoporous Si otherwise denoted as n-Si and p-Si bulk after the spark plasma sintering (SPS), showed considerable reduction in the lattice thermal conductivity, 2 orders of magnitude compared to single crystal silicon. This drastic decrease in lattice thermal conductivity was attributed to effective phonon scattering by the nanograins (40 nm) and nanopores (100 nm) with sizes close to the mean free path of phonons. In the case of both doped silicon samples, the p-Si showed a rather higher lattice thermal conductivity compared to the n-Si sample. This was attributed to the incomplete doping of Sb in n-Si, which forms precipitates and contributes to phonon scattering. Apart from the differences in thermal conductivity as a result of the different dopant, the electrical conductivity and carrier mobility of the dopant varied as well. The maximum power output for both n-Si and p-Si were 1.14 and 1.81 W m^{-2} respectively under a temperature difference of 40 K. Additionally, a study of the effects of porosity and the pore size on the bulk lattice thermal conductivity showed a decrease in the thermal conductivity when porosity increased and pore size decreased. This suggests that an increase in porosity and reduction in pore size cause significant drop in the thermal conductivity. It goes on to outline the importance of selecting the right diatomite precursor. The figure of merit for both n and p-Si were found to increase with increasing temperature, suggesting a medium to high temperature application. However, the highest zT (thermoelectric dimensionless figure of merit) obtained shows it has not reached a practical level yet and could be increased *via* the choice of dopant in the n-Si type. In another related study by Szczech *et al.*,[117] Mg_2Si was magnesiothermically produced from diatomite and potential application in thermoelectrics analyzed. Silicides have already been tipped to be potential candidates for thermoelectric materials as mentioned earlier. In their study, an estimated Mg_2Si grain size of 20–36 nm suggests a potential increase in zT of the thermoelectric material, based on an earlier report.[242] In this report,[242] nanostructures less than 10 nm cause significant decrease in thermal conductivity. Interestingly, nanostructures with relatively big grain sizes (up to 150 nm) could also cause significant decrease in the thermal conductivity, thus suggesting an expected increase in the zT of diatomite based Mg_2Si.

6.2 Solar energy harvesting

The use of solar energy covers a broad spectrum of applications, ranging from direct conversion of solar energy to electricity and for photocatalysis. The latter is an area where the potential use of diatomite has received great interest.

6.2.1 Dye sensitized solar cells. The interaction of diatom frustules with light is fascinating and has been adequately studied.[243–247] The interesting optical properties observed are the main motivations for the interest in diatoms for potential applications in solar energy harvesting technologies. It is reported that diatoms are efficient light harvesting organisms, and this is further backed by their ability to produce their own food like plants do with chlorophyll.[248,249] This suggests the potential to channel such light trapping properties into energy harvesting based on solar energy technologies. Harnessing energy from the sun is one of the eco-friendliest ways of producing energy. A number of materials find applications in this field, but one that has seen massive commercialization is silicon based solar cells. Silicon is cheap, less toxic and offers tunable optical and electronic properties.[57] Albeit these advantages, the high surface reflectance of silicon based solar cells remains a huge setback in their entire efficiency, which has over the years inspired the introduction of some promising solar

energy harvesting. These are dye sensitized solar cells (DSSC), organic based solar cells, quantum solar cells and several others.[250–253] Among the above-mentioned technologies, DSSC have received a lot of attention as far as diatomite application is concerned. Aside from this, DSSC has attracted widespread interest in the scientific community due to the prospects of efficiently harnessing solar energy at a low cost.[56] Previous progress made in this field is fully discussed in excellent reviews by Sun *et al.*[57] and Jeffryes *et al.*[55] From the introduction of DSSC, an efficiency of 7% was reported,[254] but this has further been increased to 10%.[255] DSSC is mostly based on nanocrystalline anatase titania (TiO_2) due to their competitive optical, electrical and biological properties as compared to other reported oxides like ZnO, SnO_2, Nb_2O_5.[57] Despite its suitability, there is a limitation with the surface area of TiO_2. As reported,[256] TiO_2 does not offer very high surface areas provided by nanoparticles. Incorporating DE in the design of TiO_2 based DSSC provides a high specific surface area capable of promoting the solar cell efficiency.[57] Naturally occurring diatomite is known to have a refractive index of 1.43,[243] and porous anatase titania thin films have a refractive index between 1.7 and 2.5.[257] A combination of diatomite and porous anatase titania results in layers with high dielectric constant and light scattering within the pore array.[57] With improved light scattering, there is a possibility to use less dye or reduce the photoanode layer, resulting in further reduction in production cost.[55] Aside from the opportunity to reduce the cost, a reduced photoanode layer improves the efficiency significantly by decreasing the electron diffusion distance between the dye and the conductive glass electrode. This eventually leads to a decreased electron-electrolyte recombination, leading to the increased efficiency of the DSSC. A recent study based on this same approach was reported by Bandara *et al.*[258] In their study, they incorporated DE in the preparation of the TiO_2 based photoelectrode and reported an enhanced efficiency (35%) and improved short current density (39%), which were attributed to the enhanced light harvesting ability provided by DE. The incorporation of diatomite into DSSC presents an eco-friendly and more importantly an effective way to improve the interaction of light with the dye.

6.2.2 Photocatalyst. Chemical reactions facilitated through photoelectrochemical processes have seen tremendous admiration in recent times and this has seen widespread application in environmental waste treatment and hydrogen evolution *via* water splitting in fuel cells.[259–264] The possibility of using solar energy to accelerate chemical reactions is an interesting area of research and this is made possible with the help of semiconductor photocatalysts. Although promising progress has been made in these areas, efforts are still being undertaken to improve overall efficiency of photocatalysts. The most widely known photocatalyst is TiO_2, and reasons for its widespread use in solar energy harvesting have been presented earlier. Aside from the conventional use in DSSC, TiO_2 is also used as a semiconductor photocatalyst. However, setbacks addressed with its applications in DSSC are no different for applications as photocatalyst.[256] In addition to the setback mentioned earlier, the use of TiO_2 is limited by its wide bandgap, 3.2 eV, which implies irradiation only in the ultraviolet range of the electromagnetic spectrum. This seriously limits their efficiency to 4–5%.[265] Based on their interesting matter–light interaction, diatomite has seen huge attention as a way to improve the efficiency of semiconductor photocatalysts. It is worth noting that in the related reports, diatomite was the supporting material. In previous years a number of nanocomposites based on TiO_2,[46,48,52,53,98,120,145] Bi_2MoO_6,[266] BiOCl,[267] Bi_2S_3,[268] Ag_3PO_4,[269,270] Fe–Mn binary oxide,[271] ZnO[272–274] and Cu_2O–ZnO[150] *etc.* as precursor materials and diatomite as a supporting material have been reported. In one such report by Zhang *et al.*,[48] a photocatalyst based on precursor TiO_2 and diatomite as a supporting material was reported. The TiO_2/diatomite photocatalyst was more effective in degrading gaseous formaldehyde than pristine TiO_2 under UV radiation. This difference in photocatalytic performance between the composite photocatalyst and TiO_2 was attributed to the potential of diatomite to accelerate a good dispersion of TiO_2 nanoparticles and a strong absorption capacity for formaldehyde. Other works focusing on materials apart from the well-known TiO_2 include a report by Cai *et al.*,[266] where a facile approach to synthesize nano-sized Bi_2MoO_6/diatomite composite as a high performance photocatalyst under visible light irradiation was demonstrated. Their as-synthesized nano-sized Bi_2MoO_6/diatomite composite had significantly higher photocatalytic efficiency for Rhodamine B (RhB) degradation than the pristine Bi_2MoO_6 under visible light illumination. The high surface area of diatomite promotes the formations of composites with nanostructures suitable for efficient photocatalytic activities. In their work, the synthesized nano-sized Bi_2MoO_6/diatomite composite had Bi_2MoO_6 nanoflakes homogeneously attached to the surface of diatomite, unlike as-prepared pure Bi_2MoO_6. In the pure Bi_2MoO_6 sample, agglomerates were formed and such morphologies are reported to limit the overall photocatalytic activity due to the reduction of the active sites for photocatalysis. The degradation efficiency of the prepared nanocomposite increased with increasing Bi_2MoO_6. However, further increase to 80% Bi_2MoO_6 to diatomite ratio resulted in a significant drop in the photocatalytic activity of the nanocomposite due to the formation of aggregates of Bi_2MoO_6 on the surface of the nanocomposite. In another work by Xiao *et al.*,[268] a semiconductor photocatalyst based diatomite and Bi_2S_3 was reported. In their work, the nanocomposite DE-Bi_2S_3 showed better photocatalytic activity than the pure Bi_2S_3 towards the degradation of Cr(IV), a bioaccumulated pollutant in wastewater. The improved photocatalytic activity was attributed to the ability of diatomite to prevent the aggregation of Bi_2S_3 monomers. Diatomite is reported to monodisperse Bi_2S_3 and also facilitates the absorption of Cr(IV) on its surface, thus enhancing the photocatalytic activity. Another promising nanocomposite based on a Cu_2O–ZnO system immobilized on diatomite was reported by Zhu *et al.*[150] Diatomaceous earth, playing the role of the supporting material, enhanced the photocatalytic activity of the hybrid towards the degradation of red water produced from TNT production. Natural DE used in their work played the same role as reports presented above. The high surface area of diatomite provided a bigger contact surface between the photocatalyst and

the liquid due to the improved dispersion of Cu_2O–ZnO on its surface. It should be noted that in all the literature addressed, the authors report of a stable nanocomposite photocatalyst which can be reused. The micro–nano structure of diatomite appears to inspire morphologies suitable for catalytic activity in almost all the works reported.

6.2.3 Silicon and polymer based solar cells. The application of diatomite in solar energy harvesting has been extended to silicon and polymer based solar cells.[71,84,112] In silicon based solar cells, solar energy is directly converted to electrical energy. In these reported applications, diatomite derived materials served as an anti-reflective coating, causing

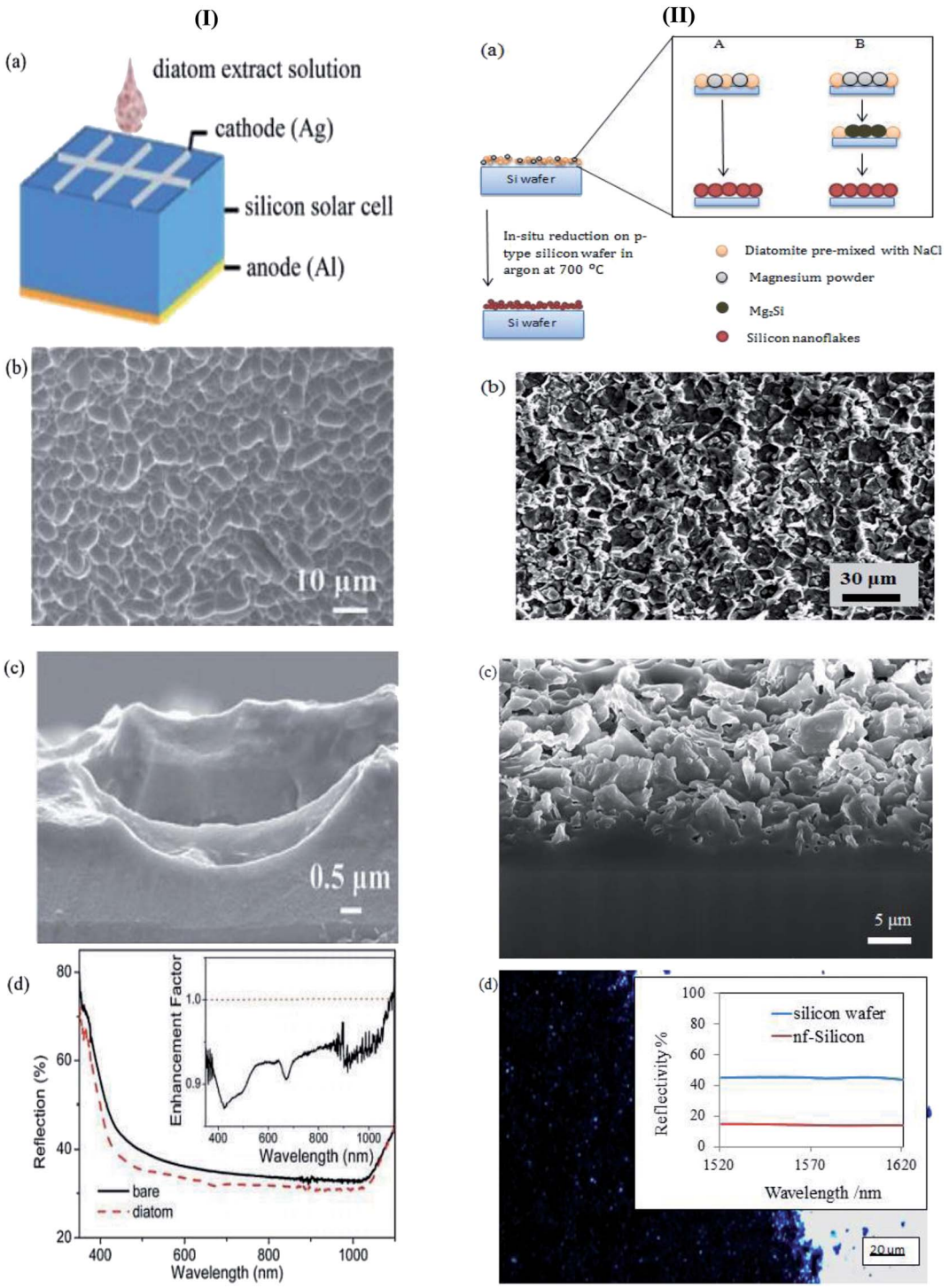

Fig. 12 Schematic illustration of the 2 approaches reported to suppress surface reflectivity of silicon based solar cell (I) (a) schematic illustration of synthesis process (b and c) SEM images diatom extract (d) surface reflectivity of diatom extract[71] and (II) (a) schematic illustration of synthesis process (b and c) SEM images of silicon nanoflakes (d) surface reflectivity of silicon nanoflakes.[112]

a significant reduction in the surface reflectance of silicon based solar cells. One major setback of silicon based solar cells is their high surface reflectivity, which affects the overall efficiency of this solar cell type. A huge part of the electromagnetic radiation from the sun is not accounted for due to this high surface reflectivity. The measured surface reflectivity of polished silicon are given as 54, 35 and 31% for the UV range (300–400 nm), visible (400–800 nm) and near-IR (1200–2000 nm) respectively.[275] To reduce the surface reflectivity, a number of approaches are employed including the use of anti-reflective coating, and surface modification of wafer surface resulting in what is best known as black silicon (BSi).[71,275] Although these solutions offer improved surface properties, they are often complex, require non-eco-friendly processing and costly.[71,112] In a study by Chen *et al.*[71] a spin-coated chlorophyll extract from diatom algae caused a significant reduction of the surface reflectivity of silicon wafer to 13% (350–1100 nm). Another approach using diatomite to reduce the surface reflectivity of silicon was demonstrated by Aggrey *et al.*[112] In their work, a black silicon-like coating, referred to in their work as "silicon nanoflakes", was formed on the wafer surface after an *in situ* magnesiothermic reduction of diatomite on the surface. The silicon nanoflakes coating caused a significant drop in the surface reflectivity to 15% (1520–1620 nm). The two strategies reported have been summarized in Fig. 12,[71,112] both significant in another related work, McMillon-Brown *et al.*[84] enhanced the light trapping ability of their polymer based solar cell. Organic photovoltaics (OPV), although attractive for several reasons like being lightweight, flexible and transparent, have a huge setback. The highest power conversion efficiency (PCE) to be reported is 11.5%.[276] The PCE of organic solar cells are known to be dependent on the thickness of the active layer.[84] Even though an increase in the thickness of the active layer provides more absorption, charge extraction for thick active layers is limited by the low charge mobility of the organic semiconducting blend. For this reason, the thickness of the active layer is normally restricted between 100 and 300 nm. In order to improve the active-layer absorption a number of approaches have been suggested to redirect and improve light trapping, but most of them require complex and expensive processes.[277–280] It is reported that DE improves the light absorption of active materials when in close proximity and this is quite expected because the interesting optical DE exhibits.[246] As such, the incorporation of DE into the design of OPVs could improve the active layer absorption through improved light scattering. Through the addition of DE to their active layer, they obtained the same PCE as standard thickness cells with 36% thinner active layer. This confirms DE inclusion in OPV can help optimize them by tackling the issues with thickness limitations. In these reports the potential use of diatomite to complement bulk silicon and polymer based solar are analyzed and may be crucial for improved solar cell performance. The fascinating optical properties obviously enhance light absorption of these solar cell types and could go a long way to improve their efficiency.

7. Other potential energy applications

The target to increase the efficiency of green energy technologies comes with a lot of stiff criteria for energy materials. Already, notable breakthroughs have been reported about the use of diatomite in some energy harvesting and storage applications such as solar energy applications,[46,52,71,84,98,112,258,268] thermal energy storage,[72,76,89,195] thermoelectrics[36,117] and electrical energy storage systems (batteries and supercapacitors).[45,49,59,60,62,63,100,144] The successes attained to date will certainly serve as a catalyst to foster DE studies in energy applications. The widespread potential applications of DE can be attributed to a combination of factors. Diatomite is an attractive silica precursor, a workable template for new materials and most importantly possesses a naturally formed nanoporous structure highly desired and required in new energy materials. Much more can be expected from the use of diatomite as a template for electrodes of batteries based on Na, K, Mg, Al *etc.* and other battery types as research is still on-going in these areas. Current energy materials are expected to possess nanostructures suitable for typically functional applications in energy systems and concurrently exhibit good structural stability. It is not surprising that DE has gained such huge attention for the replacement of existing silica precursors used for outstandingly good yet structurally poor Si based anode materials. DE may receive a lot more attention as researchers continue to find ways of nanostructuring electrode materials and separators for electrochemical devices. Another potential area, currently unexplored to the best of our knowledge, is the use of DE as a precursor for the growth and formation of quartz for piezoelectric applications. As a naturally occurring siliceous material, DE qualifies to be used as a precursor for quartz formation. This gap in the potential of DE was previously addressed by Korsunsky *et al.*[121] Using a nanostructured silica precursor for the growth and formation of nanostructured piezo quartz could allow for a simple and straightforward synthesis route unlike the protocols reported in previous studies.[281,282] Nanostructured quartz films on silicon substrates have been synthesized *via* wet chemistry in recent studies.[283,284] Currently, the electronic grade of quartz is produced *via* a long hydrothermal process developed by Spezia, where the large crystals are cut and polished.[285] Subsequent processes such as shaping and integration are performed in order to obtain thinner oscillators with higher resonance frequencies.[286] The existing process is complex and expensive and has triggered a lot of interest in cheap and straightforward routes such as sol–gel chemistry, chemical solution deposition and hydrothermal synthesis.[287–291] Different silica precursors like amorphous silica colloids, tetraethoxysilane silica (TEOS), and dry amorphous silica have been used in these reports.[281–284] Earlier studies emphasized the importance of synthesis conditions such as the silica precursor, catalyst, humidity and thermal treatment.[292–296] As far as the silica precursor is concerned, there is yet to be a work on nanostructured quartz synthesized using DE. DE is naturally abundant, eco-friendly, cheap and most importantly possesses nanoscale morphologies which make it a suitable

candidate as a silica precursor for quartz formation. Improving existing and developing future energy materials could see a more substantive approach towards DE as long as the search for cheaper and eco-friendlier ways to produce reliable and efficient energy materials stays on.

8. Conclusion

Diatomaceous earth has been explored in several forms for different energy applications. Regardless of their state of application, DE has shown promising results thus prompting further interest amongst scientists. Indeed, the fascinating naturally formed nanostructure of DE is paramount in their contributions reported to date. Using DE as a template and precursor for new energy materials seems to offer cheaper, simpler and eco-friendlier synthesis protocols compared to most protocols carried out without it. The reported synthesis routes: impregnation technology, displacement reactions, wet chemistry and deposition and etching are well established processes. In general, these synthesis routes seek to utilize or preserve the nanoporous structure of DE.

- The impregnation technology makes use of the nanoporous structure of DE to form nanocomposites by impregnating DE with the active material. DE serves as a supporting material in this process. The impregnation technology comes with a simple set-up and is normally performed at low temperatures.
- In displacement reactions, the main objective is to preserve the nanostructure of DE in Si based material after reduction reactions at relatively higher temperatures than in the impregnation technology. DE plays the role of a precursor and a template for the new material produced using the displacement reaction.
- Deposition techniques and wet chemistry routes provide platforms to produce new materials and hybrid systems by covering the surface and sometimes internal pores of DE. In the deposition and wet chemistry routes, DE plays the role of a template and in some cases both a template and supporting material.

Among these synthesis routes, further studies and modifications of displacement reactions have led to the introduction of notable non-conventional methods, which offer somewhat better control over the outcome of the typical silica to silicon conversion that takes place in this process. A better control over the outcome of displacement reactions means a better chance to control the nanoscale morphology of silicon-based materials produced from DE. Another important aspect of these synthesis processes is the role that some prior treatments performed on DE play on the nanostructure and properties of the final products. Prior treatments, mainly mechanical and thermal, affect the powder properties of DE prior to the main synthesis processes. Prior treatments such as calcination, mechanical milling, microwave heating and vacuum drying are all crucial for the full implementation of DE as the next generation energy material. DE is obviously an ideal and near perfect material for emerging energy materials, but this expectation relies heavily on the right combination of synthesis processes. The preference for DE over other siliceous materials is related to the neat naturally formed nanostructure of the former. The goal of almost all principal synthesis processes is to preserve this structure for intended applications. As far as synthesis is concerned, the main threat to the nanoscale morphology of DE comes from the high temperature and extreme mechanical treatments. Apart from displacement reactions with rather high temperatures used, the other main synthesis processes require relatively low temperatures, although pre-treatments may involve high temperature treatment. The quest to preserve the nanostructure has benefited from several ideas such as the use of inorganic salts. Inorganic salts represent a means of scavenging the enormous heat evolved in displacement reactions and thus may help preserve the nanostructure to some extent. Achieving further improvement places greater demands on the understanding of the kinetics and thermodynamics of silica to silicon transformations mostly facilitated by Mg and Al in DE-related studies. A better understanding of the reaction kinetics will inform the search for best reaction parameters which could complement inorganic salts to improve nanostructure preservation. Even though particle size reduction is reportedly beneficial for battery applications, this may not be suitable treatment for applications where high porosity is required and most importantly for bio-templating purposes, since the individual frustules end up badly fragmented. It is extremely important to find the right balance between particle size reduction and the preservation of nanoscale morphology of DE in order to obtain powders with suitable free surface characteristics for intended applications. For bio-templating purposes, it is imperative for frustules to be free from impurities blocking the pores. Thermal pre-treatment *via* microwave heating is reported to be effective in eliminating impurities from the pores. The ideal DE precursor with empty pores, suitable particle size and unbroken frustules may be achievable only through laboratory cultivation of diatoms which is not very economical, thus exploiting a synergy between different pre-treatments and synthesis process to obtain workable precursors is much desired. As far as applications are concerned, the prospects of DE in the ever increasing and demanding energy sector applications are indisputable based on accounts provided in the reviewed literature. In thermal energy storage, DE has been successfully incorporated together with active materials to form shape-stable phase change materials that deliver enhanced performance due to the high degree of encapsulation or impregnation of PCMs. So far, the available literature shows that DE-based nPCMs offer a high phase change temperature but this occurs at the expense of the latent heat storage ability. Thus, future works could concentrate on optimizing phase change temperatures in order to further improve the storage capability of PCMs. Incorporating DE in the design of supercapacitor electrodes has shown enormous increase in supercapacitor performance such as high specific capacitance and excellent cycling stability. This has been partly attributed to the nanoscale morphology of DE that is able to prevent agglomeration and large volume changes during cycling. Properties such as high reversibility and good cycling during charge–discharge have been ascribed to the high surface

area and porosity offered by DE. Developing facile and highly efficient synthesis processes remain a crucial step in the realization of DE as supporting material or template for electrode material for supercapacitors. In battery development, DE has seen tremendous interest as a precursor for silica and silicon-based anode materials for Li-ion batteries, where significant successes have been widely reported. DE based anodes have delivered superior electrochemical performance due to their heterogeneous network and porous structure. Additionally, further application of carbon coating has been reported to optimize the electrochemical performance of these anodes to offer a higher specific capacity due to decreased diffusion length owing to the high surface area of the treated DE and the contribution from carbon. Here, other forms of conductive coatings can be investigated in varying structures in order to optimize further the electrochemical performance while also looking at other forms of treatment of the diatoms. The development of solid-state batteries, the potential battery of the future could necessitate the use of DE as a template and supporting material for the design of battery electrodes considering the recent successes reported for this battery type, where huge volume changes and dendrite formation were minimized by DE incorporation into the design of the electrode. Quite some progress has been made in reducing the shuttling effect of polysulfides in Li–S batteries by preparing a DE-based composite electrode. The improved battery stability after using DE in Li–S batteries presents a path to design composite electrode materials where DE is a competitive candidate as a supporting material. The possibility and temptation to use Si as a thermoelectric material could be realized in the nearest future following early success reported in preparing nanoporous Si thermoelectric generators, where promising results were obtained. Alongside nanoporous Si, a rather well-known thermoelectric material based on Mg and Si (Mg_2Si) with interesting nanoscale morphologies could be developed from DE, to offer outstanding *zT*. Indeed, the realization of these possibilities hinges critically on the proper synthesis processes, which have the potential of preserving the hierarchical nanostructure of DE for the intended applications. Solar energy harvesting is another area which has seen tremendous interest in potential DE implementation, not only because they act as template for active materials but due to the interesting optical properties they possess. Dye sensitized solar cells (DSSC) and photocatalysis are areas of solar energy harvesting technology that received a lot of attention as far as the use of diatomite is concerned, although isolated cases in silicon and polymer based solar cells have been reported recently. DE has been successfully incorporated into TiO_2 systems of solar cells to improve efficiency where the enhancement has been attributed to the high surface area of the diatomite contribution. Also, the low band width of TiO_2 which limits irradiation to only the UV range of the electromagnetic spectrum has been improved by using DE as supporting material for systems in the past. It is worth noting that though the incorporation of DE in such systems results in improvement in properties, the present state only uses DE as supporting material and not the main active material. Capitalizing on these strengths could pave the way for full implementation of DE in DSSC and photocatalysis where minimal quantities of the active materials may be required, thus reducing the cost. Thus far, DE offered an alternative approach to enhancing energy performance of materials in an eco-friendlier and cost-effective manner. While all these studies suggest the undeniable depth of usefulness DE would yield in the energy industry, the full potential of DE could remain untapped. At present, to the best of our knowledge there is no comparative study of different DE cultures and their performance in applications. It would be interesting to synthesize DE-based energy materials based on different individual cultures and to understand the relationship between their nanoscale structure and performance. Of course, the task is challenging and time consuming, but any study dedicated to this will help realize the full potential of DE. Potentially, specific cultures may be found to be suitable for particular applications.

Conflicts of interest

There are no conflicts to declare.

Acknowledgements

The authors wish to acknowledge the support from the Royal Society of London under projects IEC/R2/170223 and IEC/R2/202254.

References

1 R. Calvert, Diatomaceous earth, *J. Chem. Educ.*, 1930 Dec, 7(12), 2829.
2 M. M. Ghobara, M. M. Ghobara, M. M. Ghobara and A. Mohamed, Diatomite in Use: Nature, Modifications, Commercial Applications and Prospective Trends, *Diatoms: Fundamentals and Applications*, 2019 Jun 28, 471–509.
3 T. D. Kelly, G. R. Matos, D. A. Buckingham, C. A. DiFrancesco, K. E. Porter and C. Berry, Historical statistics for mineral and material commodities in the United States, *US Geological Survey data series*. 2010 Feb;vol. 140, pp. 01–06.
4 P. Zahajská, S. Opfergelt, S. C. Fritz, J. Stadmark and D. J. Conley, What is diatomite?, *Quat. Res.*, 2020 Jul, **96**, 48–52.
5 J. Murray and A. F. Renard. *Report on deep-sea deposits based on the specimens collected during the voyage of HMS Challenger in the years 1872 to 1876*, HM Stationery Office, 1891.
6 P. S. Conger, Accumulation of diatomaceous deposits, *J. Sediment. Res.*, 1942, **12**(2), 55–66.
7 G. K. Pedersen, Anoxic events during sedimentation of a Palaeogene diatomite in Denmark, *Sedimentology*, 1981 Aug, **28**(4), 487–504.
8 F. L. Kadey Jr, *Diatomite. Industrial Rocks and Minerals*. 1983, vol. 1, pp. 677–708.

9 W. E. Dean, M. Leinen and D. A. Stow, Classification of deep-sea, fine-grained sediments, *J. Sediment. Res.*, 1985 Mar 1, **55**(2), 250–256.
10 K. Minoura, T. Susaki and K. Horiuchi, Lithification of biogenic siliceous sediments: Evidence from Neogene diatomaceous sequences of northeast Japan, *Sediment. Geol.*, 1996 Dec 1, **107**(1–2), 45–59.
11 S. D. Inglethorpe. Industrial minerals laboratory manual: diatomite. *British Geological Survey*; 1993.
12 S. Akin, J. M. Schembre, S. K. Bhat and A. R. Kovscek, Spontaneous imbibition characteristics of diatomite, *J. Pet. Sci. Eng.*, 2000 Mar 1, **25**(3–4), 149–165.
13 R. B. Owen, Sedimentological characteristics and origins of diatomaceous deposits in the East African Rift System, *Sedimentation in Continental Rifts*, 2002, pp.233–246.
14 P. R. Moyle and T. P. Dolley, *U.S. Geological Survey Chapter D, With or Without Salt-a Comparison of Marine and Continental-Lacustrine Diatomite Deposits*, 2003.
15 S. Martinovic, M. Vlahovic, T. Boljanac and L. Pavlovic, Preparation of filter aids based on diatomites, *Int. J. Miner. Process.*, 2006 Sep 1, **80**(2–4), 255–260.
16 B. Yılmaz and N. Ediz, The use of raw and calcined diatomite in cement production, *Cem. Concr. Compos.*, 2008 Mar 1, **30**(3), 202–211.
17 X. Qi, M. Liu, Z. Chen and R. Liang, Preparation and properties of diatomite composite superabsorbent, *Polym. Adv. Technol.*, 2007 Mar, **18**(3), 184–193.
18 A. NIKPAY, Diatomaceous earths as alternatives to chemical insecticides in stored grain, *Insect Sci.*, 2006 Dec, **13**(6), 421–429.
19 D. Li, Y. K. Joo, N. E. Christians and D. D. Minner, Inorganic soil amendment effects on sand-based sports turf media, *Crop Sci.*, 2000 Jul, **40**(4), 1121–1125.
20 M. Green, E. Fielder, B. Scrosati, M. Wachtler and J. S. Moreno, Structured silicon anodes for lithium battery applications, *Electrochem. Solid State Lett.*, 2003 Mar 5, **6**(5), A75.
21 J. Rong, C. Masarapu, J. Ni, Z. Zhang and B. Wei, Tandem structure of porous silicon film on single-walled carbon nanotube macrofilms for lithium-ion battery applications, *ACS Nano*, 2010 Aug 24, **4**(8), 4683–4690.
22 C. K. Chan, H. Peng, G. Liu, K. McIlwrath, X. F. Zhang, R. A. Huggins and Y. Cui, High-performance lithium battery anodes using silicon nanowires, *Nat. Nanotechnol.*, 2008 Jan, **3**(1), 31–35.
23 T. Song, J. Xia, J. H. Lee, D. H. Lee, M. S. Kwon, J. M. Choi, J. Wu, S. K. Doo, H. Chang, W. I. Park and D. S. Zang, Arrays of sealed silicon nanotubes as anodes for lithium ion batteries, *Nano Lett.*, 2010 May 12, **10**(5), 1710–1716.
24 X. Chen, K. Gerasopoulos, J. Guo, A. Brown, C. Wang, R. Ghodssi and J. N. Culver, Virus-enabled silicon anode for lithium-ion batteries, *ACS Nano*, 2010 Sep 28, **4**(9), 5366–5372.
25 L. F. Cui, L. Hu, J. W. Choi and Y. Cui, Light-weight free-standing carbon nanotube-silicon films for anodes of lithium ion batteries, *ACS Nano*, 2010 Jul 27, **4**(7), 3671–3678.
26 T. Takamura, M. Uehara, J. Suzuki, K. Sekine and K. Tamura, High capacity and long cycle life silicon anode for Li-ion battery, *J. Power Sources*, 2006 Aug 25, **158**(2), 1401–1404.
27 U. Kasavajjula, C. Wang and A. J. Appleby, Nano-and bulk-silicon-based insertion anodes for lithium-ion secondary cells, *J. Power Sources*, 2007 Jan 1, **163**(2), 1003–1039.
28 H. Kim, M. Seo, M. H. Park and J. Cho, A critical size of silicon nano-anodes for lithium rechargeable batteries, *Angew. Chem., Int. Ed.*, 2010 Mar 15, **49**(12), 2146–2149.
29 N. Liu, H. Wu, M. T. McDowell, Y. Yao, C. Wang and Y. Cui, A yolk-shell design for stabilized and scalable Li-ion battery alloy anodes, *Nano Lett.*, 2012 Jun 13, **12**(6), 3315–3321.
30 N. Liu, Z. Lu, J. Zhao, M. T. McDowell, H. W. Lee, W. Zhao and Y. Cui, A pomegranate-inspired nanoscale design for large-volume-change lithium battery anodes, *Nat. Nanotechnol.*, 2014 Mar, **9**(3), 187–192.
31 R. Yi, F. Dai, M. L. Gordin, S. Chen and D. Wang, Micro-sized Si-C composite with interconnected nanoscale building blocks as high-performance anodes for practical application in lithium-ion batteries, *Adv. Energy Mater.*, 2013 Mar, **3**(3), 295–300.
32 N. Liu, K. Huo, M. T. McDowell, J. Zhao and Y. Cui, Rice husks as a sustainable source of nanostructured silicon for high performance Li-ion battery anodes, *Sci. Rep.*, 2013 May 29, **3**(1), 1–7.
33 J. Song, S. Chen, M. Zhou, T. Xu, D. Lv, M. L. Gordin, T. Long, M. Melnyk and D. Wang, Micro-sized silicon–carbon composites composed of carbon-coated sub-10 nm Si primary particles as high-performance anode materials for lithium-ion batteries, *J. Mater. Chem. A*, 2014, **2**(5), 1257–1262.
34 M. Wu, J. E. Sabisch, X. Song, A. M. Minor, V. S. Battaglia and G. Liu, In situ formed Si nanoparticle network with micron-sized Si particles for lithium-ion battery anodes, *Nano Lett.*, 2013 Nov 13, **13**(11), 5397–5402.
35 C. Shen, M. Ge, L. Luo, X. Fang, Y. Liu, A. Zhang, J. Rong, C. Wang and C. Zhou, *In situ* and *ex situ* TEM study of lithiation behaviours of porous silicon nanostructures, *Sci. Rep.*, 2016 Aug 30, **6**(1), 1.
36 P. A. Zong, D. Makino, W. Pan, S. Yin, C. Sun, P. Zhang, C. Wan and K. Koumoto, Converting natural diatomite into nanoporous silicon for eco-friendly thermoelectric energy conversion, *Mater. Des.*, 2018 Sep 15, **154**, 246–253.
37 Y. Nishimoto and K. Namba, Investigation of texturization for crystalline silicon solar cells with sodium carbonate solutions, *Sol. Energy Mater. Sol. Cells*, 2000 Apr 1, **61**(4), 393–402.
38 J. Yoo, Reactive ion etching (RIE) technique for application in crystalline silicon solar cells, *Sol. Energy*, 2010 Apr 1, **84**(4), 730–734.
39 D. Z. Dimitrov and C. H. Du, Crystalline silicon solar cells with micro/nano texture, *Appl. Surf. Sci.*, 2013 Feb 1, **266**, 1–4.
40 X. Liu, P. R. Coxon, M. Peters, B. Hoex, J. M. Cole and D. J. Fray, Black silicon: fabrication methods, properties

and solar energy applications, *Energy Environ. Sci.*, 2014, **7**(10), 3223–3263.

41 M. Otto, M. Algasinger, H. Branz, B. Gesemann, T. Gimpel, K. Füchsel, T. Käsebier, S. Kontermann, S. Koynov, X. Li and V. Naumann, Black silicon photovoltaics, *Adv. Opt. Mater.*, 2015 Feb, **3**(2), 147–164.

42 J. Lv, T. Zhang, P. Zhang, Y. Zhao and S. Li, Review application of nanostructured black silicon, *Nanoscale Res. Lett.*, 2018 Dec, **13**(1), 1–10.

43 S. Karaman, A. Karaipekli, A. Sarı and A. Bicer, Polyethylene glycol (PEG)/diatomite composite as a novel form-stable phase change material for thermal energy storage, *Sol. Energy Mater. Sol. Cells*, 2011 Jul 1, **95**(7), 1647–1653.

44 M. S. Wang, L. Z. Fan, M. Huang, J. Li and X. Qu, Conversion of diatomite to porous Si/C composites as promising anode materials for lithium-ion batteries, *J. Power Sources*, 2012 Dec 1, **219**, 29–35.

45 Y. X. Zhang, M. Huang, F. Li, X. L. Wang and Z. Q. Wen, One-pot synthesis of hierarchical MnO2-modified diatomites for electrochemical capacitor electrodes, *J. Power Sources*, 2014 Jan 15, **246**, 449–456.

46 Y. Chen, Q. Wu, C. Zhou and Q. T. Jin, Enhanced photocatalytic activity of La and N co-doped TiO_2/diatomite composite, *Powder Technol.*, 2017, **322**, 296–300.

47 D. R. Huang, Y. J. Jiang, R. L. Liou, C. H. Chen, Y. A. Chen and C. H. Tsai, Enhancing the efficiency of dye-sensitized solar cells by adding diatom frustules into TiO2 working electrodes, *Appl. Surf. Sci.*, 2015 Aug 30, **347**, 64–72.

48 G. Zhang, Z. Sun, Y. Duan, R. Ma and S. Zheng, Synthesis of nano-TiO_2/diatomite composite and its photocatalytic degradation of gaseous formaldehyde, *Appl. Surf. Sci.*, 2017 Aug 1, **412**, 105–112.

49 B. Campbell, R. Ionescu, M. Tolchin, K. Ahmed, Z. Favors, K. N. Bozhilov, C. S. Ozkan and M. Ozkan, Carbon-coated, diatomite-derived nanosilicon as a high rate capable Li-ion battery anode, *Sci. Rep.*, 2016 Oct 7, **6**(1), 1–9.

50 Y. X. Zhang, F. Li, M. Huang, Y. Xing, X. Gao, B. Li, Z. Y. Guo and Y. M. Guan, Hierarchical NiO moss decorated diatomites *via* facile and templated method for high performance supercapacitors, *Mater. Lett.*, 2014 Apr 1, **120**, 263–266.

51 X. L. Guo, M. Kuang, F. Li, X. Y. Liu, Y. X. Zhang, F. Dong and D. Losic, Engineering of three dimensional (3-D) diatom@ TiO2@ MnO2 composites with enhanced supercapacitor performance, *Electrochim. Acta*, 2016 Feb 1, **190**, 159–167.

52 Y. Chen and K. Liu, Preparation and characterization of nitrogen-doped TiO2/diatomite integrated photocatalytic pellet for the adsorption-degradation of tetracycline hydrochloride using visible light, *Chem. Eng. J.*, 2016 Oct 15, **302**, 682–696.

53 R. Zuo, G. Du, W. Zhang, L. Liu, Y. Liu, L. Mei and Z. Li, Photocatalytic degradation of methylene blue using TiO2 impregnated diatomite, *Adv. Mater. Sci. Eng.*, 2014 Jan 1, **2014**, 170148.

54 D. Losic, J. G. Mitchell and N. H. Voelcker, Diatomaceous lessons in nanotechnology and advanced materials, *Adv. Mater.*, 2009 Aug 7, **21**(29), 2947–2958.

55 C. Jeffryes, J. Campbell, H. Li, J. Jiao and G. Rorrer, The potential of diatom nanobiotechnology for applications in solar cells, batteries, and electroluminescent devices, *Energy Environ. Sci.*, 2011, **4**(10), 3930–3941.

56 Y. Wang, J. Cai, Y. Jiang, X. Jiang and D. Zhang, Preparation of biosilica structures from frustules of diatoms and their applications: current state and perspectives, *Appl. Microbiol. Biotechnol.*, 2013 Jan, **97**(2), 453–460.

57 X. W. Sun, Y. X. Zhang and D. Losic, Diatom silica, an emerging biomaterial for energy conversion and storage, *J. Mater. Chem. A*, 2017, **5**(19), 8847–8859.

58 R. Ragni, S. R. Cicco, D. Vona and G. M. Farinola, Multiple routes to smart nanostructured materials from diatom microalgae: a chemical perspective, *Adv. Mater.*, 2018 May, **30**(19), 1704289.

59 F. Zhou, Z. Li, Y. Y. Lu, B. Shen, Y. Guan, X. X. Wang, Y. C. Yin, B. S. Zhu, L. L. Lu, Y. Ni and Y. Cui, Diatomite derived hierarchical hybrid anode for high performance all-solid-state lithium metal batteries, *Nat. Commun.*, 2019 Jun 6, **10**(1), 1.

60 Y. Zhang, R. Zhang, S. Chen, H. Gao, M. Li, X. Song, H. L. Xin and Z. Chen, Diatomite-Derived Hierarchical Porous Crystalline-AmorphousNetwork for High-Performance and Sustainable Si Anodes, *Adv. Funct. Mater.*, 2020 Dec, **30**(50), 2005956.

61 J. Li, J. Xu, Z. Xie, X. Gao, J. Zhou, Y. Xiong, C. Chen, J. Zhang and Z. Liu, Diatomite-Templated Synthesis of Freestanding 3D Graphdiyne for Energy Storage and Catalysis Application, *Adv. Mater.*, 2018 May, **30**(20), 1800548.

62 Z. Wang, J. Zhao, S. Liu, F. Cui, J. Luo, Y. Wang, S. Zhang, C. Zhang and X. Yang, Cultured Diatoms Suitable for the Advanced Anode of Lithium Ion Batteries, *ACS Sustainable Chem. Eng.*, 2021 Jan 7, **9**(2), 844–852.

63 M. V. Blanco, V. Renman, F. Vullum-Bruer and A. M. Svensson, Nanostructured diatom earth SiO 2 negative electrodes with superior electrochemical performance for lithium ion batteries, *RSC Adv.*, 2020, **10**(55), 33490–33498.

64 M. De Stefano, W. H. Kooistra and D. Marino, morphology of the diatom genus campyloneis (bacillariophyceae, bacillariophyta), with a description of campyloneis juliae sp. nov. and an evaluation of the function of the valvocopulae 1, *J. Phycol.*, 2003 Aug, **39**(4), 735–753.

65 D. Losic, R. J. Pillar, T. Dilger, J. G. Mitchell and N. H. Voelcker, Atomic force microscopy (AFM) characterisation of the porous silica nanostructure of two centric diatoms, *J. Porous Mater.*, 2007 Mar 1, **14**(1), 61–69.

66 B. Tesson, M. J. Genet, V. Fernandez, S. Degand, P. G. Rouxhet and V. Martin-Jezequel, Surface chemical composition of diatoms, *ChemBioChem*, 2009 Aug 2011, **17**(12), 10.

67 E. Kiefer, L. Sigg and P. Schosseler, Chemical and spectroscopic characterization of algae surfaces, *Environ. Sci. Technol.*, 1997 Feb 27, **31**(3), 759–764.

68 E. G. Vrieling, T. P. Beelen, Q. Sun, S. Hazelaar, R. A. van Santen and W. W. Gieskes, Ultrasmall, small, and wide angle X-ray scattering analysis of diatom biosilica: interspecific differences in fractal properties, *J. Mater. Chem.*, 2004, **14**(13), 1970–1975.

69 F. E. Round, R. M. Crawford and D. G. Mann, *Diatoms: biology and morphology of the genera*, Cambridge university press, 1990 May 25.

70 A. I. Salimon, P. V. Sapozhnikov, J. Everaerts, O. Y. Kalinina, C. Besnard, C. Papadaki, J. Cvjetinovic, E. S. Statnik, Y. Kan, P. Aggrey and V. Kalyaev, A Mini-Atlas of diatom frustule electron microscopy images at different magnifications. Materials Today:, *Proceedings*, 2020 Jan 1, **33**, 1924–1933.

71 C. T. Chen, F. C. Hsu, J. Y. Huang, C. Y. Chang, T. Y. Chang, H. M. Lin, T. Y. Lin and Y. F. Chen, Effects of a thermally stable chlorophyll extract from diatom algae on surface textured Si solar cells, *RSC Adv.*, 2015, **5**(44), 35302–35306.

72 S. G. Jeong, J. Jeon, O. Chung, S. Kim and S. Kim, Evaluation of PCM/diatomite composites using exfoliated graphite nanoplatelets (xGnP) to improve thermal properties, *J. Therm. Anal. Calorim.*, 2013 Nov, **114**(2), 689–698.

73 Z. Sun, Y. Zhang, S. Zheng, Y. Park and R. L. Frost, Preparation and thermal energy storage properties of paraffin/calcined diatomite composites as form-stable phase change materials, *Thermochim. Acta*, 2013 Apr 20, **558**, 16–21.

74 B. Xu and Z. Li, Paraffin/diatomite composite phase change material incorporated cement-based composite for thermal energy storage, *Appl. Energy*, 2013 May 1, **105**, 229–237.

75 Y. Konuklu, O. Ersoy and O. Gokce, Easy and industrially applicable impregnation process for preparation of diatomite-based phase change material nanocomposites for thermal energy storage, *Appl. Therm. Eng.*, 2015 Dec 5, **91**, 759–766.

76 X. Li, J. G. Sanjayan and J. L. Wilson, Fabrication and stability of form-stable diatomite/paraffin phase change material composites, *Energy Build.*, 2014 Jun 1, **76**, 284–294.

77 T. Nomura, N. Okinaka and T. Akiyama, Impregnation of porous material with phase change material for thermal energy storage, *Mater. Chem. Phys.*, 2009 Jun 15, **115**(2–3), 846–850.

78 M. Li, Z. Wu and H. Kao, Study on preparation and thermal properties of binary fatty acid/diatomite shape-stabilized phase change materials, *Sol. Energy Mater. Sol. Cells*, 2011 Aug 1, **95**(8), 2412–2416.

79 M. Li, H. Kao, Z. Wu and J. Tan, Study on preparation and thermal property of binary fatty acid and the binary fatty acids/diatomite composite phase change materials, *Appl. Energy*, 2011 May 1, **88**(5), 1606–1612.

80 R. Wen, X. Zhang, Z. Huang, M. Fang, Y. Liu, X. Wu, X. Min, W. Gao and S. Huang, Preparation and thermal properties of fatty acid/diatomite form-stable composite phase change material for thermal energy storage, *Sol. Energy Mater. Sol. Cells*, 2018 May 1, **178**, 273–279.

81 A. Sarı and A. Biçer, Thermal energy storage properties and thermal reliability of some fatty acid esters/building material composites as novel form-stable PCMs, *Sol. Energy Mater. Sol. Cell.*, 2012 Jun 1, **101**, 114–122.

82 Z. Sun, W. Kong, S. Zheng and R. L. Frost, Study on preparation and thermal energy storage properties of binary paraffin blends/opal shape-stabilized phase change materials, *Sol. Energy Mater. Sol. Cell.*, 2013 Oct 1, **117**, 400–407.

83 Z. Li, N. Zhang, Y. Sun, H. Ke and H. Cheng, Application of diatomite as an effective polysulfides adsorbent for lithium-sulfur batteries, *J. Energy Chem.*, 2017 Nov 1, **26**(6), 1267–1275.

84 L. McMillon-Brown, M. Mariano, Y. L. Lin, J. Li, S. M. Hashmi, A. Semichaevsky, B. P. Rand and A. D. Taylor, Light-trapping in polymer solar cells by processing with nanostructured diatomaceous earth, *Org. Electron.*, 2017 Dec 1, **51**, 422–427.

85 G. Wu, S. Ma, Y. Bai and H. Zhang, The surface modification of diatomite, thermal, and mechanical properties of poly (vinyl chloride)/diatomite composites, *J. Vinyl Addit. Technol.*, 2019 Mar, **25**(s2), E39–E47.

86 M. J. Abden, Z. Tao, Z. Pan, L. George and R. Wuhrer, Inclusion of methyl stearate/diatomite composite in gypsum board ceiling for building energy conservation, *Appl. Energy*, 2020 Feb 1, **259**, 114113.

87 C. Li, M. Wang, B. Xie, H. Ma and J. Chen, Enhanced properties of diatomite-based composite phase change materials for thermal energy storage, *Renewable Energy*, 2020 Mar 1, **147**, 265–274.

88 Y. Konuklu, O. Ersoy, F. Erzin and T. YÖ, Experimental study on preparation of lauric acid/microwave-modified diatomite phase change material composites, *Sol. Energy Mater. Sol. Cells*, 2019 Jun 1, **194**, 89–94.

89 B. Xu and Z. Li, Paraffin/diatomite/multi-wall carbon nanotubes composite phase change material tailor-made for thermal energy storage cement-based composites, *Energy*, 2014 Aug 1, **72**, 371–380.

90 P. Zhang, Y. Cui, K. Zhang, S. Wu, D. Chen and Y. Gao, Enhanced thermal storage capacity of paraffin/diatomite composite using oleophobic modification, *J. Clean. Prod.*, 2021 Jan 10, **279**, 123211.

91 A. Sharma, V. V. Tyagi, C. R. Chen and D. Buddhi, Review on thermal energy storage with phase change materials and applications, *Renew. Sustain. Energy Rev.*, 2009 Feb 1, **13**(2), 318–345.

92 M. M. Kenisarin and K. M. Kenisarina, Form-stable phase change materials for thermal energy storage, *Renew. Sustain. Energy Rev.*, 2012 May 1, **16**(4), 1999–2040.

93 D. Losic, J. G. Mitchell and N. H. Voelcker, Complex gold nanostructures derived by templating from diatom frustules, *Chem. Commun.*, 2005, (39), 4905–4907.

94 D. Losic, J. G. Mitchell, R. Lal and N. H. Voelcker, Rapid fabrication of micro-and nanoscale patterns by replica molding from diatom biosilica, *Adv. Funct. Mater.*, 2007 Sep 24, **17**(14), 2439–2446.

95 H. Li, C. Jeffryes, T. Gutu and J. Jiao, Peptide-mediated deposition of nanostructured TiO_2 into the periodic structure of diatom biosilica and its integration into the fabrication of a dye-sensitized solar cell device, *Materials Research Society Online Proceedings Library (OPL)*, 2009, p. 1189.

96 Y. Yu, J. Addai-Mensah and D. Losic, Synthesis of self-supporting gold microstructures with three-dimensional morphologies by direct replication of diatom templates, *Langmuir*, 2010 Sep 7, **26**(17), 14068–14072.

97 J. Toster, K. S. Iyer, W. Xiang, F. Rosei, L. Spiccia and C. L. Raston, Diatom frustules as light traps enhance DSSC efficiency, *Nanoscale*, 2013, **5**(3), 873–876.

98 D. Liu, W. Yuan, P. Yuan, W. Yu, D. Tan, H. Liu and H. He, Physical activation of diatomite-templated carbons and its effect on the adsorption of methylene blue (MB), *Appl. Surf. Sci.*, 2013 Oct 1, **282**, 838–843.

99 K. Li, X. Liu, T. Zheng, D. Jiang, Z. Zhou, C. Liu, X. Zhang, Y. Zhang and D. Losic, Tuning MnO_2 to FeOOH replicas with bio-template 3D morphology as electrodes for high performance asymmetric supercapacitors, *Chem. Eng. J.*, 2019 Aug 15, **370**, 136–147.

100 Y. Yang, A. Li, X. Cao, F. Liu, S. Cheng and X. Chuan, Use of a diatomite template to prepare a MoS_2/amorphous carbon composite and exploration of its electrochemical properties as a supercapacitor, *RSC Adv.*, 2018, **8**(62), 35672–35680.

101 Q. J. Le, M. Huang, T. Wang, X. Y. Liu, L. Sun, X. L. Guo, D. B. Jiang, J. Wang, F. Dong and Y. X. Zhang, Biotemplate derived three dimensional nitrogen doped graphene@ MnO2 as bifunctional material for supercapacitor and oxygen reduction reaction catalyst, *J. Colloid Interface Sci.*, 2019 May 15, **544**, 155–163.

102 K. Chen, C. Li, L. Shi, T. Gao, X. Song, A. Bachmatiuk, Z. Zou, B. Deng, Q. Ji, D. Ma and H. Peng, Growing three-dimensional biomorphic graphene powders using naturally abundant diatomite templates towards high solution processability, *Nat. Commun.*, 2016 Nov 7, **7**(1), 1–9.

103 F. Li, Y. Xing, M. Huang, K. L. Li, T. T. Yu, Y. X. Zhang and D. Losic, MnO 2 nanostructures with three-dimensional (3D) morphology replicated from diatoms for high-performance supercapacitors, *J. Mater. Chem. A*, 2015, **3**(15), 7855–7861.

104 D. B. Jiang, B. Y. Zhang, T. X. Zheng, Y. X. Zhang and X. Xu, One-pot synthesis of η-Fe2O3 nanospheres/diatomite composites for electrochemical capacitor electrodes, *Mater. Lett.*, 2018 Mar 15, **215**, 23–26.

105 Z. Hu, K. Ma, W. Tian, F. Wang, H. Zhang, J. He, K. Deng, Y. X. Zhang, H. Yue and J. Ji, Manganese dioxide anchored on hierarchical carbon nanotubes/graphene/diatomite conductive architecture for high performance asymmetric supercapacitor, *Appl. Surf. Sci.*, 2020 Apr 1, **508**, 144777.

106 K. Masuko, M. Shigematsu, T. Hashiguchi, D. Fujishima, M. Kai, N. Yoshimura, T. Yamaguchi, Y. Ichihashi, T. Mishima, N. Matsubara and T. Yamanishi, Achievement of more than 25% conversion efficiency with crystalline silicon heterojunction solar cell, *IEEE J. Photovolt.*, 2014 Sep 10, **4**(6), 1433–1435.

107 *Applications of piezoelectric quartz crystal microbalances*, ed. Lu C and Czanderna AW, Elsevier; 2012 Dec 2.

108 N. Neophytou, Prospects of low-dimensional and nanostructured silicon-based thermoelectric materials: findings from theory and simulation, *Eur. Phys. J. B*, 2015 Apr, **88**(4), 1–2.

109 A. Morata, M. Pacios, G. Gadea, C. Flox, D. Cadavid, A. Cabot and A. Tarancón, Large-area and adaptable electrospun silicon-based thermoelectric nanomaterials with high energy conversion efficiencies, *Nat. Commun.*, 2018 Nov 12, **9**(1), 1–8.

110 Q. J. Le, T. Wang, D. N. Tran, F. Dong, Y. X. Zhang and D. Losic, Morphology-controlled MnO 2 modified silicon diatoms for high-performance asymmetric supercapacitors, *J. Mater. Chem. A*, 2017, **5**(22), 10856–10865.

111 L. F. Guo, S. Y. Zhang, J. Xie, D. Zhen, Y. Jin, K. Y. Wan, D. G. Zhuang, W. Q. Zheng and X. B. Zhao, Controlled synthesis of nanosized Si by magnesiothermic reduction from diatomite as anode material for Li-ion batteries. International Journal of Minerals, *J. Mater. Metall.*, 2020 Apr, **27**(4), 515–525.

112 P. Aggrey, B. Abdusatorov, Y. Kan, I. A. Salimon, S. A. Lipovskikh, S. Luchkin, D. M. Zhigunov, A. I. Salimon and A. M. Korsunsky, In situ formation of nanoporous silicon on a silicon wafer *via* the magnesiothermic reduction reaction (MRR) of diatomaceous earth, *Nanomaterials*, 2020 Apr, **10**(4), 601.

113 G. Leng, G. Qiao, Z. Jiang, G. Xu, Y. Qin, C. Chang and Y. Ding, Micro encapsulated & form-stable phase change materials for high temperature thermal energy storage, *Appl. Energy*, 2018 May 1, **217**, 212–220.

114 P. Aggrey, A. I. Salimon, B. Abdusatorov, S. S. Fedotov and A. M. Korsunsky, The structure and phase composition of nano-silicon as a function of calcination conditions of diatomaceous earth, *Mater. Today: Proc.*, 2020 Jan 1, **33**, 1884–1892.

115 S. Martinovic, M. Vlahovic, T. Boljanac and L. Pavlovic, Preparation of filter aids based on diatomites, *Int. J. Miner. Process.*, 2006 Sep 1, **80**(2–4), 255–260.

116 R. Zheng, Z. Ren, H. Gao, A. Zhang and Z. Bian, Effects of calcination on silica phase transition in diatomite, *J. Alloys Compd.*, 2018 Aug 15, **757**, 364–371.

117 J. R. Szczech and S. Jin, Mg2Si nanocomposite converted from diatomaceous earth as a potential thermoelectric nanomaterial, *J. Solid State Chem.*, 2008 Jul 1, **181**(7), 1565–1570.

118 N. Ediz, İ. Bentli and İ. Tatar, Improvement in filtration characteristics of diatomite by calcination, *Int. J. Miner. Process.*, 2010 Apr 28, **94**(3–4), 129–134.

119 B. Yılmaz and N. Ediz, The use of raw and calcined diatomite in cement production, *Cem. Concr. Compos.*, 2008 Mar 1, **30**(3), 202–211.

120 Y. Xia, F. Li, Y. Jiang, M. Xia, B. Xue and Y. Li, Interface actions between TiO2 and porous diatomite on the

structure and photocatalytic activity of TiO2-diatomite, *Appl. Surf. Sci.*, 2014 Jun 1, **303**, 290–296.

121 A. M. Korsunsky, Y. D. Bedoshvili, J. Cvjetinovic, P. Aggrey, K. I. Dragnevski, D. A. Gorin, A. I. Salimon and Y. V. Likhoshway, Siliceous diatom frustules–A smart nanotechnology platform, *Mater. Today: Proc.*, 2020 Jan 1, **33**, 2032–2040.

122 X. Tang, G. Wen and Y. Song, Novel scalable synthesis of porous silicon/carbon composite as anode material for superior lithium-ion batteries, *J. Alloys Compd.*, 2018 Mar 30, **739**, 510–517.

123 J. Wang, D. H. Liu, Y. Y. Wang, B. H. Hou, J. P. Zhang, R. S. Wang and X. L. Wu, Dual-carbon enhanced silicon-based composite as superior anode material for lithium ion batteries, *J. Power Sources*, 2016 Mar 1, **307**, 738–745.

124 D. Lončarević and Ž. Čupić The perspective of using nanocatalysts in the environmental requirements and energy needs of industry. in *Industrial Applications of Nanomaterials*, Elsevier, 2019 Jan 1, pp. 91–122.

125 K. Schulte and F. R. L. VonF, High-density polyethylene fiber/polyethylene matrix composites, *Compr. Compos. Mater. II*, 2000, 231–248.

126 M. D. Wakeman and C. D. Rudd, Compression molding of thermoplastic composites, *Compr. Compos. Mater. II*, 2000, 915–963.

127 J. I. A. Pei-ying, Application of impregnation technology in the die castings [J], *China National Knowledge Infrastructure*, Shaanxi Coal, 2006, p. 4.

128 H. Nazir, M. Batool, F. J. Osorio, M. Isaza-Ruiz, X. Xu, K. Vignarooban, P. Phelan and A. M. Kannan, Recent developments in phase change materials for energy storage applications: A review, *Int. J. Heat Mass Transfer*, 2019 Feb 1, **129**, 491–523.

129 L. N. Vakhitova. Fire retardant nanocoating for wood protection. in *Nanotechnology in Eco-efficient Construction*, Woodhead Publishing, 2019 Jan 1, pp. 361–391.

130 F. Rodríguez-Reinoso and A. Sepúlveda-Escribano. Porous carbons in adsorption and catalysis. in *Handbook of surfaces and interfaces of materials*, Academic Press, 2001 Jan 1, pp. 309–355.

131 V. P. Lehto and J. Riikonen. Drug loading and characterization of porous silicon materials, in *Porous silicon for biomedical applications*, Woodhead Publishing, 2014 Jan 1, pp. 337–355.

132 P. Liu, X. Gu, L. Bian, L. Peng and H. He, Capric acid/intercalated diatomite as form-stable composite phase change material for thermal energy storage, *J. Therm. Anal. Calorim.*, 2019 Oct, **138**(1), 359–368.

133 P. Liu, X. Gu, L. Bian, X. Cheng, L. Peng and H. He, Thermal properties and enhanced thermal conductivity of capric acid/diatomite/carbon nanotube composites as form-stable phase change materials for thermal energy storage, *ACS Omega*, 2019 Feb 11, **4**(2), 2964–2972.

134 W. Jia, C. Wang, T. Wang, Z. Cai and K. Chen, Preparation and performances of palmitic acid/diatomite form-stable composite phase change materials, *Int. J. Energy Res.*, 2020 May, **44**(6), 4298–4308.

135 T. Weege. Basic impregnation techniques [for windings]. *InProceedings: Electrical Insulation Conference and Electrical Manufacturing and Coil Winding Conference*, IEEE, 1997 Sep 25, pp. 709–715.

136 Y. Zhao and J. Xie, Practical applications of vacuum impregnation in fruit and vegetable processing, *Trends Food Sci. Technol.*, 2004 Sep 1, **15**(9), 434–451.

137 U. Sabu, G. Logesh, M. Rashad, A. Joy and M. Balasubramanian, Microwave assisted synthesis of biomorphic hydroxyapatite, *Ceram. Int.*, 2019 Apr 15, **45**(6), 6718–6722.

138 N. Amini, V. S. Haritos and A. Tanksale, Microwave assisted pretreatment of eucalyptus sawdust enhances enzymatic saccharification and maximizes fermentable sugar yield, *Renewable energy*, 2018 Nov 1, **127**, 653–660.

139 T. Qian, J. Li and Y. Deng, Pore structure modified diatomite-supported PEG composites for thermal energy storage, *Sci. Rep.*, 2016 Sep 1, **6**(1), 1–4.

140 J. Zong, D. Wang, Y. Jin, X. Gao and X. Wang. Preparation of Stearic acid/Diatomite Composite Phase Change Material, in *E3S Web of Conferences* 2021, EDP Sciences, vol. 245, p. 03070.

141 J. Jin, L. Liu, R. Liu, H. Wei, G. Qian, J. Zheng, W. Xie, F. Lin and J. Xie, Preparation and thermal performance of binary fatty acid with diatomite as form-stable composite phase change material for cooling asphalt pavements, *Constr. Build. Mater.*, 2019 Nov 30, **226**, 616–624.

142 T. Wang, Q. Le, J. Zhang, Y. Zhang and W. Li, Carbon cloth@ T-Nb_2O_5@ MnO_2: A rational exploration of manganese oxide for high performance supercapacitor, *Electrochim. Acta*, 2017 Nov 1, **253**, 311–318.

143 S. Feng and R. Xu, New materials in hydrothermal synthesis, *Acc. Chem. Res.*, 2001 Mar 20, **34**(3), 239–247.

144 C. Jing, X. Liu, X. Liu, D. Jiang, B. Dong, F. Dong, J. Wang, N. Li, T. Lan and Y. Zhang, Crystal morphology evolution of Ni–Co layered double hydroxide nanostructure towards high-performance biotemplate asymmetric supercapacitors, *CrystEngComm*, 2018, **20**(46), 7428–7434.

145 K. Li, S. Feng, C. Jing, Y. Chen, X. Liu, Y. Zhang and L. Zhou, Assembling a double shell on a diatomite skeleton ternary complex with conductive polypyrrole for the enhancement of supercapacitors, *Chem. Commun.*, 2019, **55**(91), 13773–13776.

146 Y. Jia, W. Han, G. Xiong and W. Yang, Layer-by-layer assembly of TiO_2 colloids onto diatomite to build hierarchical porous materials, *J. Colloid Interface Sci.*, 2008 Jul 15, **323**(2), 326–331.

147 J. He, D. Chen, Y. Li, J. Shao, J. Xie, Y. Sun, Z. Yan and J. Wang, Diatom-templated TiO_2 with enhanced photocatalytic activity: biomimetics of photonic crystals, *Appl. Phys. A*, 2013 Nov, **113**(2), 327–332.

148 B. Wang, F. C. de Godoi, Z. Sun, Q. Zeng, S. Zheng and R. L. Frost, Synthesis, characterization and activity of an immobilized photocatalyst: natural porous diatomite supported titania nanoparticles, *J. Colloid Interface Sci.*, 2015 Jan 15, **438**, 204–211.

149 J. Ouwehand, E. Van Eynde, E. De Canck, S. Lenaerts, A. Verberckmoes and P. Van Der Voort, Titania-functionalized diatom frustules as photocatalyst for indoor air purification, *Applied Catalysis B: Environmental*, 2018 Jun 15, **226**, 303–310.

150 Q. Zhu, Y. Zhang, F. Zhou, F. Lv, Z. Ye, F. Fan and P. K. Chu, Preparation and characterization of Cu_2O–ZnO immobilized on diatomite for photocatalytic treatment of red water produced from manufacturing of TNT, *Chem. Eng. J.*, 2011 Jun 15, **171**(1), 61–68.

151 J. Fang, Q. Liu, W. Zhang, J. Gu, Y. Su, H. Su, C. Guo and D. Zhang, Ag/diatomite for highly efficient solar vapor generation under one-sun irradiation, *J. Mater. Chem. A*, 2017, **5**(34), 17817–17821.

152 F. A. Khan, Synthesis of Nanomaterials: Methods & Technology. In *Applications of Nanomaterials in Human Health*, Springer, Singapore, 2020, pp. 15–21.

153 *Nanomaterials: Synthesis, characterization, and applications*, ed. Haghi AK, Zachariah AK and Kalariakkal N, CRC Press, 2013 Mar 11.

154 Y. B. Pottathara, Y. Grohens, V. Kokol, N. Kalarikkal and S. Thomas. Synthesis and processing of emerging two-dimensional nanomaterials, in *Nanomaterials Synthesis*, Elsevier, 2019 Jan 1, pp. 1–25.

155 R. J. Varghese, S. Parani, S. Thomas, O. S. Oluwafemi and J. Wu. Introduction to nanomaterials: synthesis and applications, in *Nanomaterials for Solar Cell Applications*, 2019 Jan 1, pp. 75–95, Elsevier.

156 T. C. Mokhena, M. J. John, M. A. Sibeko, V. C. Agbakoba, M. J. Mochane, A. Mtibe, T. H. Mokhothu, T. S. Motsoeneng, M. M. Phiri, M. J. Phiri and P. S. Hlangothi. Nanomaterials: Types, synthesis and characterization, in *Nanomaterials in Biofuels Research*, Springer, Singapore, 2020, pp. 115–141.

157 Z. Xing, J. Lu and X. Ji, A brief review of metallothermic reduction reactions for materials preparation, *Small Methods*, 2018 Dec, **2**(12), 1800062.

158 A. Bogacz, S. Rumianowski, W. Szymanski and W. Szklarski. Technology of light lanthanide metals production, in *Advances in Molten Salts*, Begell House, 1999 Jan 1.

159 U. B. Pal, D. E. Woolley and G. B. Kenney, Emerging SOM technology for the green synthesis of metals from oxides, *Jom*, 2001 Oct, **53**(10), 32–35.

160 K. Yasuda, K. Saegusa and T. H. Okabe, Aluminum subhalide as a reductant for metallothermic reduction, *High Temp. Mater. Processes*, 2011 Aug 1, **30**(4), 411–423.

161 M. A. Rhamdhani, M. A. Dewan, G. A. Brooks, B. J. Monaghan and L. Prentice, Alternative Al production methods: Part 1–a review of indirect carbothermal routes, *Miner. Process. Extr. Metall.*, 2013 Jun 1, **122**(2), 87–104.

162 H. P. Martin, R. Ecke and E. Müller, Synthesis of nanocrystalline silicon carbide powder by carbothermal reduction, *J. Eur. Ceram. Soc.*, 1998 Nov 1, **18**(12), 1737–1742.

163 D. J. Fray, Emerging molten salt technologies for metals production, *JOM*, 2001 Oct, **53**(10), 27–31.

164 Z. Xing, N. Gao, Y. Qi, X. Ji and H. Liu, Influence of enhanced carbon crystallinity of nanoporous graphite on the cathode performance of microbial fuel cells, *Carbon*, 2017 May 1, **115**, 271–278.

165 Z. Bao, M. R. Weatherspoon, S. Shian, Y. Cai, P. D. Graham, S. M. Allan, G. Ahmad, M. B. Dickerson, B. C. Church, Z. Kang and H. W. Abernathy Iii, Chemical reduction of three-dimensional silica micro-assemblies into microporous silicon replicas, *Nature*, 2007 Mar, **446**(7132), 172–175.

166 F. Gallego-Gómez, M. Ibisate, D. Golmayo, F. J. Palomares, M. Herrera, J. Hernández, S. I. Molina and L. C. Blanco Á, Light emission from nanocrystalline Si inverse opals and controlled passivation by atomic layer deposited Al2O3, *Adv. Mater.*, 2011 Nov 23, **23**(44), 5219–5223.

167 E. K. Richman, C. B. Kang, T. Brezesinski and S. H. Tolbert, Ordered mesoporous silicon through magnesium reduction of polymer templated silica thin films, *Nano Lett.*, 2008 Sep 10, **8**(9), 3075–3079.

168 C. Y. Khripin, D. Pristinski, D. R. Dunphy, C. J. Brinker and B. Kaehr, Protein-directed assembly of arbitrary three-dimensional nanoporous silica architectures, *ACS Nano*, 2011 Feb 22, **5**(2), 1401–1409.

169 Y. Zhang and J. Huang, Hierarchical nanofibrous silicon as replica of natural cellulose substance, *J. Mater. Chem.*, 2011, **21**(20), 7161–7165.

170 J. K. Yoo, J. Kim, Y. S. Jung and K. Kang, Scalable fabrication of silicon nanotubes and their application to energy storage, *Adv. Mater.*, 2012 Oct 23, **24**(40), 5452–5456.

171 W. Deqing and S. Ziyuan, Aluminothermic reduction of silica for the synthesis of alumina-aluminum-silicon composite, *J. Mater. Synth. Process.*, 2001 Sep, **9**(5), 241–246.

172 J. Cui, Y. Cui, S. Li, H. Sun, Z. Wen and J. Sun, Microsized porous SiO x@ C composites synthesized through aluminothermic reduction from rice husks and used as anode for lithium-ion batteries, *ACS Appl. Mater. Interfaces*, 2016 Nov 9, **8**(44), 30239–30247.

173 N. Lin, Y. Han, J. Zhou, K. Zhang, T. Xu, Y. Zhu and Y. Qian, A low temperature molten salt process for aluminothermic reduction of silicon oxides to crystalline Si for Li-ion batteries, *Energy Environ. Sci.*, 2015, **8**(11), 3187–3191.

174 Z. W. Zhou, Y. T. Liu, X. M. Xie and X. Y. Ye, Aluminothermic reduction enabled synthesis of silicon hollow microspheres from commercialized silica nanoparticles for superior lithium storage, *Chem. Commun.*, 2016, **52**(54), 8401–8404.

175 Y. Lai, J. R. Thompson and M. Dasog, Metallothermic reduction of silica nanoparticles to porous silicon for drug delivery using new and existing reductants, *Chem. - Eur. J.*, 2018 Jun 4, **24**(31), 7913–7920.

176 I. M. Morsi, K. E. Barawy, M. B. Morsi and S. R. Abdel-Gawad, Silicothermic reduction of dolomite ore under inert atmosphere, *Can. Metall. Q.*, 2002 Jan 1, **41**(1), 15–28.

177 J. Zhou, H. Zhao, N. Lin, T. Li, Y. Li, S. Jiang, J. Tian and Y. Qian, Silicothermic reduction reaction for fabricating interconnected Si–Ge nanocrystals with fast and stable Li-storage, *J. Mater. Chem. A*, 2020, **8**(14), 6597–6606.

178 G. D. Sun and G. H. Zhang, Study on the preparation of molybdenum silicides by the silicothermic reduction of MoS_2, *J. Alloys Compd.*, 2017 Dec 25, **728**, 295–306.
179 M. Li, C. Ke and J. Zhang, Synthesis of ZrB2 powders by molten-salt participating silicothermic reduction, *J. Alloys Compd.*, 2020 Sep 5, **834**, 155062.
180 J. Entwistle, A. Rennie and S. Patwardhan, A review of magnesiothermic reduction of silica to porous silicon for lithium-ion battery applications and beyond, *J. Mater. Chem. A*, 2018, **6**(38), 18344–18356.
181 L. Batchelor, A. Loni, L. T. Canham, M. Hasan and J. L. Coffer, Manufacture of mesoporous silicon from living plants and agricultural waste: an environmentally friendly and scalable process, *Silicon*, 2012 Oct, **4**(4), 259–266.
182 W. Luo, X. Wang, C. Meyers, N. Wannenmacher, W. Sirisaksoontorn, M. M. Lerner and X. Ji, Efficient fabrication of nanoporous Si and Si/Ge enabled by a heat scavenger in magnesiothermic reactions, *Sci. Rep.*, 2013 Jul 17, **3**(1), 1–7.
183 Z. Favors, W. Wang, H. H. Bay, Z. Mutlu, K. Ahmed, C. Liu, M. Ozkan and C. S. Ozkan, Scalable synthesis of nano-silicon from beach sand for long cycle life Li-ion batteries, *Sci. Rep.*, 2014 Jul 8, **4**(1), 1–7.
184 W. Wang, Z. Favors, R. Ionescu, R. Ye, H. H. Bay, M. Ozkan and C. S. Ozkan, Monodisperse porous silicon spheres as anode materials for lithium ion batteries, *Sci. Rep.*, 2015 Mar 5, **5**(1), 1–6.
185 C. Li, C. Liu, W. Wang, Z. Mutlu, J. Bell, K. Ahmed, R. Ye, M. Ozkan and C. S. Ozkan, Silicon derived from glass bottles as anode materials for lithium ion full cell batteries, *Sci. Rep.*, 2017 Apr 19, **7**(1), 1.
186 L. Shen, X. Guo, X. Fang, Z. Wang and L. Chen, Magnesiothermically reduced diatomaceous earth as a porous silicon anode material for lithium ion batteries, *J. Power Sources*, 2012 Sep 1, **213**, 229–232.
187 L. Shen, Z. Wang and L. Chen, Carbon-coated hierarchically porous silicon as anode material for lithium ion batteries, *RSC Adv.*, 2014, **4**(29), 15314–15318.
188 W. Wu, M. Wang, R. Wang, D. Xu, H. Zeng, C. Wang, Y. Cao and Y. Deng, Magnesio-mechanochemical reduced SiOx for high-performance lithium ion batteries, *J. Power Sources*, 2018 Dec 15, **407**, 112–122.
189 J. Liang, X. Li, Z. Hou, W. Zhang, Y. Zhu and Y. Qian, A deep reduction and partial oxidation strategy for fabrication of mesoporous Si anode for lithium ion batteries, *ACS Nano*, 2016 Feb 23, **10**(2), 2295–2304.
190 T. Chen, J. Wu, Q. Zhang and X. Su, Recent advancement of SiOx based anodes for lithium-ion batteries, *J. Power Sources*, 2017 Sep 30, **363**, 126–144.
191 W. Luo, X. Chen, Y. Xia, M. Chen, L. Wang, Q. Wang, W. Li and J. Yang, Surface and interface engineering of silicon-based anode materials for lithium-ion batteries, *Adv. Energy Mater.*, 2017 Dec, **7**(24), 1701083.
192 N. Sarier and E. Onder, Organic phase change materials and their textile applications: an overview, *Thermochim. Acta*, 2012 Jul 20, **540**, 7–60.
193 Z. Zhang, G. Shi, S. Wang, X. Fang and X. Liu, Thermal energy storage cement mortar containing n-octadecane/expanded graphite composite phase change material, *Renewable energy*, 2013 Feb 1, **50**, 670–675.
194 S. G. Jeong, J. Jeon, J. H. Lee and S. Kim, Optimal preparation of PCM/diatomite composites for enhancing thermal properties, *Int. J. Heat Mass Transfer*, 2013 Jul 1, **62**, 711–717.
195 B. Xu and Z. Li, Performance of novel thermal energy storage engineered cementitious composites incorporating a paraffin/diatomite composite phase change material, *Appl. Energy*, 2014 May 15, **121**, 114–122.
196 J. Huang, B. Wu, S. Lyu, T. Li, H. Han, D. Li, J. K. Wang, J. Zhang, X. Lu and D. Sun, Improving the thermal energy storage capability of diatom-based biomass/polyethylene glycol composites phase change materials by artificial culture methods, *Sol. Energy Mater. Sol. Cells*, 2021 Jan 1, **219**, 110797.
197 G. Xiong, K. P. Hembram, R. G. Reifenberger and T. S. Fisher, MnO2-coated graphitic petals for supercapacitor electrodes, *J. Power Sources*, 2013 Apr 1, **227**, 254–259.
198 Q. Wu, Y. Liu and Z. Hu, Flower-like NiO microspheres prepared by facile method as supercapacitor electrodes, *J. Solid State Electrochem.*, 2013 Jun 1, **17**(6), 1711–1716.
199 G. Wang, L. Zhang and J. Zhang, A review of electrode materials for electrochemical supercapacitors, *Chem. Soc. Rev.*, 2012, **41**(2), 797–828.
200 Z. Wang, C. Ma, H. Wang, Z. Liu and Z. Hao, Facilely synthesized Fe2O3–graphene nanocomposite as novel electrode materials for supercapacitors with high performance, *J. Alloys Compd.*, 2013 Mar 5, **552**, 486–491.
201 R. Liang, H. Cao and D. Qian, MoO 3 nanowires as electrochemical pseudocapacitor materials, *Chem. Commun.*, 2011, **47**(37), 10305–10307.
202 Q. Liao and C. Wang, Amorphous FeOOH nanorods and Co 3 O 4 nanoflakes as binder-free electrodes for high-performance all-solid-state asymmetric supercapacitors, *CrystEngComm*, 2019, **21**(4), 662–672.
203 W. Wei, X. Cui, W. Chen and D. G. Ivey, Manganese oxide-based materials as electrochemical supercapacitor electrodes, *Chem. Soc. Rev.*, 2011, **40**(3), 1697–1721.
204 L. Peng, X. Peng, B. Liu, C. Wu, Y. Xie and G. Yu, Ultrathin two-dimensional MnO2/graphene hybrid nanostructures for high-performance, flexible planar supercapacitors, *Nano Lett.*, 2013 May 8, **13**(5), 2151–2157.
205 Y. X. Zhang, W. Huo, K. Li, Q. Sun and T. Cao, *Supercapacitor nanomaterials, Advanced Nanomaterials for Electrochemical-Based Energy Conversion and Storage*, Elsevier, 2020, pp. 295–324.
206 L. Hu, B. Qu, L. Chen and Q. Li, Low-temperature preparation of ultrathin nanoflakes assembled tremella-like NiO hierarchical nanostructures for high-performance lithium-ion batteries, *Mater. Lett.*, 2013 Oct 1, **108**, 92–95.
207 Y. J. Mai, J. P. Tu, X. H. Xia, C. D. Gu and X. L. Wang, Co-doped NiO nanoflake arrays toward superior anode

materials for lithium ion batteries, *J. Power Sources*, 2011 Aug 1, **196**(15), 6388–6393.

208 Q. Wu, Z. Hu and Y. Liu, A novel electrode material of NiO prepared by facile hydrothermal method for electrochemical capacitor application, *J. Mater. Eng. Perform.*, 2013 Aug, **22**(8), 2398–2402.

209 L. Marcinauskas, Ž. Kavaliauskas and V. Valinčius, Carbon and nickel oxide/carbon composites as electrodes for supercapacitors, *J. Mater. Sci. Technol.*, 2012 Oct 1, **28**(10), 931–936.

210 A. S. Arico, P. Bruce, B. Scrosati, J. M. Tarascon and W. Van Schalkwijk, Nanostructured materials for advanced energy conversion and storage devices, *Mater. Sustainable Energy Appl.*, 2011, 148–159.

211 W. Qi, J. G. Shapter, Q. Wu, T. Yin, G. Gao and D. Cui, Nanostructured anode materials for lithium-ion batteries: principle, recent progress and future perspectives, *J. Mater. Chem. A*, 2017, **5**(37), 19521–19540.

212 W. S. Kim, Y. Hwa, J. H. Shin, M. Yang, H. J. Sohn and S. H. Hong, Scalable synthesis of silicon nanosheets from sand as an anode for Li-ion batteries, *Nanoscale*, 2014, **6**(8), 4297–4302.

213 Y. Yao, M. T. McDowell, I. Ryu, H. Wu, N. Liu, L. Hu, W. D. Nix and Y. Cui, Interconnected silicon hollow nanospheres for lithium-ion battery anodes with long cycle life, *Nano Lett.*, 2011 Jul 13, **11**(7), 2949–2954.

214 T. H. Hwang, Y. M. Lee, B. S. Kong, J. S. Seo and J. W. Choi, Electrospun core–shell fibers for robust silicon nanoparticle-based lithium ion battery anodes, *Nano Lett.*, 2012 Feb 8, **12**(2), 802–807.

215 M. Ashuri, Q. He and L. L. Shaw, Silicon as a potential anode material for Li-ion batteries: where size, geometry and structure matter, *Nanoscale*, 2016, **8**(1), 74–103.

216 H. K. Liu, Z. P. Guo, J. Z. Wang and K. Konstantinov, Si-based anode materials for lithium rechargeable batteries, *J. Mater. Chem.*, 2010, **20**(45), 10055–10057.

217 P. Li, G. Zhao, X. Zheng, X. Xu, C. Yao, W. Sun and S. X. Dou, Recent progress on silicon-based anode materials for practical lithium-ion battery applications, *Energy Storage Mater.*, 2018 Nov 1, **15**, 422–446.

218 X. Li, M. Gu, S. Hu, R. Kennard, P. Yan, X. Chen, C. Wang, M. J. Sailor, J. G. Zhang and J. Liu, Mesoporous silicon sponge as an anti-pulverization structure for high-performance lithium-ion battery anodes, *Nat. Commun.*, 2014 Jul 8, **5**(1), 1–7.

219 P. Li, J. Y. Hwang and Y. K. Sun, Nano/microstructured silicon–graphite composite anode for high-energy-density Li-ion battery, *ACS Nano*, 2019 Feb 13, **13**(2), 2624–2633.

220 X. Ding, X. Liu, Y. Huang, X. Zhang, Q. Zhao, X. Xiang, G. Li, P. He, Z. Wen, J. Li and Y. Huang, Enhanced electrochemical performance promoted by monolayer graphene and void space in silicon composite anode materials, *Nano Energy*, 2016 Sep 1, **27**, 647–657.

221 X. Tao, Y. Liu, W. Liu, G. Zhou, J. Zhao, D. Lin, C. Zu, O. Sheng, W. Zhang, H. W. Lee and Y. Cui, Solid-state lithium–sulfur batteries operated at 37 C with composites of nanostructured Li7La3Zr2O12/carbon foam and polymer, *Nano Lett.*, 2017 May 10, **17**(5), 2967–2972.

222 R. Bouchet, S. Maria, R. Meziane, A. Aboulaich, L. Lienafa, J. P. Bonnet, T. N. Phan, D. Bertin, D. Gigmes, D. Devaux and R. Denoyel, Single-ion BAB triblock copolymers as highly efficient electrolytes for lithium-metal batteries, *Nat. Mater.*, 2013 May, **12**(5), 452–457.

223 Z. Xue, D. He and X. Xie, Poly (ethylene oxide)-based electrolytes for lithium-ion batteries, *J. Mater. Chem. A*, 2015, **3**(38), 19218–19253.

224 A. Manthiram, Y. Fu, S. H. Chung, C. Zu and Y. S. Su, Rechargeable lithium–sulfur batteries, *Chem. Rev.*, 2014 Dec 10, **114**(23), 11751–11787.

225 L. Chen and L. L. Shaw, Recent advances in lithium–sulfur batteries, *J. Power Sources*, 2014 Dec 1, **267**, 770–783.

226 A. Manthiram, S. H. Chung and C. Zu, Lithium–sulfur batteries: progress and prospects, *Adv. Mater.*, 2015 Mar, **27**(12), 1980–2006.

227 Z. W. Seh, Y. Sun, Q. Zhang and Y. Cui, Designing high-energy lithium–sulfur batteries, *Chem. Soc. Rev.*, 2016, **45**(20), 5605–5634.

228 P. Cong, S. Chen and H. Chen, Effects of diatomite on the properties of asphalt binder, *Constr. Build. Mater.*, 2012 May 1, **30**, 495–499.

229 L. Xu, X. Gao, Z. Li and C. Gao, Removal of fluoride by nature diatomite from high-fluorine water: an appropriate pretreatment for nanofiltration process, *Desalination*, 2015 Aug 3, **369**, 97–104.

230 S. LeBlanc, Thermoelectric generators: Linking material properties and systems engineering for waste heat recovery applications, *Sustainable Mater. Technol.*, 2014 Dec 1, **1**, 26–35.

231 K. Biswas, J. He, I. D. Blum, C. I. Wu, T. P. Hogan, D. N. Seidman, V. P. Dravid and M. G. Kanatzidis, High-performance bulk thermoelectrics with all-scale hierarchical architectures, *Nature*, 2012 Sep, **489**(7416), 414–418.

232 Z. Chen, X. Zhang and Y. Pei, Manipulation of phonon transport in thermoelectrics, *Adv. Mater.*, 2018 Apr, **30**(17), 1705617.

233 P. A. Zong, R. Hanus, M. Dylla, Y. Tang, J. Liao, Q. Zhang, G. J. Snyder and L. Chen, Skutterudite with graphene-modified grain-boundary complexion enhances zT enabling high-efficiency thermoelectric device, *Energy Environ. Sci.*, 2017, **10**(1), 183–191.

234 Q. Zhang, Z. Zhou, M. Dylla, M. T. Agne, Y. Pei, L. Wang, Y. Tang, J. Liao, J. Li, S. Bai and W. Jiang, Realizing high-performance thermoelectric power generation through grain boundary engineering of skutterudite-based nanocomposites, *Nano Energy*, 2017 Nov 1, **41**, 501–510.

235 G. Schierning, Silicon nanostructures for thermoelectric devices: A review of the current state of the art, *Phys. Status Solidi A*, 2014 Jun, **211**(6), 1235–1249.

236 C. B. Vining, Desperately seeking silicon, *Nature*, 2008 Jan, **451**(7175), 132–133.

237 A. I. Boukai, Y. Bunimovich, J. Tahir-Kheli, J. K. Yu, W. A. Goddard Iii and J. R. Heath, Silicon nanowires as

efficient thermoelectric materials, *nature*, 2008 Jan, **451**(7175), 168–171.

238 A. I. Hochbaum, R. Chen, R. D. Delgado, W. Liang, E. C. Garnett, M. Najarian, A. Majumdar and P. Yang, Enhanced thermoelectric performance of rough silicon nanowires, *Nature*, 2008 Jan, **451**(7175), 163–167.

239 S. K. Bux, R. G. Blair, P. K. Gogna, H. Lee, G. Chen, M. S. Dresselhaus, R. B. Kaner and J. P. Fleurial, Nanostructured bulk silicon as an effective thermoelectric material, *Adv. Funct. Mater.*, 2009 Aug 10, **19**(15), 2445–2452.

240 V. Lysenko, S. Perichon, B. Remaki and D. Barbier, Thermal isolation in microsystems with porous silicon, *Sens. Actuators, A*, 2002 Apr 30, **99**(1–2), 13–24.

241 G. Gesele, J. Linsmeier, V. Drach, J. Fricke and R. Arens-Fischer, Temperature-dependent thermal conductivity of porous silicon, *J. Phys. D: Appl. Phys.*, 1997 Nov 7, **30**(21), 2911.

242 M. S. Dresselhaus, G. Chen, M. Y. Tang, R. G. Yang, H. Lee, D. Z. Wang, Z. F. Ren, J. P. Fleurial and P. Gogna, New directions for low-dimensional thermoelectric materials, *Adv. Mater.*, 2007 Apr 20, **19**(8), 1043–1053.

243 T. Fuhrmann, S. Landwehr, M. El Rharbi-Kucki and M. Sumper, Diatoms as living photonic crystals, *Appl. Phys. B: Lasers Opt.*, 2004 Feb, **78**(3), 257–260.

244 S. Yamanaka, R. Yano, H. Usami, N. Hayashida, M. Ohguchi, H. Takeda and K. Yoshino, Optical properties of diatom silica frustule with special reference to blue light, *J. Appl. Phys.*, 2008 Apr 1, **103**(7), 074701.

245 J. Noyes, M. Sumper and P. Vukusic, Light manipulation in a marine diatom, *J. Mater. Res.*, 2008 Dec, **23**(12), 3229–3235.

246 X. Chen, C. Wang, E. Baker and C. Sun, Numerical and experimental investigation of light trapping effect of nanostructured diatom frustules, *Sci. Rep.*, 2015 Jul 9, **5**(1), 1–9.

247 J. Romann, J. C. Valmalette, A. Røyset and M. A. Einarsrud, Optical properties of single diatom frustules revealed by confocal microspectroscopy, *Opt. Lett.*, 2015 Mar 1, **40**(5), 740–743.

248 W. H. Kooistra, R. Gersonde, L. K. Medlin and D. G. Mann. The origin and evolution of the diatoms: their adaptation to a planktonic existence. *Evolution of primary producers in the sea*. 2007 Jan 1, pp. 207–49.

249 E. V. Armbrust, The life of diatoms in the world's oceans, *Nature*, 2009 May, **459**(7244), 185–192.

250 F. Gaspari and S. Quaranta, *2.5 PV Materials*, Elsevier Ltd., 2018, vol. 2.

251 J. Baxter, Z. Bian, G. Chen, D. Danielson, M. S. Dresselhaus, A. G. Fedorov, T. S. Fisher, C. W. Jones, E. Maginn, U. Kortshagen and A. Manthiram, Nanoscale design to enable the revolution in renewable energy, *Energy Environ. Sci.*, 2009, **2**(6), 559–588.

252 C. Z. Hotz. Quantum Dots, in *Molecular Biomethods Handbook*, Humana Press, 2008, pp. 697–710.

253 D. Wöhrle and D. Meissner, Organic solar cells, *Adv. Mater.*, 1991 Mar, **3**(3), 129–138.

254 B. O'regan and M. Grätzel, A low-cost, high-efficiency solar cell based on dye-sensitized colloidal TiO 2 films, *Nature*, 1991 Oct, **353**(6346), 737–740.

255 M. K. Nazeeruddin, A. Kay, I. Rodicio, R. Humphry-Baker, E. Müller, P. Liska, N. Vlachopoulos and M. Grätzel, Conversion of light to electricity by cis-X2bis (2, 2'-bipyridyl-4, 4'-dicarboxylate) ruthenium (II) charge-transfer sensitizers (X= Cl-, Br-, I-, CN-, and SCN-) on nanocrystalline titanium dioxide electrodes, *J. Am. Chem. Soc.*, 1993 Jul, **115**(14), 6382–6390.

256 D. Losic, G. Triani, P. J. Evans, A. Atanacio, J. G. Mitchell and N. H. Voelcker, Controlled pore structure modification of diatoms by atomic layer deposition of TiO 2, *J. Mater. Chem.*, 2006, **16**(41), 4029–4034.

257 Y. Tachibana, H. Y. Akiyama and S. Kuwabata, Optical simulation of transmittance into a nanocrystalline anatase TiO_2 film for solar cell applications, *Sol. Energy Mater. Sol. Cell.*, 2007 Jan 23, **91**(2–3), 201–206.

258 T. M. Bandara, M. Furlani, I. Albinsson, A. Wulff and B. E. Mellander, Diatom frustules enhancing the efficiency of gel polymer electrolyte based dye-sensitized solar cells with multilayer photoelectrodes, *Nanoscale Adv.*, 2020, **2**(1), 199–209.

259 K. Maeda, K. Teramura, D. Lu, T. Takata, N. Saito, Y. Inoue and K. Domen, Photocatalyst releasing hydrogen from water, *Nature*, 2006 Mar, **440**(7082), 295.

260 S. Y. Lee and S. J. Park, TiO2 photocatalyst for water treatment applications, *J. Ind. Eng. Chem.*, 2013 Nov 25, **19**(6), 1761–1769.

261 A. Kudo and Y. Miseki, Heterogeneous photocatalyst materials for water splitting, *Chem. Soc. Rev.*, 2009, **38**(1), 253–278.

262 A. Kudo, Development of photocatalyst materials for water splitting, *Int. J. Hydrogen Energy*, 2006 Feb 1, **31**(2), 197–202.

263 A. Primo, A. Corma and H. García, Titania supported gold nanoparticles as photocatalyst, *Phys. Chem. Chem. Phys.*, 2011, **13**(3), 886–910.

264 K. M. Lee, C. W. Lai, K. S. Ngai and J. C. Juan, Recent developments of zinc oxide based photocatalyst in water treatment technology: a review, *Water Res.*, 2016 Jan 1, **88**, 428–448.

265 W. Choi, A. Termin and M. R. Hoffmann, The role of metal ion dopants in quantum-sized TiO_2: correlation between photoreactivity and charge carrier recombination dynamics, *J. Phys. Chem.*, 2002 May 1, **98**(51), 13669–13679.

266 L. Cai, J. Gong, J. Liu, H. Zhang, W. Song and L. Ji, Facile preparation of nano-Bi_2MoO_6/diatomite composite for enhancing photocatalytic performance under visible light irradiation, *Materials*, 2018 Feb, **11**(2), 267.

267 Z. Jia, T. Li, Z. Zheng, J. Zhang, J. Liu, R. Li, Y. Wang, X. Zhang, Y. Wang and C. Fan, The BiOCl/diatomite composites for rapid photocatalytic degradation of ciprofloxacin: Efficiency, toxicity evaluation, mechanisms and pathways, *Chem. Eng. J.*, 2020 Jan 15, **380**, 122422.

268 L. Xiao, X. Zhang and G. Yan, Diatomite-Bi2S3 composite photocatalyst: enhanced photocatalytic performance for

visible light reduction of Cr (VI), *Mater. Res. Express*, 2019 Mar 6, **6**(6), 065902.

269 P. Zhu, Y. Chen, M. Duan, M. Liu and P. Zou, Structure and properties of Ag_3PO_4/diatomite photocatalysts for the degradation of organic dyes under visible light irradiation, *Powder Technol.*, 2018 Aug 1, **336**, 230–239.

270 H. B. Fan, Q. F. Ren, S. L. Wang, Z. Jin and Y. Ding, Synthesis of the Ag/Ag_3PO_4/diatomite composites and their enhanced photocatalytic activity driven by visible light, *J. Alloys Compd.*, 2019 Feb 15, **775**, 845–852.

271 J. Pang, F. Fu, W. Li, L. Zhu and B. Tang, Fe-Mn binary oxide decorated diatomite for rapid decolorization of methylene blue with H_2O_2, *Appl. Surf. Sci.*, 2019 Jun 1, **478**, 54–61.

272 P. Tanniratt, T. Wasanapiarnpong, C. Mongkolkachit and P. Sujaridworakun, Utilization of industrial wastes for preparation of high performance ZnO/diatomite hybrid photocatalyst, *Ceram. Int.*, 2016 Nov 15, **42**(15), 17605–17609.

273 R. D. Soltani, A. Khataee, M. Mashayekhi and M. Safari, Photocatalysis of formaldehyde in the aqueous phase over ZnO/diatomite nanocomposite, *Turk. J. Chem.*, 2016 May 17, **40**(3), 402–411.

274 R. D. Soltani and Z. Haghighat, Visible light photocatalysis of a textile dye over ZnO nanostructures covered on natural diatomite, *Turk. J. Chem.*, 2016 May 17, **40**(3), 454–466.

275 S. J. Cho, T. An and G. Lim, Three-dimensionally designed anti-reflective silicon surfaces for perfect absorption of light, *Chem. Commun.*, 2014, **50**(99), 15710–15713.

276 J. Zhao, Y. Li, G. Yang, K. Jiang, H. Lin, H. Ade, W. Ma and H. Yan, Efficient organic solar cells processed from hydrocarbon solvents, *Nat. Energy*, 2016 Jan 25, **1**(2), 1–7.

277 J. Kong, M. M. Beromi, M. Mariano, T. Goh, F. Antonio, N. Hazari and A. D. Taylor, Colorful polymer solar cells employing an energy transfer dye molecule, *Nano Energy*, 2017 Aug 1, **38**, 36–42.

278 H. A. Atwater and A. Polman, Plasmonics for improved photovoltaic devices, *Mater. Sustainable Energy Appl.*, 2011, 1.

279 R. Betancur, P. Romero-Gomez, A. Martinez-Otero, X. Elias, M. Maymó and J. Martorell, Transparent polymer solar cells employing a layered light-trapping architecture, *Nat. Photonics*, 2013 Dec, **7**(12), 995–1000.

280 Y. Liu, C. Kirsch, A. Gadisa, M. Aryal, S. Mitran, E. T. Samulski and R. Lopez, Effects of nano-patterned *versus* simple flat active layers in upright organic photovoltaic devices, *J. Phys. D: Appl. Phys.*, 2012 Dec 17, **46**(2), 024008.

281 J. F. Bertone, J. Cizeron, R. K. Wahi, J. K. Bosworth and V. L. Colvin, Hydrothermal synthesis of quartz nanocrystals, *Nano Lett.*, 2003 May 14, **3**(5), 655–659.

282 X. Jiang, Y. B. Jiang and C. J. Brinker, Hydrothermal synthesis of monodisperse single-crystalline alpha-quartz nanospheres, *Chem. Commun.*, 2011, **47**(26), 7524–7526.

283 A. Carretero-Genevrier, M. Gich, L. Picas, J. Gazquez, G. L. Drisko, C. Boissiere, D. Grosso, J. Rodriguez-Carvajal and C. Sanchez, Soft-chemistry–based routes to epitaxial α-quartz thin films with tunable textures, *Science*, 2013 May 17, **340**(6134), 827–831.

284 A. Carretero-Genevrier and M. Gich, Preparation of macroporous epitaxial quartz films on silicon by chemical solution deposition, *J. Visualized Exp.*, 2015, (106), e53543.

285 F. Iwasaki and H. Iwasaki, Historical review of quartz crystal growth, *J. Cryst. Growth*, 2002 Apr 1, **237**, 820–827.

286 A. Laschitsch and D. Johannsmann, High frequency tribological investigations on quartz resonator surfaces, *J. Appl. Phys.*, 1999 Apr 1, **85**(7), 3759–3765.

287 Y. Xia and G. M. Whitesides, Soft lithography, *Annu. Rev. Mater. Sci.*, 1998 Aug, **28**(1), 153–184.

288 C. Boissiere, D. Grosso, A. Chaumonnot, L. Nicole and C. Sanchez, Aerosol route to functional nanostructured inorganic and hybrid porous materials, *Adv. Mater.*, 2011 Feb 1, **23**(5), 599–623.

289 C. Sanchez, C. Boissiere, D. Grosso, C. Laberty and L. Nicole, Design, synthesis, and properties of inorganic and hybrid thin films having periodically organized nanoporosity, *Chem. Mater.*, 2008 Feb 12, **20**(3), 682–737.

290 C. J. Brinker and G. W. Scherer, Sol-gel science: the physics and chemistry of sol-gel processing, Academic press, San Diego, 1990.

291 D. Grosso, How to exploit the full potential of the dip-coating process to better control film formation, *J. Mater. Chem.*, 2011, **21**(43), 17033–17038.

292 X. Jiang, L. Bao, Y. S. Cheng, D. R. Dunphy, X. Li and C. J. Brinker, Aerosol-assisted synthesis of monodisperse single-crystalline α-cristobalite nanospheres, *Chem. Commun.*, 2012, **48**(9), 1293–1295.

293 P. Bruhns and R. X. Fischer, Crystallization of cristobalite and tridymite in the presence of vanadium, *Eur. J. Mineral.*, 2000 May 1, **12**(3), 615–624.

294 A. M. Venezia, V. La Parola, A. Longo and A. Martorana, Effect of alkali ions on the amorphous to crystalline phase transition of silica, *J. Solid State Chem.*, 2001 Nov 1, **161**(2), 373–378.

295 V. G. Pol, A. Gedanken and J. Calderon-Moreno, Deposition of gold nanoparticles on silica spheres: a sonochemical approach, *Chem. Mater.*, 2003 Mar 11, **15**(5), 1111–1118.

296 D. C. Altamirano-Juárez, C. Carrera-Figueiras, M. G. Garnica-Romo, M. L. Mendoza-Lopez, M. B. Ortuno-Lopez, M. E. Pérez-Ramos, A. Ramos-Mendoza, C. Rivera-Rodríguez, H. Tototzintle-Huitle, J. J. Valenzuela-Jauregi and M. A. Vidales-Hurtado, Effects of metals on the structure of heat-treated sol-gel SiO2 glasses, *J. Phys. Chem. Solids*, 2001 Nov 1, **62**(11), 1911–1917.